The role of Thioredoxin-interacting protein in T cell receptor signalling

Dissertation

submitted to the
Combined Faculty of Natural Sciences and Mathematics
of the Ruperto Carola University of Heidelberg, Germany
for the degree of
Doctor of Natural Sciences

M. Sc. Stefanie Dünnbier
born in Neuruppin, Germany

4th July 2019

Dissertation

submitted to the

Combined Faculty of Natural Sciences and Mathematics

of the Ruperto Carola University of Heidelberg, Germany

for the degree of

Doctor of Natural Sciences

Presented by

M. Sc. Stefanie Dünnbier

born in Neuruppin, Germany

Oral examination: 10th September 2019

The role of Thioredoxin-interacting protein in T cell receptor signalling

Referees: Prof. Dr. Frauke Melchior

Prof. Dr. Peter H. Krammer

„Das Glück – kein Reiter wird's erjagen.

Es ist nicht dort und ist nicht hier.

Lern überwinden, lern entsagen,

und ungeahnt erblüht es dir.“

Theodor Fontane

Danksagung

An dieser Stelle möchte ich meinen besonderen Dank nachstehenden Personen entgegenbringen, ohne deren Mithilfe die Anfertigung dieser Dissertation niemals zustande gekommen wäre:

- Prof. Dr. Peter H. Krammer, dass er mir ermöglicht hat unter seiner Aufsicht an diesem Projekt zu arbeiten. Ich schätze alle Möglichkeiten, die mir während meiner Zeit in seinem Labor geboten wurden sowie die zahlreichen Einblicke in die Geschichte der Immunologie.
- Den Mitgliedern meines „Thesis Advisory"-Komitees, Frau Prof. Dr. Frauke Melchior und Herr Prof. Dr. Peter Angel für die Betreuung sowie die vielen konstruktiven Kommentare, Vorschläge und Diskussionen.
- Dr. Karin Müller-Decker, dass Sie sich dazu bereit erklärt hat Mitglied meiner Prüfungskommission zu sein.
- Dr. Karsten Gülow für seine hervorragende direkte Betreuung. Er war immer und jederzeit gerne für Probleme ansprechbar und hatte für (fast) jedes Problem eine Lösung parat. Mit seiner Motivation und seinem Engagement konnte er mir auch in schwierigen Situationen weiterhelfen.
- Dr. Corinna Link für ihre große Hilfe bei der Zusammenstellung und dem Korrekturlesen dieser Arbeit.
- Der gesamten Abteilung D030, insbesondere Dr. Tina Oberacker und Dr. Anne Schröder sowie den anderen Promovierenden – Kevin Bode, Dr. Corinna Link, Tobias Hein, Maria Nolte, Dr. Fatmire Bujupi – für das tolle Arbeitsumfeld, ihre Hilfsbereitschaft, die vielen Diskussionen und die sehr freundschaftliche Atmosphäre.
- Kevin Bode und Dr. Corinna Link, für eine fröhliche Atmosphäre in unserem gemeinsamen Schreibraum und dass sie immer ein offenes Ohr für mich hatten. Sie haben mich auch in schwierigen Situationen immer aufgemuntert. Kevin: „Steffi, Lächeln hilft!" ☺
- Diana Vobis, Marlene Pach sowie meinen Azubis Hannah Kempf, Lena Vogelbacher und Lea Günther für ihre sehr große Hilfe bei der technischen Umsetzung, welche maßgeblich zum Gelingen dieser Arbeit beigetragen hat.
- Meiner Familie und meinen Freunden außerhalb des Labors die mich auch in schwierigen Phasen während meiner Zeit als Doktorandin aufgemuntert und unterstützt haben.
- Mein größter Dank gilt dem wichtigsten Menschen in meinem Leben – meinem Ehemann, Mario, für deine geduldige, liebevolle und bereichernde Unterstützung sowie für dein Verständnis während der Zeit meiner Doktorarbeit. Danke, dass du immer für mich da bist und ich immer auf dich zählen kann.

Contents

Abstract

T cell receptor (TCR) engagement and subsequent signalling are a prerequisite to initiate a T cell immune response. In recent years, our group investigated the underlying mechanisms of TCR signalling and identified Thioredoxin-interacting protein (TXNIP) as a possible regulator of a T cell immune response.

This study examined the role of TXNIP in TCR signalling. Following TCR stimulation, TXNIP expression was reduced due to accelerated proteasomal degradation as well as decreased protein synthesis. Since TXNIP is a negative regulator of Trx, activation-induced downregulation of TXNIP expression resulted in increased Trx activity.

Using TXNIP knockout (KO) T cells as a model system, this study revealed that TXNIP has an impact on gene expression upon TCR engagement. By analysing stimulation-induced whole genome expression of TXNIP KO cells in comparison to control cells, this study demonstrated that TXNIP acts as a transcriptional inhibitor. TXNIP affects transcription of CD95L, GMCSF, GZMB, IFNG, IL2, TNFA and EGR2. These genes are involved in T cell activation, differentiation, cytokine signalling as well as cell death and designated as NFκB, AP1 as well as NFAT targets. Thus, TXNIP might control gene expression by regulating the activity of one or various transcription factors. Expression of CD95L upon TCR stimulation mediates activation-induced cell death (AICD) in apoptosis-sensitive T cells. In accordance with increased stimulation-induced CD95L expression, AICD was enhanced in TXNIP KO cells compared to control cells. This result underlines the important role of TXNIP in TCR signalling.

Taken together, this study demonstrates that TXNIP is involved in TCR signalling by acting as transcriptional inhibitor. Hence, TXNIP might be considered as a potential therapeutic target to shape T cell responses *e.g.* in autoimmune or tumour diseases.

Zusammenfassung

T-Zell-Rezeptor (TCR)-Stimulation und die daraus resultierende Aktivierung von intrazellulären Signalkaskaden bilden die Grundlage zur Initiation einer spezifischen Immunantwort. In den letzten Jahren hat unsere Gruppe die dem TCR-Signalweg zugrundeliegenden molekularen Mechanismen im Detail untersucht und entdeckt, dass das Thioredoxin-interacting protein (TXNIP) ein möglicher Regulator der T-Zell-Immunantwort ist.

Die vorliegende Studie untersuchte die Rolle von TXNIP in der TCR-Signalgebung. Stimulation des TCRs führte zu einer Reduzierung der TXNIP-Expression aufgrund von verstärktem proteasomalem Abbau und verringerter Proteinbiosynthese. Da TXNIP ein negativer Regulator von Thioredoxin (Trx) ist, ging die aktivierungs-induzierte Reduktion von TXNIP mit einer gesteigerten Aktivität von Trx einher.

Durch die Generierung von TXNIP knockout (KO)-T-Zellen als Modellsystem, konnte in dieser Studie gezeigt werden, dass TXNIP einen Einfluss auf die aktivierungs-induzierte Transkription hat. Anhand einer Genomexpressionsanalyse von TCR-stimulierten TXNIP KO-Zellen im Vergleich zu Kontroll-Zellen demonstrierte diese Studie, dass TXNIP als Inhibitor der stimulations-abhängigen Transkription in T-Zellen wirkt. Die Expression von TXNIP reguliert die Transkription von CD95L, GMCSF, GZMB, IFNG, IL2, TNFA und EGR2. Die Expression dieser Gene spielt eine wichtige Rolle in der Aktivierung, Differenzierung, Zytokin-Signalgebung sowie auch beim Zelltod von T-Zellen und unterliegt der Regulation durch verschiedene Transkriptionsfaktoren wie NFκB, AP1 und NFAT. Dies deutet darauf hin, dass TXNIP die Aktivität von einem oder mehreren Transkriptionsfaktoren regulieren könnte. Expression des CD95L nach TCR-Stimulation löst in Apoptose-sensitiven T-Zellen aktivierungs-induzierten Zelltod (AICD) aus. Dementsprechend resultierte die erhöhte CD95L-Expression in einem Anstieg des AICDs in TCR-stimulierten TXNIP KO-Zellen im Vergleich zu Kontroll-Zellen. Dieses Ergebnis bekräftigt, dass TXNIP in der TCR-Signalgebung eine wichtige Funktion übernimmt.

Zusammengefasst demonstriert die vorliegende Studie, dass TXNIP als negativer Regulator der Genexpression die TCR-Signalgebung beeinflusst. Diese Funktion von TXNIP könnte als potentieller therapeutischer Angriffspunkt zur Modulation von T-Zell-Immunantworten, z.B. bei Autoimmun- oder Krebserkrankungen, genutzt werden.

Abbreviations

$1,25(OH)_2D_3$	1,25-dihydroxyvitamin D_3
7AAD	7-Aminoactinomycin D
ACAD	activated cell autonomous death
ADPGK	ADP-dependent glucokinase
AET	2-aminoethylisothiouronium-bromide
AICD	activation-induced cell death
AIDS	acquired immune deficiency syndrome
AIF	apoptosis inducing factor
ALPS	autoimmune lymphoproliferative syndrome
AP1	activator protein 1
Apaf-1	apoptotic protease activating factor-1
APC	antigen presenting cell
APO	apoptosis antigen-1
APS	ammonium persulfate
ASK-1	apoptosis signal-regulating kinase 1
BCR	B cell receptor
BSA	bovine serum albumin
Ca^{2+}	calcium
CAR	chimeric antigen receptor
CD	cluster of differentiation
c-FLIP	cellular FLICE inhibitory protein
CFSE	carboxyfluorescein succinimidyl ester
ChIP	chromatin immunoprecipitation
ChoRE	carbohydrate response elements
ChREBP	carbohydrate response element binding protein
CHX	cycloheximide
Co-IP	protein complex immunoprecipitation
Cys	cysteine
DAG	diacylglycerol
DC	dendritic cell
DcR	decoy receptor
DD	death domain
DED	death effector domain
DISC	death-inducing signalling complex
DMSO	dimethyl sulfoxide
dNTP	deoxyribonucleotide triphosphate
DR	death receptor
EDA	ectodermal dysplasia
EDTA	ethylenediaminetetraacetic acid
EGR	early growth response
ELISA	enzyme-linked immunosorbent assay
EMSA	electrophoretic mobility shift assay
EndoG	endonuclease G
ER	endoplasmic reticulum
ETC	electron transport chain
EV	empty vector
FADD	Fas-associated death domain
Fas	first apoptosis signal

FasL	Fas ligand
FCHL	familial combined hyperlipidemia
FCS	fetal calf serum
FITC	fluorescein isothiocyanate
FLICE	FADD-like interleukin-1β-converting enzyme
FOXO1	forkhead box protein O1
gld	generalised lymphoproliferative disease
GLUT1	glucose transporter type 1
GMCSF	granulocyte macrophage colony stimulating factor
GPx	glutathione peroxidase
Grx	glutaredoxin
gRNA	guideRNA
GSH	glutathione
GSSG	glutathione disulfide
GZMB	granzyme B
h	hour(s)
H_2DCFDA	2'-7'-dichlorodihydrofluorescein diacetate
H_2O_2	hydrogen peroxide
HAT	histone acetyltransferase
HDAC	histone deacetylase
HRP	horseradish peroxidase
HtrA2/Omi	high-temperature requirement A2/Omi
IAP	inhibitor of apoptosis protein
ICAD	inhibitor of caspase-activated DNase
IFNG	Interferon gamma
Iono	ionomycin
IKK	inhibitor of NFκB kinase
IκBα	inhibitor of NFκB α
IL	interleukin
IP_3	inositol-1,4,5-trisphosphate
ITAM	immunoreceptor tyrosine-based activation motif
KO	knockout
LAT	linker for activation of T cells
LB	lysogeny broth
LC	clasto-Lactacystin β-lactone
Lck	leukocyte-specific protein tyrosine kinase
lpr	lymphoproliferation
MAPK	mitogen-activated protein kinase
MFI	mean fluorescence intensity
$MgCl_2$	magnesium chloride
MHC	major histocompatibility complex
min	minutes
Mlx	Max-like protein X
NAC	N-acetyl-cysteine
NFAT	nuclear factor of activated T cells
NFκB	nuclear factor kappa-light-chain-enhancer of activated B cells
NF-Y	nuclear factor Y
NGF	nerve growth factor
OPG	osteoprotegerin

PAMP	pathogen associated molecular pattern
PBLs	peripheral blood leukocytes
PBS	phosphate buffered saline
PCR	polymerase chain reaction
PHA	phytohemagglutinin
PI3K	phosphatidylinositol 3 kinase
PIP_2	phosphatidylinositol-4,5-bisphosphate
PKCθ	protein kinase Cθ
PLCγ1	phospholipase Cγ1
PMA	phorbol 12-myristate-13-acetate
PRR	pattern recognition receptor
PTP	protein tyrosine phosphatases
qRT-PCR	quantitative Real Time-PCR
RasGRP	Ras guanyl nucleotide-releasing protein
Ref1	redox factor 1
R	receptor
RIP1	receptor-interacting protein 1
ROS	reactive oxygen species
RPMI	Roswell Park Memorial Institute
RNR	ribonucleotide reductase
RT	room temperature
RTK	receptor tyrosine kinases
RT-PCR	reverse transcription-PCR
SAHA	suberoylanilide hydroxamic acid
SDS	sodium dodecyl sulfate
SDS-PAGE	SDS-polyacrylamide gel electrophoresis
Smac/DIABLO	second mitochondria-derived activator of caspases/direct inhibitor of apoptosis protein-binding protein with low isoelectric point
SOD	superoxide dismutase
tBid	truncated Bid
TBP-2	Trx-binding protein 2
TBS	tris buffered saline
TBS-T	TBS-tween20
TCR	T cell receptor
TEMED	N,N,N',N' – tetramethylethylenediamine
TL1A	TNF-like protein 1A
TNF	tumour necrosis factor
TNFR	tumour necrosis factor receptor
TRAIL	TNF-related apoptosis inducing ligand
Trx	thioredoxin
TrxR	Trx reductase
TXNIP	thioredoxin-interacting protein
U/ml	units per ml
VDUP1	vitamin D_3 upregulated protein 1
WT	wild type
ZAP70	ζ-chain associated protein kinase of 70 kDa

1 Introduction

1.1 The immune system

The immune system protects the human body against *e.g.* invading pathogens or transformed cells. Thus, the main task is the discrimination between self and non-self structures termed antigens. Classically, the immune system can be divided into two major subsystems: the innate and the adaptive immunity. Despite these subsystems utilise different underlying defence strategies, during an immune response they act in concert [1].

1.1.1 Innate immunity

The evolutionary well conserved innate immune system represents the first line of defence and can be sufficient for the elimination of an infection. Innate immunity is based on the recognition of conserved pathogen structures termed pathogen associated molecular patterns (PAMPs) by a specific set of pattern recognition receptors (PRRs). The detection of common patterns enables the innate immune system to respond quickly to a variety of pathogens regardless of their unique antigens. Macrophages, mast cells, granulocytes, natural killer cells and dendritic cells (DCs) are cells of the innate immune system. They have different functions *e.g.* phagocytosis and lysis of pathogens as well as infected cells and can activate the adaptive immune system by presenting antigens [2].

1.1.2 Adaptive Immunity

The adaptive immune system consists of T and B lymphocytes and, in contrast to the innate immune system, is characterised by antigen-specific immune responses. Each lymphocyte responds to a particular antigenic structure recognised by its specific TCR and B cell receptor (BCR). The surface receptors of B lymphocytes bind to native antigens whereas TCRs recognise only antigens that are processed and loaded onto major histocompatibility complexes (MHC) on antigen presenting cells (APCs) [3].

The thymus is the major central lymphoid organ for the development of T cells [4, 5]. T lymphocytes arise from bone marrow-derived lymphoid precursor cells which migrate to the thymus to undergo maturation [6]. In the course of T cell development, genes encoding the TCR are rearranged *via* somatic recombination [3, 7]. This process generates a diverse TCR repertoire with unique specificities ensuring a response against a wide variety of antigens. However, these randomly produced TCRs can also recognise self-antigens. Such self-reactive T cells must be eliminated to avoid autoimmune responses. Hence, T cell reactivity is tightly controlled by a selection process, before mature naïve T cells migrate to peripheral lymphoid organs like the lymph nodes or the spleen [8, 9]. However, this central selection process in the thymus is imperfect and some self-reactive T cells escape into the periphery where they are further controlled by different mechanisms. For instance, recognition of the respective self-antigen mediates repetitive TCR stimulation resulting in the deletion of the self-reactive T cell *via* activation-induced cell death (AICD) [10, 11].

Activation of mature naive T lymphocytes requires interaction with an APC and the resulting T cell response is determined by three signals. Binding of the TCR to an antigen-loaded MHC on the surface of an APC guarantees antigen specificity and is the first signal. The second signal as referred to co-stimulation and the third signal represented by cytokines shape the phenotype of the T cell and the T cell immune response. The second and third signal can be interpreted as regulatory signals while TCR engagement and the subsequent signalling are a prerequisite to initiate a T cell response [12].

1.2 TCR signalling

TCR signalling requires the formation of a functional TCR complex including the TCR itself which is composed of an α- and β-chain and the associated CD3 complex consisting of a ζ-homodimer and two heterodimers comprising CD3δ:ε and CD3γ:ε (Figure 1.1) [13–16]. The transmembrane α- and β-chain are essential for the recognition of antigen-loaded MHC complexes but they cannot initiate further intracellular signalling due to their short cytoplasmic tails. Thus, TCR downstream signalling relies on the large cytoplasmic chains of the TCR-associated CD3 complex which have to be phosphorylated at immunoreceptor

tyrosine-based activation motifs (ITAMs) [17–20]. Following TCR stimulation, ITAM phosphorylation at the CD3 chains is caused due to the recruitment of protein tyrosine kinases Fyn and leukocyte-specific protein tyrosine kinase (Lck) [21]. Phosphorylated ITAMs serve as docking sites for kinases like the ζ-chain associated protein kinase of 70 kDa (ZAP70) [22]. Lck mediates phosphorylation of ITAM-bound ZAP70 [23] resulting in its activation and, hence, phosphorylation of substrates such as the linker for activation of T cells (LAT). Phosphorylated LAT initiates the recruitment of further adapter and signalling molecules including phospholipase Cγ1 (PLCγ1) [24, 25] which is a key molecule in TCR signalling as it mediates the hydrolysis of phosphatidylinositol-4,5-bisphosphate (PIP_2) to diacylglycerol (DAG) and inositol-1,4,5-trisphosphate (IP_3) [26]. The generation of the second messengers DAG and IP_3 separates TCR signalling into two branches. Production of IP_3 results in the opening of calcium (Ca^{2+}) channels in the endoplasmic reticulum (ER) and plasma membrane leading to a rise of the cytosolic Ca^{2+} concentration [27]. This increased Ca^{2+} level activates the phosphatase calcineurin which in turn dephosphorylates transcription factor nuclear factor of activated T cells (NFAT). Dephosphorylation uncovers a nuclear localisation sequence which facilitates nuclear translocation and, thus, NFAT-specific gene transcription [28].

PLCγ1-mediated formation of DAG induces activation of several proteins like Ras guanyl nucleotide-releasing protein (RasGRP) and the protein kinase Cθ (PKCθ). RasGRP triggers the mitogen-activated protein kinase (MAPK) signalling cascade which results in phosphorylation and nuclear translocation of activator protein 1 (AP1) [29, 30]. PKCθ activity allows degradation of the inhibitor of NFκB α (IκBα) by the inhibitor of NFκB kinase (IKK) complex which finally leads to translocation of nuclear factor kappa-light-chain-enhancer of activated B cells (NFκB) to the nucleus [31]. Moreover, it has been reported that PKCθ translocates to mitochondria where it triggers the formation of the second messenger hydrogen peroxide (H_2O_2). Mitochondria-derived H_2O_2 further promotes activation of AP1 and NFκB [32, 33].

Conclusively, stimulation of the TCR results in the concerted induction of multiple signalling pathways converging at the activation of the three major transcription factors: NFAT, AP1 and NFκB. Regulation of a T cell immune response following TCR stimulation relies on the tight control of gene expression mediated by the balanced activation of these transcription factors [34–36].

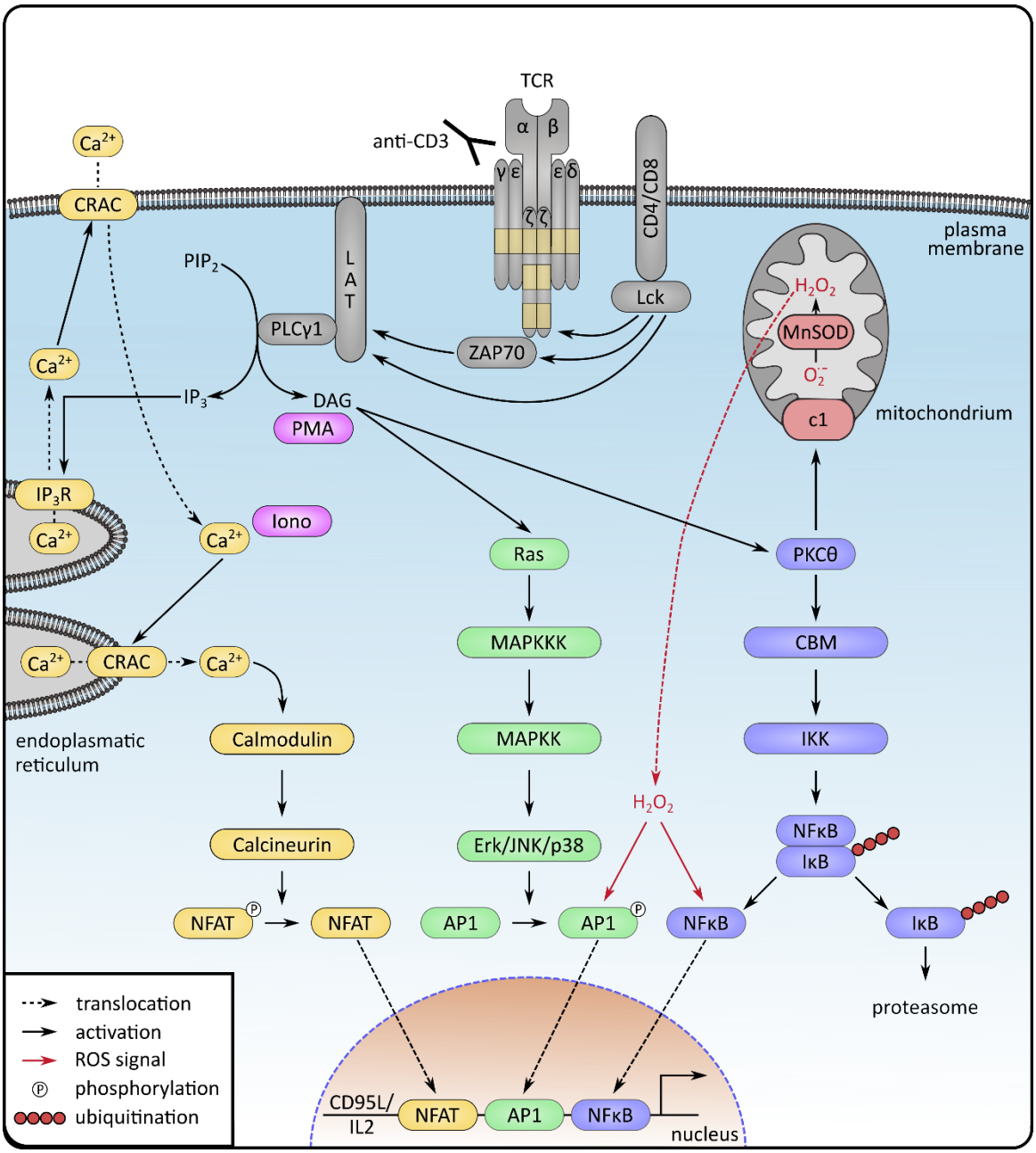

Figure 1.1: TCR signalling.
Stimulation of the TCR activates the proximal TCR signalling machinery (grey) resulting in the generation of DAG and IP_3. IP_3 induces a rise of intracellular Ca^{2+} leading to NFAT activation (yellow), while DAG mediates activation of AP1 (green) and NFκB (blue). In parallel, production of mitochondrial-derived ROS, especially H_2O_2, amplifies activation of NFκB and AP1. See text for details. Modified from: [37]. CRAC - Ca^{2+} release activated channels, IP_3R - IP_3 receptor, CBM complex - a protein complex comprising Carma1, Bcl10 and MALT1, c1 -respiratory complex I, $O_2^{\cdot-}$ - superoxide anion

1.2.1 *In vitro* TCR stimulation

Stimulation of the TCR can be mimicked *in vitro* by utilising one of two different techniques (Figure 1.1). The commonly used pharmacological way of imitated TCR stimulation includes the simultaneous treatment with phorbol-12-myristate-13-acetate (PMA) and ionomycin (Iono). PMA, a DAG mimetic, initiates the activation of PKCθ and RasGRP, whereas Iono, a calcium ionophore, replaces IP_3 resulting in a rise of cytosolic Ca^{2+} concentration [38]. Alternatively, stimulation of the TCR can be achieved by the use of crosslinked or plate-bound agonistic anti-CD3 antibodies [39]. Although both techniques result in T cell activation, it should be noted that PMA/Iono bypasses the TCR whereas CD3 stimulation uses the proximal TCR-mediated signalling machinery.

1.2.2 Oxidative signalling in T cells

The term ROS comprises highly reactive molecules like superoxide anions and H_2O_2. ROS arise as a byproduct of cellular metabolism and have long been considered to exert toxic effects including the damage of lipids, DNA or proteins. However, in the past decades evidence accumulated that ROS play a key role as second messengers in many physiologic processes *e.g.* TCR signalling. Since H_2O_2, in comparison to other ROS molecules, is a mild oxidant, electrically neutral, exhibits an enhanced half-life and can easily diffuse through membranes, it is the major contributor of oxidative signalling [40, 41]. H_2O_2-mediated signalling relies on the oxidation of proteins containing cysteine (Cys) residues resulting in modification of their structure and function. In general, oxidation of Cys residues is reversible and reduction is mediated by the action of cellular reductants such as thioredoxin (Trx) and glutathione which are mandatory for the maintenance of redox homeostasis [42, 43]. For further details about the generation and regulation of ROS see chapter 1.4.

1.2.2.1. Generation of the TCR-derived oxidative signal

TCR engagement is accompanied by transient production of low levels of ROS, especially superoxide anions and H_2O_2 [41, 44]. The generation of these second messengers represents a major hallmark of TCR signalling since antioxidant treatment can abrogate T cell differentiation, proliferation as well as AICD [45–48]. Despite the fact that various sources were reported to be involved in TCR-mediated ROS generation including the

mitochondrial electron transport chain [33, 49], 5-lipoxygenase [50] and NAPDH oxidases [51, 52], mitochondria were recently identified as the main source of ROS involved in AICD [33]. Mitochondrial ROS production is induced by PKCθ-mediated activation of the alternative, glycolytic enzyme ADP-dependent glucokinase (ADPGK) which results in a functional change of the mitochondrial respiratory chain and the release of superoxide anions primarily at complex I [53]. In addition, TCR-induced mitochondrial fission is required for ROS release [54]. The mitochondrial manganese superoxide dismutase (MnSOD, also known as SOD2) especially contributes to the rapid dismutation of complex I-produced superoxide anions into H_2O_2 [33, 53]. Thereupon, H_2O_2 diffuses into the cytoplasm where it acts on various redox-sensitive proteins of the TCR signalling cascade [53, 55].

1.2.2.2. Influence of oxidative signals on TCR signalling

Phosphorylation of proteins is an important post-translational modification [56] and plays a key role in the regulation of protein functions as well as signal transduction during TCR signalling. Protein phosphorylation is controlled by protein tyrosine phosphatases (PTPs) as well as receptor tyrosine kinases (RTKs). Due to the presence of oxidation-sensitive Cys residues in their active centre, PTPs represent a well-known target of redox regulation [43]. H_2O_2-dependent oxidation and, thus, inactivation of PTPs results in increased and sustained protein phosphorylation by PTKs [41, 57, 58]. Since TCR signalling is based on multiple phosphorylations, oxidation-dependent changes in PTP activity are crucial for T cell stimulation.

1.2.2.3. NFκB

NFκB is a major regulator of gene expression and amongst others involved in the transcriptional response during T cell activation, proliferation as well as cell death [59, 60]. NFκB represents a family of transcription factors which consists of five proteins including RelA (p65), RelB, cRel, p50 and p52. The NFκB subunits form both homo- as well as heterodimers while the p50/p65 heterodimer is commonly referred to as NFκB. In resting cells, NFκB is sequestered in the cytoplasm by IκB. Signal-induced IκB phosphorylation and proteasomal degradation allows the release and subsequent nuclear translocation of NFκB. In the nucleus, various posttranslational modifications of NFκB as well as chromatin

remodelling of target genes are mandatory for NFκB DNA binding and full transcription [61, 62]. Over the last decades, the redox status of cells has been implicated in NFκB activation. In the cytoplasm, ROS-mediated oxidation processes enhance the signalling pathway resulting in NFκB nuclear translocation. In contrast, in the nucleus reducing conditions regulate NFκB DNA binding and transcriptional activity [63]. The redox regulator Trx is considered to be the specific reductant which promotes NFκB DNA binding activity by reduction of a Cys residue within the DNA binding domain of the p50 subunit [64–67]. Although NFκB activity does not generally depend on redox regulation, antioxidant treatment demonstrated a major role of ROS in NFκB regulation specifically in T cells [40, 68, 69].

1.2.2.4. AP1

Similar to NFκB, AP1 is a redox-sensitive transcription factor [70] and implicated in the transcriptional regulation following TCR stimulation [71]. AP1 proteins are homo- or heterodimers composed of Jun, Fos, JDP, ATF and Maf subunits which bind to a common DNA element termed AP1-binding site [72]. Activation of AP1 is amongst others controlled at the level of transcription and by posttranslational modifications such as phosphorylation [73, 74] which are mainly regulated by redox-mediated inhibition of MAPK-specific phosphatases resulting in the increased activity of MAPK signalling cascades [75]. In addition, AP1 harbours a conserved Cys residue situated in the DNA binding domain which is reduced by redox factor 1 (Ref1) and Trx to potentiate DNA binding activity of AP1 in the nucleus [70, 76, 77].

1.2.3 TCR stimulation and restimulation

TCR signalling can result in proliferation as well as in cell death. Which path is taken following TCR engagement mainly depends on the activation status of the T cell as well as the costimulatory environment. Upon first antigen exposure, T cells differentiate and proliferate while showing an apoptosis-resistant phenotype (Figure 1.2). However, these activated T cells become sensitive to apoptosis in later stages of an immune response. Thus, repeated antigen encounter and consequently TCR restimulation results in CD95L-mediated AICD [78].

These contradictory results of TCR stimulation are also reflected in a dual function of the cytokine interleukin 2 (IL2). During the clonal expansion and effector phase of a T cell immune response IL2 serves as essential growth and survival factor while in the contraction phase IL2 is contributing to T cell apoptosis. It was suggested that IL2 sensitises T cells to AICD by enhancing CD95L expression and/or by reducing the expression of anti-apoptotic proteins [79–82]. CD95L-mediated AICD is in detail explained in section 1.3.4.

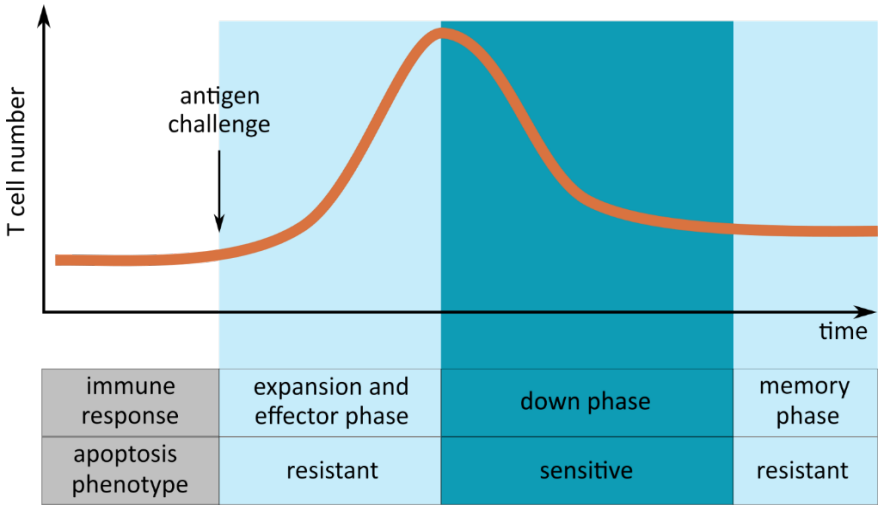

Figure 1.2: Time course of a T cell immune response and apoptotic phenotypes of T cells.
Upon antigen challenge, naïve T cells expand, differentiate and exhibit an apoptosis-resistant phenotype. Over time, activated T cells shift towards an apoptosis-sensitive phenotype and induction of apoptosis mediates termination of an acquired immune response. However, some antigen-specific T cells survive and differentiate into apoptosis-resistant memory T cells. See text for details. Modified from: [78].

1.3 Apoptosis

In multicellular organisms regulated elimination of cells is a necessity for development, homeostasis as well as aging. A number of morphologically and functionally distinguishable types of cell death have been identified *e.g.* apoptosis, necrosis, necroptosis, macroautophagy and pyroptosis [83–87].

Apoptosis is an active and genetically defined process of cell death which mediates removal of *e.g.* redundant, aged, infected, mutated or damaged cells. It is characterised by various morphological and biochemical features including nuclear condensation, DNA fragmentation, cytoplasmic shrinkage and plasma membrane blebbing. In the course of apoptotic cellular dismantling, plasma membrane integrity is maintained and prevents leakage of intracellular content which could elicited an inflammatory immune response. Therefore, apoptosis is in general a non-immunogenic process [88–90].

1.3.1 Apoptosis in homeostasis and pathophysiology

During its whole life span, the human body undergoes continuous inner renewal. Daily, billions of cells die in the course of natural cell turnover which is based on two substantial features: cell division and cell death. In this context, cells are generally eliminated by apoptosis to ensure an efficient and immediate removal of cells which is essential for the maintenance of tissue functions and, hence, a healthy organism [91, 92].

Since the immune system arises by an excess production of cells, apoptosis represents a keyregulatory mechanism for cellular homeostasis and prevention of autoimmunity. During development in the thymus, approximately 97 % of the T cell precursors die by apoptosis due to the generation of non-functional TCRs or TCRs responding to self-antigens [93, 94]. In addition, apoptotic cell demise is essential to restrict self-reactive T cells in the periphery as well as to remove clonally expanded T cells after an immune response. Thus, T cell apoptosis is mandatory for the maintenance of central and peripheral tolerance as well as T cell homeostasis [95, 96].

The importance of apoptosis is further emphasised by different pathologies associated with either insufficient or enhanced cell death. On the one hand, inadequate cell demise can cause abnormalities such as cancer or autoimmunity. Cancer is accompanied with an imbalanced cell growth due to increased proliferation or resistance to apoptosis [97]. In autoimmune diseases, self-reactive T cells fail to undergo apoptosis and, hence, can cause tissue damage as seen in type 1 diabetes, systemic lupus erythematosus or rheumatoid arthritis [98, 99]. On the other hand, many diseases like neurodegenerative disorders and AIDS are caused by an excess of apoptosis [97]. HIV infections are characterised by a virus-induced depletion of T cells resulting in an impaired immune defence termed AIDS and infected individuals finally die due to opportunistic infections or cancer [100–102]. A better understanding of the apoptotic signalling cascades and, thus, the molecular mechanisms underlying apoptotic resistance or sensitivity is important to develop new therapeutic approaches for apoptosis-related diseases.

1.3.2 Apoptotic signalling pathways

Apoptosis is initiated and executed by the action of Cys-dependent aspartate-specific proteases termed caspases. Caspases are synthesised as inactive precursors (pro-

caspases) and become active by proteolytic cleavage by a protease or autocatalysis. On the basis of their features in the apoptotic process, caspases can be subdivided into two classes: initiator caspases (*e.g.* caspase-8/9/10) and effector caspases (*e.g.* caspase-3/6/7). Death signals mediate the induction of initiator caspases which in turn proteolytically activate effector caspases. The latter degrade a broad spectrum of proteins including cytoskeletal components resulting in cell shrinkage, nuclear condensation and membrane blebbing. In addition, degradation of the inhibitor of caspase-activated DNase (ICAD) by effector caspases leads to CAD nuclear translocation which mediates DNA fragmentation [103–105].

Two signalling pathways initiate apoptosis: the intrinsic pathway which is triggered by various environmental stressors and the extrinsic pathway which is induced by binding of death ligands to their respective cell surface receptors (Figure 1.3). Although each signalling pathway utilises distinct molecules, they are linked and can influence each other at multiple levels [106].

1.3.2.1. Mitochondria and cell death – the intrinsic pathway

The mitochondria-dependent intrinsic apoptotic pathway is triggered by various environmental stressors such as growth factor deprivation, radiation, viral infections or oxidative stress (Figure 1.3) [88, 107]. These stress-induced signals mediate permeabilisation of mitochondrial membranes resulting in the release of cytochrome c into the cytosol [108]. Subsequently, cytochrome c binds the cytosolic adaptor protein apoptotic protease activating factor-1 (Apaf-1) in an ATP-dependent manner and facilitates its oligomerisation. The complex of cytochrome c and Apaf-1 is termed apoptosome and forms a platform for the recruitment and processing of procaspase-9 into its active form. Finally, caspase-9 triggers activation of downstream effector caspases caspase-3/6/7 and, thus, execution of apoptosis [107, 109, 110].

Bcl-2 proteins are major regulators of the mitochondrial events of the intrinsic apoptotic pathway. The mammalian Bcl-2 protein family consists of more than 20 proteins including members with anti-apoptotic functions *e.g.* Bcl-2, Bcl-x_L and Mcl-1 as well as pro-apoptotic functions *e.g.* Bax, Bak, Bid and Bim. The initiation of the mitochondrial pathway is regulated by the ratio of anti- and pro-apoptotic Bcl-2 proteins [107].

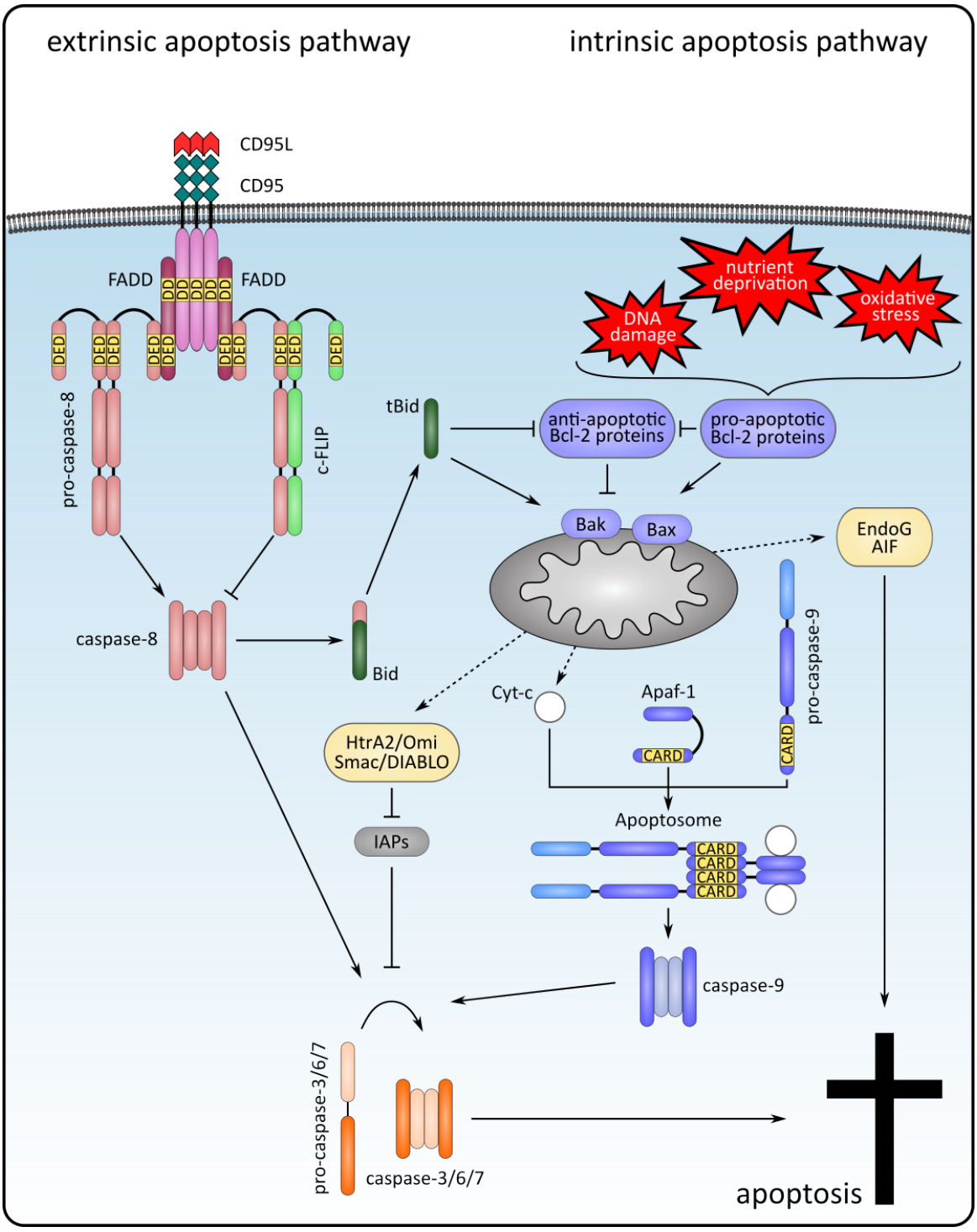

Figure 1.3: Pathways of apoptosis.
Apoptosis is mediated by two pathways: the extrinsic pathway which is initiated upon binding of death ligands to death receptors or the intrinsic pathway which is induced by a Bcl-2 family member-regulated permeabilisation of mitochondrial membranes in response to variety of stress stimuli. Both pathways are based on different core signalling machineries, however, they ultimately result in the activation of caspases which are essential for the initiation and execution of apoptosis. See text for details. Modified from: [111].

Besides cytochrome c, further pro-apoptotic proteins such as second mitochondria-derived activator of caspases/direct inhibitor of apoptosis protein-binding protein with low isoelectric point (Smac/DIABLO), high-temperature requirement A2/Omi (HtrA2/Omi), apoptosis inducing factor (AIF) and Endonuclease G (EndoG) are kept enclosed in the mitochondria and are released into the cytosol upon its permeabilisation. Cytosolic Smac/DIABLO as well as HtrA2/Omi antagonise inhibitor of apoptosis proteins (IAPs) which inhibit the function of caspases and the ripoptosome, a signalling platform triggering cell death [112–114]. Furthermore, HtrA2/Omi is able to initiate caspase-independent apoptosis due to its serine protease activity [110, 114]. Following release from the mitochondria, AIF and EndoG translocate into the nucleus. Nuclear flavoprotein AIF triggers chromatin condensation [115] whereas EndoG, a sequence-unspecific DNAse, mediates DNA degradation [110, 116].

1.3.2.2. Death receptor-induced apoptosis – the extrinsic pathway

The extrinsic pathway is governed by various death receptors (DRs) which act as cell surface sensors for extracellular death ligands. DRs are a subgroup of the tumour necrosis factor receptor (TNFR) superfamily and possess a type I transmembrane structure as well as Cys-rich extracellular domains. Moreover, they contain a cytoplasmic motif termed death domain (DD) which is essential for signal transduction and, thus, for induction of apoptosis [117, 118]. Hitherto, eight human DRs have been described: first apoptosis signal (Fas, also known as CD95, apoptosis antigen-1 (APO-1) or DR2, [119–121]), TNFR1 (DR1, CD120a), DR3 (APO-3), TNF-related apoptosis inducing ligand (TRAIL)-R1 (DR4, APO-2), TRAIL-R2 (DR5), DR6, nerve growth factor (NGF)-R and ectodermal dysplasia (EDA)-R [122, 123]. In addition, another subgroup belonging to the TNFR superfamily and consisting of four decoy receptors (DcRs) named osteoprotegerin (OPG), DcR1 (TRAIL-R3), DcR2 (TRAIL-R4) and DcR3 has been identified [124]. The DcRs can bind to death ligands but in contrast to the DRs, they cannot transduce the signal into the cell due to the absence of the DD. Therefore, it is suggested that the DcRs compete with DRs for ligands and, hence, rather inhibit apoptosis [124, 125].

Death ligands are type II transmembrane proteins and belong to the TNF ligand superfamily [126]. So far, the following ligands have been identified: Fas ligand (FasL, CD95L, APO-1L) which binds to Fas and DcR3, TNFα the cognate ligand of TNF-R1, TNF-like

protein 1A (TL1A) that binds to DR3 and DcR3 and lastly TRAIL (APO-2L) which is the cognate ligand to TRAIL-R1 and TRAIL-R2 as well as to the DcRs TRAIL-R3, TRAIL-R4 and OPG [127–131]. Besides the membrane-bound form also soluble types of death ligands have been reported. These soluble ligands arise through cleavage by specific metalloproteases [132–134].

Signal transduction of DR-death ligand complexes into the cell relies on the formation of a multimeric protein complexes termed death-inducing signalling complex (DISC) [135]. As shown in Figure 1.3, the CD95-DISC is composed of oligomerised receptors, the adapter protein Fas-associated death domain (FADD, also known as MORT-1) and pro-caspase-8 (FADD-like interleukin-1β-converting enzyme (FLICE), MACH) [136–138]. Recruitment of the individual components to the CD95-DISC is mediated by homotypic interactions between the DD of CD95 and FADD as well as between the death effector domain (DED) of FADD and procapsaes-8 [135, 137, 138]. Activation of procaspase-8 at the DISC dependents on high local concentrations of procaspase-8 which facilitates cleavage in an autocatalytic manner [139, 140]. Active caspase-8 is a heterotetramer composed of two large (p18) and two small (p10) subunits [138, 141] which in turn activates effector caspases resulting in apoptosis execution [128].

On the basis of the quantity of active caspase-8 generated at the CD95-DISC, two different cell types can be distinguished. Type I cells exhibit sufficient amounts of caspase-8 to directly induce apoptosis, while apoptosis of type II cells depends on amplification by the mitochondrial pathway due to reduced DISC formation. In type II cells, caspase-8-mediated cleavage of Bid to truncated Bid (tBid) triggers permeabilisation of mitochondria membranes and, thus, apoptosome formation [78, 142–144].

DR-mediated apoptosis is tightly controlled. At the CD95-DISC level, the major regulator is cellular FLICE inhibitory protein (c-FLIP). Hitherto, three isoforms of c-FLIP were identified at the protein level: c-FLIP$_S$ (short), c-FLIP$_L$ (long) and c-FLIP$_R$ (Raji). While c-FLIP$_S$ as well as c-FLIP$_R$ exhibit anti-apoptotic functions by blocking recruitment and, hence, activation of caspase-8, the role of c-FLIP$_L$ is ambivalent as pro- or anti-apoptotic functions have been reported [145–148].

However, formation of the DISC does not necessarily lead to apoptosis since the outcome of DR engagement depends on the molecules involved in DISC assembly. For instance, TNFα, a critical regulator of inflammation, mediates an alternative signalling cascade by

the recruitment of receptor-interacting protein 1 (RIP1) which activates NFκB and finally results in survival [149, 150].

1.3.3 The CD95/CD95L system

The CD95/CD95L system plays a major role in the regulation of immune responses by mediating deletion of activated T cells [95, 151] and by contributing to the elimination of self-reactive T cells in the periphery [10, 11]. In both scenarios, TCR restimulation initiates CD95L transcription which results in AICD. Moreover, CD95L-mediated apoptosis plays an important role in the removal of virus-infected or cancer cells by cytotoxic T cells [78, 124]. The receptor CD95 is expressed in almost all tissues whereby especially activated T cells exhibit high expression levels [78, 152]. In contrast, the expression of the ligand CD95L is restricted to activated natural killer cells as well as to activated T cells [153–155]. However, constitutive expression of CD95L contributes to the protection of immune privileged tissues like testis or brain from invading, activated immune cells and, thus, inflammation [156–158].

The physiological importance of the CD95/CD95L system is illustrated by the fact that mutation in CD95 or CD95L are associated with diseases in mice and humans. Mice bearing the homozygous *lpr/lpr* (lymphoproliferation) allele have a mutation in the *cd95* gene. The *lpr* mutation is caused by an insertion of an early transposable element into an intron of the cd95 gene which results in premature termination and aberrant splicing of the CD95 mRNA transcript. However, *lpr* mice still express a small amount of wild type CD95 mRNA and protein [159–162]. Mice homozygous for *gld* (generalised lymphoproliferative disease) carry a point mutation in the cd95l gene resulting in the expression of a dysfunctional CD95L [162–164]. Both mice strains develop lymphadenopathy as well as splenomegaly and suffer from autoimmune disorder syndromes caused by accumulation of peripheral lymphocytes due to impaired AICD [162, 164, 165]. In humans, mutations in the CD95 or CD95L gene cause an autoimmune disorder termed autoimmune lymphoproliferative syndrome (ALPS). ALPS patients exhibit first signs of autoimmunity during childhood (Canal Smith syndrome) and have an enhanced risk to develop lymphomas [166, 167].

1.3.4 CD95L-mediated AICD

Induction of apoptosis is an essential regulatory mechanism for the termination of an acquired immune response and, thus, for the maintenance of T cell homeostasis. The time course of a T cell immune response is characterised by different phases (Figure 1.2). Upon first antigen contact, T cells proliferate and differentiate while showing an apoptosis-resistant phenotype. However, over time these activated T cells become sensitive to apoptosis and at the end of an immune response the majority of T cells die *via* apoptosis. Only few T cells survive and differentiate into memory T cells which can expand quickly when reencountering their respective antigen [78]. Two apoptotic pathways trigger the elimination of T cells after an immune response: activated cell autonomous death (ACAD) and AICD. ACAD is initiated by deprivation of survival factors *e.g.* IL2 which in turn activates Bim leading to induction of the intrinsic apoptotic signalling pathway. AICD is mediated by TCR restimulation resulting in the expression of CD95L and subsequent activation of the extrinsic apoptosis pathway. Both apoptosis types have different roles in T cell elimination. ACAD is associated with the termination of an acute immune response. In this scenario, antigen concentrations are low and levels of survival factors are reduced. Impaired elimination of a trigger of an immune response remains antigen levels high resulting in TCR restimulation and, hence, AICD which increases the risk of a chronic inflammation [95, 151, 168, 169].

During T cell development in the thymus, reactivity of T cells is tightly controlled by a selection process which ensures elimination of self-reactive T cells. However, this central selection process is imperfect and some self-reactive T cells escape into the periphery where they are further controlled by different mechanisms. Recognition of self-antigens by peripheral self-reactive T cells leads to repetitive TCR stimulation resulting in AICD. Thus, AICD is one important mechanism maintaining peripheral tolerance and preventing autoimmune diseases [10, 11].

A number of studies demonstrate that CD95L-mediated AICD affects the efficiency of anti-tumour immune responses. AICD-mediated deletion of tumour-specific T cells by repetitive TCR stimulation due to high concentrations of tumour antigens or upon immunotherapy facilitates tumour growth. The underlying mechanism contributing to treatment-induced AICD of tumour-specific T cells are not well understood but the extent of tumour burden may play a decisive role [170–173].

Chimeric antigen receptor (CAR) T cells are genetically engineered T cells which produce an artificial TCR recognising tumour antigens and one approach utilised as cancer immunotherapy. Antigen recognition *via* hyperactive CARs results in repetitive stimulation which induces CD95L expression leading to AICD-mediated deletion of CAR T cells [174]. Hence, a thorough selection of CAR constructs with moderate rather than high reactivity increases anti-tumour potency. A better understanding of the molecular mechanism regulating CD95L-mediated AICD is important to tailor T cell immune responses in terms of preventing autoimmunity or to enhance the efficacy of T cell-mediated anti-tumour responses.

1.3.4.1. In vitro model for CD95L-mediated AICD

For the analysis of CD95L-mediated AICD, an *in vitro* model has been established. Freshly isolated resting primary human T cells ("day 0" T cells, apoptosis-resistant) are incubated and, thereby, activated with phytohemagglutinin (PHA) overnight ("day 1" T cells). Subsequently, "day 1" T cells are cultured in the presence of IL2 for additional five days, resulting in T cells ("day 6" cells) exhibiting an apoptosis-sensitive phenotype and, hence, representing T cells in the deletion phase of an immune response [132].

1.4 ROS

ROS is a term summarising molecules more reactive than molecular oxygen itself including radicals such as hydroxyl radical and superoxide anions as well as non-radical derivatives like H_2O_2. ROS are produced as a byproduct of cellular metabolism and have the potential to exert toxic effects resulting in the damage of lipids, DNA or proteins. The harmful features of ROS are connected to various pathologic conditions such as cancer, neurodegenerative disorders and chronic inflammation. These diseases exhibit an impaired redox homeostasis and consequently increased generation of ROS. The imbalance between ROS production and detoxification is designated as oxidative stress. In contrast to their potentially harmful characteristics, ROS play a key role in signal transduction and function as second messengers in many physiologic processes. In this context, ROS production is tightly regulated [175].

1.4.1 Cellular sources of ROS

In general, ROS are produced by the reduction of oxygen to superoxide anions. This reaction is catalysed by several cellular enzymes *e.g.* xanthine oxidases [176], NADPH oxidases [177–179], cytochrome p450 [180] or peroxisomal enzymes [181]. In addition, superoxide anions arise as byproducts of aerobic metabolism during ATP-generating oxidative phosphorylation in the mitochondria. During oxidative phosphorylation a proton gradient across the inner mitochondrial membrane is induced by pumping protons through complexes of the electron transport chain (ETC) into the intermembrane space. The flow of protons along their concentration gradient back to the mitochondrial matrix fuels the ATP synthase. The energy for the generation of the proton gradient is provided by an electron flux through the ETC which comprises complex I to IV well as the small electron carriers cytochrome c and ubiquinone. Electrons enter the ETC either at complex I (NADH dehydrogenase) by oxidation of NADH or at complex II (succinate dehydrogenase) by oxidation of $FADH_2$. These electrons are then passed *via* ubiquinone to complex III (ubiquinol:cytochrome c oxidoreductase) which reduces cytochrome c. In the last step at complex IV (cytochrome c oxidase), electrons are transferred to molecular oxygen which is reduced to water [175, 182]. Studies suggested that during this process 1 – 3 % of the reduced oxygen is released in form of superoxide anions [183–185]. Production of superoxide anions primarily occurs at complex I which releases electrons into the matrix as well as complex III which either reduce oxygen in the matrix or in the intermembrane space [184, 186].

Besides uncontrolled generation of ROS as metabolic byproducts, mitochondria function as oxidative signalling organelles which produce ROS upon T cell activation. TCR-induced metabolic reprogramming is accompanied with downregulation of the mitochondrial oxygen consumption as well as a shift of glycolysis towards the mitochondrial glycerol-3-phosphate dehydrogenase (GPD) shuttle which results in the release of ROS at complex I of the ETC. This complex I-mediated ROS release is based on hyperreduction of ubiquinone and primarily induces generation of superoxide anion [53]. However, additional ROS production at complex III could not be excluded [53, 187].

Superoxide anions are the precursors of the majority of ROS and exhibit an extremely short half-life. Upon generation, superoxide anions are rapidly converted to H_2O_2 and molecular oxygen either spontaneously by contact with protons or by the enzyme

superoxide dismutases (SODs) [188]. H_2O_2 is the major contributor of oxidative damage as well as oxidative signalling. In comparison to other ROS molecules, H_2O_2 is a mild oxidant, electrically neutral, exhibits an enhanced half-life and can easily diffuse through membranes [41]. Despite its low reaction capacity, H_2O_2 can be converted into highly reactive hydroxyl radicals in the presence of reduced transition metals like iron and copper (Fenton reaction). Hence, accumulation of H_2O_2 and subsequent collateral damage is actively prevented by various antioxidant enzymes and systems [175].

1.4.2 Maintenance of cellular redox balance

Maintenance of cellular redox homeostasis relies on effective detoxification of ROS. Catalase, an enzyme which is primarily located in peroxisomes, catalyses the dismutation of H_2O_2 to water and oxygen at a very fast rate. However, due to its spatial restrictions, catalase can only convert limited amounts of H_2O_2 [189]. Therefore, further systems need to be involved in counteracting H_2O_2-induced protein oxidation. The reducing capacity of the two key antioxidant systems, namely the glutathione and the Trx system, is mandatory for various cellular redox processes. The functionality of these systems is based on two essential features. Firstly, the main components harbour Cys residues and, thus, two thiol groups in their active centre. Secondly, both systems use NADPH as electron donor [190]. The glutathione system is the major intracellular redox buffer system. Glutathione is a tripeptide composed of the amino acids glycine, Cys and glutamate which predominantly exists in its reduced form (GSH). Glutathione peroxidase (GPx) as well as Glutaredoxin (Grx) catalyse the reduction of ROS or oxidised molecules by using GSH as a substrate resulting in the formation of glutathione disulfide (GSSG) [191, 192]. Thereupon, GSH reductase mediates reduction of GSSG to GSH and, hence, restores the cellular pool of GSH [191].

1.4.3 The Trx system

Besides the glutathione system, the Trx system is another ubiquitously expressed NAPDH-dependent protein disulfide reductase system and therefore, a key player maintaining intracellular redox balance. The Trx system is composed of the redox-active protein Trx and the flavoenzyme Trx reductase (TrxR) (Figure 1.4) [190]. The importance of the Trx

system for several cellular redox processes is underlined by the fact that Trx as well as TrxR are mandatory for embryonic development [193–195]. Trx is a thiol-disulfide oxidoreductase containing a characteristic CysXXCys motif which mediates the recycling of oxidised proteins (Figure 1.4) [196].

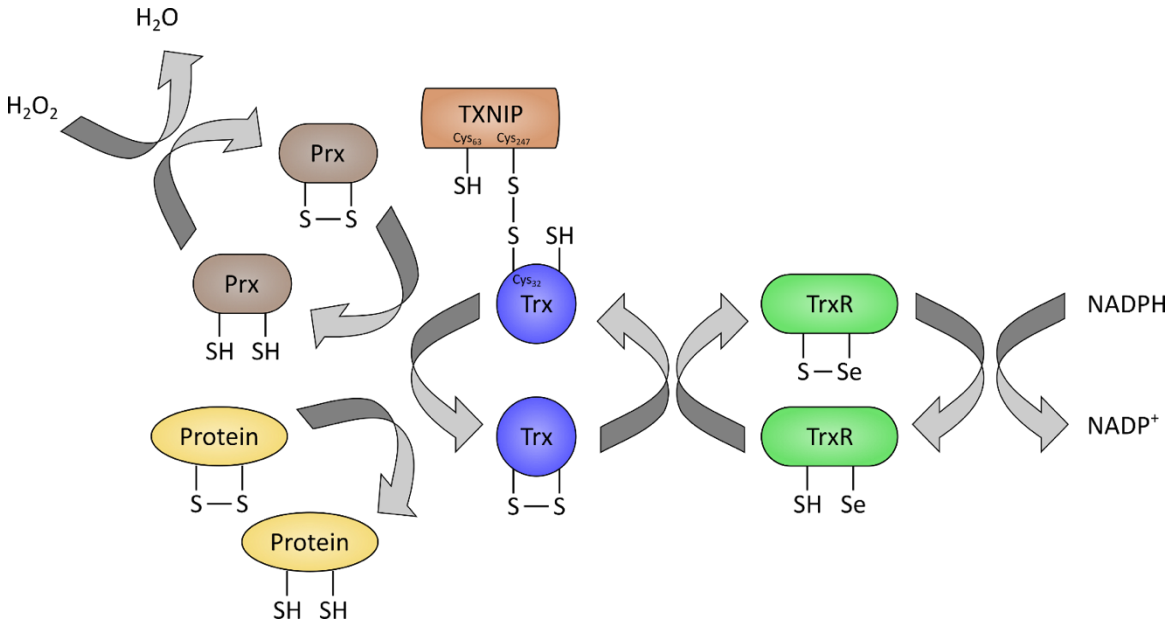

Figure 1.4: The Trx system.
Reduced Trx catalyses the reduction of cellular proteins exhibiting oxidised thiol groups by thiol-disulfide exchange resulting in the oxidation of Trx. Oxidised Trx in turn is reduced by TrxR using NADPH as an electron donor. TXNIP, a negative regulator of Trx reducing activity, contains an intramolecular disulfide which is indispensable for the formation of an intermolecular disulfide bond with reduced Trx. See text for details. Modified from: [197, 198].

Upon contact to a protein exhibiting oxidised thiol groups, Trx facilitates its reduction by thiol-disulfide exchange. The first step of this reaction is the formation of an intermolecular disulfide bond between Trx and the target protein. This initial event results in reduction of one thiol group of the substrate. Next, this unstable mixed disulfide is removed by a nucleophilic attack of the second thiol group and followed by formation of an intramolecular disulfide bond of Trx. Thus, Trx-mediated reduction of proteins results in the oxidation of Trx itself which transiently blocks its reducing function. Oxidised Trx in turn is reduced by TrxR using NADPH as an electron donor [199]. The function of Trx as an intracellular redox buffer is sustained by keeping the vast majority of Trx molecules in its reduced form [200].

The presence of three isoforms of human Trx has been reported. Trx-1, the best studied isoenzyme, is predominantly located in the cytosol and to a smaller proportion in the

nucleus [200]. However, stimulation with either UVB irradiation or vitamin D3 induces translocation of Trx1 from the cytoplasm to the nucleus [201, 202]. In comparison to Trx1, Trx2 exhibits a N-terminal mitochondrial translocation signal and, thus, is located in the mitochondria [203]. The third variant is termed SpTrx as it is highly expressed in spermatozoa [204]. Subcellular localisation of Trx1 and Trx2 requires the existence of TrxR in the respective compartment. Therefore, the cytosolic/nuclear Trx system is composed of Trx1 and TrxR1 whereas the mitochondrial system comprises Trx2 and TrxR2 [205].

Mammalian TrxRs are selenium-dependent homodimeric oxidoreductases [206]. Each monomer contains a FAD prostethic group which is important for the electron transfer from NAPDH to the substrates. Moreover, these flavoproteins exhibit two essential redox catalytic sites. One active site contains two Cys residues (CysXXXXCys motif) whereas the second active site includes one Cys as well as one selenocysteine. So far, TrxRs are the only known enzymes catalysing reduction of Trx. In addition to Trx, TrxRs reduce several other substrates like lipid hydroperoxides as well as dehydroascorbic acid indicating a broad substrate specificity which relies on the presence of the two Cys containing redox motifs [207].

The Trx system regulates a variety of cellular processes such as antioxidant response, transcription, proliferation as well as apoptosis.

Peroxiredoxins are thiol peroxidases which catalyse the removal of H_2O_2 as well as organic peroxides and, hence, contribute to the maintenance of cellular redox homeostasis. Restoration of the antioxidant function of peroxiredoxins is based on their reduction by the electron donor Trx (Figure 1.4) [208].

As mentioned in chapter 1.2.2, Trx affects gene expression and, thus, transcriptional responses. In the cytoplasm, oxidation conditions enhance signalling pathways leading to nuclear translocation of redox-dependent transcription factors like NFκB and AP1. In the nucleus, Trx promotes DNA binding activity of these transcription factors by reduction of a Cys residue within their DNA binding domain [64, 76].

Ribonucleotide reductase (RNR) catalyses the rate-limiting step of deoxyribonucleotide formation essential for DNA synthesis and repair. Both, the Trx and the glutathione system are involved in nucleotide synthesis by providing reducing equivalents to the RNR [209, 210]. However, in T lymphocytes the function of the Trx system is essential for DNA synthesis since it cannot be compensated by the glutathione system and consequently, is

indispensable for expansion of thymocytes during development as well as proliferation of T cells during immune responses [211].

Apoptosis signal-regulating kinase 1 (ASK1), a member of the MAPKKK family, is involved in various stress responses and negatively regulated by Trx. In resting cells, binding of reduced Trx to ASK1 blocks its kinase activity while stress-induced oxidation of Trx results in the release and, thus, activation of ASK1. Activated ASK1 initiates the JNK and p38 MAPK signalling cascades which control a variety of cellular functions including apoptosis [212, 213].

Due to its impact on the afore-mentioned cellular processes, the Trx system is implicated in several diseases. For instance, oxidative stress, induced by dysregulation of the Trx system, has been identified as an important causative factor for tumour development as well as initiation of neurodegenerative diseases. Moreover, enhanced Trx expression is associated with increased tumour growth and resistance to some chemotherapy treatments [214].

The activity of Trx is controlled at different levels. While diverse stress stimuli like ROS and UV irradiation mediate enhanced Trx activity by upregulation of Trx protein levels, posttranslational modifications such as thiol oxidation or inhibition of the TrxR result in suppressed Trx activity. Additionally, TXNIP can bind to the active centre of Trx and as such acts as a negative regulator that decreases the reducing activity of Trx (Figure 1.4) [214].

1.4.4 TXNIP

TXNIP is a 50 kDa protein that belongs to the α-arrestin protein family and contains a β-sheet-rich N- as well as C-terminal arrestin domain (Figure 1.5) [198, 215]. In 1994, TXNIP was originally characterised as a protein that is upregulated upon treatment with 1,25-dihydroxyvitamin D_3 ($1,25(OH)_2D_3$) in HL-60 cells and consequently termed vitamin D_3 upregulated protein 1 (VDUP1) [217]. However, the observed $1,25(OH)_2D_3$-dependent induction of TXNIP is not universally applicable since no change or even repression of TXNIP expression in response to $1,25(OH)_2D_3$ is demonstrated in different cell lines [218]. Apart from $1,25(OH)_2D_3$, expression of TXNIP can be induced by *e.g.* histone deacetylase inhibitors [219], glucose [220, 221] as well as various stress stimuli including UV light and H_2O_2 [222].

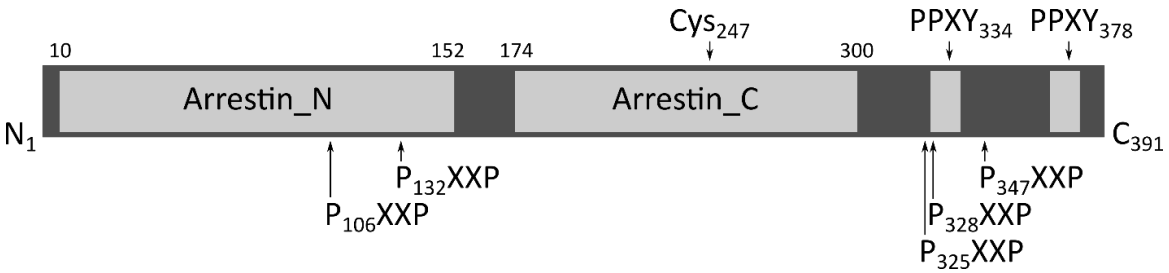

Figure 1.5: Schematic representation of the domain structure of human TXNIP.
TXNIP contains a N-terminal and a C-terminal arrestin domain as well as five PXXP motifs (SH3-binding domains) and two C-terminal PPXY motifs which are proposed to mediate protein binding and scaffold properties. Besides, Cys247 which is essential for the interaction with reduced Trx is depicted [215, 216].

In 1999, Nishiyama and co-workers discovered that TXNIP (which they referred to as Trx-binding protein 2 (TBP-2)) is an endogenous binding partner of Trx [223]. TXNIP contains an intramolecular disulfide (Cys63-Cys247) which is indispensable for the formation of a mixed disulfide with Cys32 in the catalytic centre of Trx (Figure 1.4). By blocking the redox active site of Trx, TXNIP inhibits the reducing activity of Trx [198]. Thus, TXNIP-Trx complex formation interferes with various cellular pathways regulated by Trx like antioxidant response, transcription and proliferation (described in section 1.4.3) [224]. In addition, reduced Trx activity upon TXNIP upregulation or overexpression results in a shift of the cellular redox balance to oxidation which contributes to DNA damage and aging indicating that TXNIP is a mediator of oxidative stress [221, 222, 225, 226]. Besides its role as negative regulator of Trx activity, the interaction of TXNIP with other proteins illustrates its involvement in several cellular processes such as transcription, proliferation and lipid as well as glucose metabolism.

In general, transcription is controlled by various mechanisms including reversible protein acetylation which is mediated by histone acetyltransferases (HATs) and histone deacetylases (HDACs). While gene expression is activated upon acetylation of transcription factors and/or histones, their deacetylation results in transcriptional suppression [227–229]. TXNIP is identified as a component of transcriptional corepressor complexes which associate with HDACs and inhibit NFκB-mediated gene expression. Thus, by facilitating deacetylation of NFκB, TXNIP acts as a transcriptional inhibitor [230–232].

Proliferation of cells is induced by a variety of stimuli *e.g.* growth factors and relies on cell cycle controlled by cyclins which activate cyclin-dependent kinases. TXNIP negatively

regulates cell proliferation by suppressing cyclin A promotor activity, one of the key components for mitotic cell cycle progression, by recruiting corepressor complexes [230, 233]. In addition, TXNIP mediates cell cycle arrest by blocking nuclear translocation of $p27^{kip1}$ (cyclin-dependent kinase inhibitor 1B, CDKN1B) into the cytoplasm and subsequent its proteasomal degradation. Since TXNIP regulates cell proliferation, its reduced expression in several types of tumours including renal, gastrointestinal and breast [234–236] is associated with aberrant control of the cell cycle resulting in increased proliferation. Hence, TXNIP is considered as a tumour suppressor.

Hcb-19 mouse, a model of familial combined hyperlipidemia (FCHL), exhibit alterations of the redox status *e.g.* increased $NADH/NAD^+$ ratios leading to changes in citric acid cycle and fatty acid utilisation. A TXNIP *non-sense* mutation which mediates strongly reduced TXNIP expression is identified as the causative genetic defect in Hcb-19 mouse [237, 238]. The role of TXNIP in fatty acid utilisation is validated in TXNIP KO mice which additionally show renal and hepatic dysfunction, a coagulation failure as well as dysregulation of glucose metabolism in particular enhanced glucose uptake [239–241]. The critical role of TXNIP in glucose metabolism is further illustrated by its implication in human metabolic diseases. For instance, disease progression of diabetes is associated with glucose-induced upregulation of TXNIP [221, 242]. Transcription factors involved in glucose-induced TXNIP expression include Max-like protein X (Mlx), MondoA and nuclear factor Y (NF-Y) which bind to carbohydrate response elements (ChoREs) and CCAAT motifs on the TXNIP promoter [242, 243]. In general, glucose homeostasis is regulated by three major components: the glucose transporter type 1 (GLUT1), TXNIP and the dimeric transcription factor MondoA:Mlx. Resting cells exhibit minimal metabolic activity as well as low glycolytic flux resulting in accumulation of glucose metabolites. MondoA:Mlx acts as a sensor of glucose metabolites and upon increased amounts, MondoA:Mlx is activated and initiates TXNIP expression. Increased TXNIP level in turn limits glucose uptake by facilitating internalisation of GLUT1. In contrast, proliferating cells require energy and show an increased rate of glycolysis. Enhanced glycolytic flux is accompanied by a decline of glucose metabolites which mediate dissociation of MondoA:Mlx from the TXNIP promotor resulting in reduced TXNIP transcription and in turn enhanced glucose uptake *via* GLUT1 accumulation [244–246]. The importance of TXNIP as negative regulator of glucose uptake is further underlined in T cells. Quiescent T cells cover energy

requirements *via* oxidative phosphorylation and exhibit robust TXNIP expression and low uptake of glucose. Following TCR stimulation, T cells undergo metabolic reprogramming to respond to increased energetic and biosynthetic demands of growth, proliferation, and effector function. Thus, activated T cells generate energy *via* aerobic glycolysis accompanied by enhanced glucose uptake as well as increased glycolytic flux (Warburg-like phenotype) which correlates with TXNIP suppression [247–249].

Further investigations on TXNIP KO mice reveal that TXNIP is involved in the developmental as well as functional regulation of several cell types of the immune system. TXNIP deficient mice exhibit reduced numbers as well as decreased activity of natural killer cells [250]. In addition, DCs derived from TXNIP KO mice show defective T cell activation function due to reduced cytokine secretion [251]. However, despite TXNIP deficiency did not affect T and B cell numbers as well as their development, it leads to increased proliferation of thymocytes as well as splenic T cells following stimulation [250]. Moreover, TXNIP is involved in the regulation of inflammatory responses by mediating formation of the NLRP3 inflammasome. Under conditions of oxidative stress, TXNIP dissociates from Trx which allows its binding to NLRP3 resulting in activation of the inflammasome and subsequent IL1β secretion [252].

Considering that TXNIP influences processes which play a key role in TCR signalling including redox homeostasis, gene expression, glucose metabolism as well as proliferation, TXNIP is a promising candidate to be a major regulator of T cell responses. Understanding the effect of TXNIP on TCR signalling will result in new insights which are important to shape T cell responses to prevent autoimmunity or to activate T cells in a tumour setting.

1.5 Aim of the study

TCR signalling in response to antigen recognition plays a central role in the initiation of an adaptive immune response. In the last years, our group examined the molecular mechanisms of TCR signalling and identified several proteins potentially involved in its regulation. One of these candidates is TXNIP.

The aim of this study is to examine the role of TXNIP in TCR signalling. We determined whether TXNIP expression is altered after TCR engagement in primary human T cells as well as in Jurkat T cells. In order to study the impact of TXNIP on TCR signalling, TXNIP KO T cells were generated by means of CRISPR-Cas9 technology. We intended to investigate at least three TXNIP KO clones to reduce off-target effects accompanied with the usage of single cell clones. Since TXNIP is a negative regulator of Trx activity, this study analysed the role of TXNIP on Trx activity as well as on activation-induced ROS level using TXNIP KO clones. In addition, TXNIP regulates gene expression either *via* interaction with HDACs or by modulating Trx activity. Thus, we examined the effect of TXNIP on stimulation-induced transcription in TXNIP KO clones using a whole genome array. Furthermore, AICD was determined as an additional read out for the impact of TXNIP on T cell stimulation.

In summary, this study aims at gaining novel insights regarding the role of TXNIP for T cell activation and, thus, regulation of a T cell immune response, with the long term goal of identifying factors that could be employed for manipulation of T cell immunity in autoimmune diseases and cancer.

2 Materials

2.1 Chemicals and reagents

2.1.1 Chemicals

If not stated otherwise, all chemicals were purchased from Serva, Sigma-Aldrich or Roth.

2.1.2 Reagents

Reagent	Company
7AAD (7-Aminoactinomycin D)	Sigma-Aldrich
AET (2-aminoethylisothiouronium-bromide)	Sigma-Aldrich
Ampicillin	Sigma-Aldrich
Annexin V FITC-conjugated	ImmunoTools
APG101 (human CD95-Fc fusion protein)	Apogenix
BbsI	New England Biolabs
Bicoll Separating Solution (δ = 1.077 g/ml) (Ficoll)	Biochrom
Blue Prestained Protein Standard	NEB
CFSE	Sigma-Aldrich
CHX (Cycloheximide)	Sigma-Aldrich
dNTPs (10 mM)	Life Technologies
ECL Select Western Blotting Detection Reagent	GE Healthcare
ENBREL® (Etanercept)	Pfizer
Fc:CD95L	AdipoGen Life Sciences
GeneAmp 10x PCR Buffer and $MgCl_2$	Life Technologies
H_2DCFDA (2'-7'-dichlorodihydrofluorescein diacetate)	Life Technologies
IL2	produced in our laboratory
Iono (Ionomycin)	Merck
LC (clasto-Lactacystin β-lactone)	Sigma-Aldrich
M-MulV reverse transcriptase (200 U/µl)	Life Technologies
NAC (N-acetyl-cysteine)	Sigma-Aldrich
PHA (Phytohemagglutinin)	Sigma-Aldrich
PMA (Phorbol 12-myristate-13-acetate)	Sigma-Aldrich
Power SYBR Green PCR Master Mix	Applied Biosystems
Protease Inhibitor Cocktail Set III, EDTA-free	Calbiochem
RNAse Inhibitor (20 U/µl)	Life Technologies
SAHA (Suberoylanilide hydroxamic acid, Vorinostat)	Sigma-Aldrich
T4 DNA ligase	New England Biolabs
T4 Polynucleotide Kinase	New England Biolabs
TNFα	Gift from D. Männel, University of Regensburg, Germany
Trolox	Th. Greyer
Tween 20	Gerbu

Western Lightning Plus-ECL	Perkin Elmer
zVAD	BACHEM

2.1.3 Commercial kits

Kit	Company
Amaxa® Cell Line Nucleofactor™ Kit V	Lonza
BCA Assay Kit	Thermo Scientific
Plasmid Mini Kit	Qiagen
Plasmid Maxi Kit	Qiagen
QIAquick PCR Purification Kit	Qiagen
RNeasy Mini Kit	Qiagen
Thioredoxin Activity Assay (FkTRX-04)	BIOZOL
CellTiter 96® AQ_{ueous} One Solution Cell Proliferation Assay	Promega

2.2 Buffers and solutions

Buffer/Solution	Composition
ACK buffer pH 7.2	155 mM NH_4Cl 1 mM $KHCO_3$ 0.5 mM EDTA
Annealing buffer (2 x) pH 8.0	20 mM Tris 2 mM EDTA 100 mM NaCl
Annexin-binding-buffer pH 7.4	10 mM Hepes 140 mM NaCl 2.5 mM $CaCl_2$
Blocking buffer for flow cytometry	10 % (v/v) rat serum 10 % (v/v) FCS PBS
Blocking solution for western blot	5 % (w/v) skim milk powder or 5 % (w/v) BSA TBS-T
PBS pH 7.4	137 mM NaCl 8.1 mM Na_2HPO_4 2.7 mM KCl 1.5 mM KH_2PO_4
Ponceau S solution	0.1 % (w/v) ponceau S 5 % (v/v) acetic acid
Protein lysis buffer	20 mM Hepes pH 7.9 100 mM KCl 300 mM NaCl 10 mM EDTA 0.1 % (v/v) Triton X-100

Reducing sample buffer (5 x) for western blot	50 % (v/v) glycerol 3 % (w/v) SDS 375 mM Tris pH 6.8 5 % (v/v) β-mercaptoethanol 0.25 mg/ml bromphenol blue
Resolving gel (SDS-PAGE)	24 mM Tris-HCl pH 6.8 5 % (w/v) acrylamide 0.1 % (w/v) SDS 0.03 % (w/v) APS 0.1 % (v/v) TEMED
SDS running buffer	25 mM Tris 0.19 M glycine 1 % (w/v) SDS
Stacking gel (SDS-PAGE)	37.5 mM Tris-HCl pH 8.8 10 % (w/v) acrylamide 0.1 % (w/v) SDS 0.03 % (w/v) APS 0.1 % (w/v) TEMED
TBS pH 7.5	50 mM Tris-HCl pH 7.5 150 mM NaCl
TBS-T	0.05 % (v/v) Tween 20 TBS
Western blot transfer buffer	25 mM Tris 190 mM glycine 20 % (v/v) methanol

2.3 Consumables

Consumable	**Company**
Bacterial culture tubes	Greiner-Bio-One
Costar® -96 well flat micro titer plates black	Sigma-Aldrich
Cryotubes	TPP
culture flasks / plates / dishes	TPP
FACS tubes	BD Becton Dickinson GmbH
Filter Tips, TipOne®	StarLab
MicroAmp® Optical 96 well Reaction Plate	Life Technologies
Nitrocellulose membrane 0.45 NC	GE Healthcare
Optical Adhesive Covers for qRT-PCR plates	Life Technologies
PCR tubes (0.2 ml)	Starlab
Pipette tips	Starlab
Reaction tubes (1.5 ml, 2 ml)	Eppendorf
Reaction tubes (15, 50 ml)	Greiner-Bio-One
Serological Pipets (5 ml, 10 ml, 25 ml)	Corning
Sterile filters (0.22 µm, 0.44 µM)	Merck Millipore
Syringe (2.5 ml, 5 ml, 10 ml and 50 ml)	Terumo
Whatman Blotting paper	BioRad

2.4 Culture media and supplements

2.4.1 Bacterial culture media

LB Medium for bacterial culture was autoclaved at 125°C for 30 min and stored at 4°C. For the selection of bacterial clones, LB medium and LB agar plates were supplemented with 100 µg/ml ampicillin.

Medium	Content
LB Agar	20 g/L Agar LB medium
LB medium pH 7.4	10 g/L tryptone 5 g/L yeast extract 10 g/L NaCl

2.4.2 Media for eukaryotic cell culture

In general, media were supplemented with 10 % (v/v) heat-inactivated FCS (30 min, 56 °C) and stored at 4 °C.

Reagent	Company
FCS (fetal calf serum)	Sigma-Aldrich
Freezing medium	90 % (v/v) FCS, 10 % (v/v) DMSO
Penicillin-Streptomycin (10.000 U/ml)	Life Technologies
Rat serum	Milteny Biotech
RPMI-1640 medium	Sigma-Aldrich

2.5 Biologic material

2.5.1 Bacterial strains

Strain	Experimental purpose	Company
E. coli DH5α	Vector amplification and cloning	Life Technologies

2.5.2 Eukaryotic cell line

Cell line	Characteristics	Medium
J16 (Jurkat)	human T lymphoblastoid cell line [144, 253]	RPMI-1640 + 10 % FCS

2.6 Antibodies

2.6.1 Primary Western blot antibodies

Antigen target	clone	Isotype	Dilution	Provider
β-Actin	AC-15	mouse monoclonal	1:20.000	Sigma-Aldrich
Thioredoxin-1	C63C6	rabbit monoclonal	1:1.000	Cell Signaling
TXNIP	JY2	mouse monoclonal	1:2.000	MBL
Itch	D8Q6D	rabbit monoclonal	1:1.000	Cell Signaling

2.6.2 Secondary Western blot antibodies

Specificity	Isotype	Dilution	Provider
mouse-IgG-HRP	horse	1:10.000	Cell Signaling
rabbit-IgG-HRP	goat	1:5.000	Cell Signaling

2.6.3 Antibodies for flow cytometry

Antigen target	Fluorophore	Clone	Dilution	Provider
CD3	FITC	SK7	1:100	BD Biosciences
CD95	PE	DX2	1:100	BD Biosciences

2.6.4 Stimulation antibody

Antigen target	Clone	Isotype	Stock solution	Provider
CD3	OKT3	mouse monoclonal	1 mg/ml in PBS	prepared from Hybridoma in our laboratory [32]

2.7 Materials for molecular biology

If not stated otherwise, all primers and siRNA oligonucleotides were synthesised by Sigma-Aldrich.

2.7.1 Primers for PCR, cloning and sequencing

Gene target	Primer	Sequence (5´→ 3´)
gRNA1	Forward reverse	CACCGTTCGGCTTTGAGCTTCCTC AAACGAGGAAGCTCAAAGCCGAAC
gRNA2	Forward reverse	CACCGAATATGGGTGTGTAGACTAC AAACGTAGTCTACACACCCATATTC
Oligo-dT		TTTTTTTTTTTTTTT
TXNIP-specific sequencing primer	Forward reverse	AGCAAGCCTAATGGCTACTCG AATCTAATGCCCAAGACGTCTGAT
U6	Forward	GAGGGCCTATTTCCCATGATTCC

2.7.2 Primers for qPCR

2.7.2.1 Self-designed qPCR primers

Primers for qPCR listed below were designed using the online primer designing tool Primer-BLAST (http://www.ncbi.nlm.nih.gov/tools/primer-blast/). In general, all primer pairs were designed to be intron-spanning with primer efficiencies between at least 1.7 and 2.0.

Gene target	Primer	Sequence (5´→ 3´)
GAPDH	Forward reverse	GCAAATTCCATGGCACCGT TCGCCCCACTTGATTTTGG
CD95L	Forward reverse	AAAGTGGCCCATTTAACAGGC AAAGCAGGACAATTCCATAGGTG
IL2	Forward reverse	CAACTGGAGCATTTACTGCTG TCAGTTCTGTGGCCTTCTTGG
TNFA	Forward reverse	GCCGCATCGCCGTCTCCTAC AGCGCTGAGTCGGTCACCCT
TXNIP	Forward reverse	AGACCAGCCAACAGGTGAGA TGAAGGATGTTCCCAGAGGC

2.7.2.2 Verified qPCR primers

All RT^2 qPCR Primer Assays listed below were obtained from Qiagen.

Gene target	Catalog no.
EGR2	PPH01478F
GMCSF	PPH00576C
GZMB	PPH02594A
IFNG	PPH00380C

2.7.3 siRNA oligonucleotides

Gene target	Sequence (5´→ 3´)
Non-targeting control siRNA	AAUAGCGACUAAACACAUCAA
Itch	CCAGUUGGACUCAAGGAUUUA

2.7.4 Vector

Plasmid	Company
pSpCas9(BB)-2A-GFP (PX458)	Addgene

2.8 Instruments

Instrument	Company
7500 Real time PCR systems	Life Technologies
Amaxa® Nucleofactor™ II Device	Lonza
Centrifuge 5810R	Eppendorf
Chemi-Smart 5100	Vilber Lourmat
FACS Canto II flow cytometer	BD Becton Dickinson
GeneAmp PCR system 9700	Life Technologies
GloMax®-Multi+ Detection System	Promega
Megafuge 3SR+	Haereus, Hanau, Germany
Mini-PROTEAN II® electrophoresis chamber	Biorad
Mini-PROTEAN® Tetra cell	Biorad
NanoDrop ND-1000	PeqLab
PH meter ProfiLine pH 3210	WTW
Power Supply E865	Consort
Tabletop centrifuge Fresco 17	Thermo Scientific
Thermomixer Comfort	Eppendorf

2.9 Software

Software	Company
7500 Software version 2.0.1	Life Technologies
Chemi Capt version 15.01	Vilber Lourmat
Chromas	Technelysium Pty Ltd
FACSDIVA™ 6.1.2	BD Becton Dickinson
Flow Jo version 7.6.5	FlowJo LLC
GelQuant.NET	BiochemLabSolutions
Graph Pad Prism version 6	GraphPad Software
Instinct software version 3.1.3	Promega
Microsoft Office 2010	Microsoft
NanoDrop 1000 version 3.7.1	Thermo Fisher Scientific

3 Methods

3.1 Eukaryotic cell culture

3.1.1 General culture conditions

Human T lymphoblastoid cell line Jurkat J16 were cultured in RPMI-1640 with 10 % FCS at 37 °C in a humidified incubator with a 5 % CO_2 content. Used FCS was heated for 30 min at 56 °C to inactivate complement factors. Medium was changed every 2 - 3 days and cell density was adjusted to 2 x 10^5 cells/ml. Harvesting of the cells was implemented by centrifugation for 10 min at 1500 rpm and 4 °C. All cell culture work was conducted under sterile conditions using a laminar flow hood.

3.1.2 Thawing and freezing of cells

For freezing, cells were harvested and resuspended in FCS supplemented with 10 % DMSO (freezing medium). Cryo-vials containing the cell suspension were transferred into a Mr. Frosty container filled with isopropanol (achieving a slow gradient of lowering freezing temperatures) and stored at -80 °C for 2 – 3 days. For long term storage cells were transferred to liquid nitrogen (-196 °C).

Cells were rapidly thawed in a water bath at 37 °C and immediately transferred to a centrifuge tube containing 25 ml RPMI-1640 supplemented with 10 % FCS. Thereafter, cells were centrifuged at 1500 rpm and 4°C for 10 min and resuspended in an adequate volume of fresh RPMI-1640 with 10 % FCS.

3.1.3 Isolation of human peripheral T lymphocytes

Isolation of human peripheral T cells was conducted by Ficoll-Plaque density centrifugation, followed by rosetting with AET-treated sheep erythrocytes as described before [254].

3.1.3.1 Preparation of AET-erythrocytes

Sheep red blood cells were delivered in a 1:1 ratio in Alsever solution (Fiebig Nährstofftechnik), which was removed from the erythrocytes by washing them three

times with PBS. For the preparation of the AET solution (pH=9.0) pyrogen-free, sterile water was used (0.5 g of AET diluted in 12.5 ml of water). Subsequently, washed sheep erythrocytes were mixed with 12.5 ml of AET solution and incubated for 15 min at 37 °C on a rolling device. Afterwards, AET-treated sheep red blood cells were washed four times with PBS and finally diluted in RPMI-1640 with 10 % FCS to prepare a 2 % suspension. All centrifugation steps were conducted at 1500 rpm and 20 °C for 10 min. AET-treated sheep erythrocytes were stored at 4 °C for up to three days.

3.1.3.2 Isolation of peripheral blood leukocytes

Blood of buffy coats (Blutbank, Stadtklinikum Karlsruhe) was adjusted to 200 ml with PBS. 35 ml of blood-PBS mixture was slowly layered onto 15 ml Ficoll and centrifuged at 2420 rpm and 20 °C for 20 min without brake. Peripheral blood leukocytes (PBLs) were collected from the interphase, washed twice with PBS (1000 rpm, 10 min, 20 °C and slow breaking) and resuspended in RPMI-1640 with 10 % FCS. For the depletion of adherent cells (*i.e.* monocytes and macrophages), PBLs were transferred into cell culture flasks and cultured for 1 h at 37 °C. Collection of non-adhering lymphocytes was performed by taking off cell suspension of cell culture flasks.

3.1.3.3 T cell isolation by rosetting with AET-treated sheep erythrocytes

For a “rosetting” reaction PBLs were mixed with a 2 % AET-treated sheep red blood cell solution in a 1:1 ratio. Afterwards, the mixture was centrifuged at 1000 rpm and 20 °C for 10 min (slow breaking). Next, a 50 ml tube filled with 15 ml Ficoll was carefully overlayed with the resuspended pellet (containing “rosettes” of T cells and erythrocytes) and centrifuged for 20 min at 2420 rpm and 20 °C (without brakes). After one wash with pre-warmed medium (1000 rpm, 10 min, 20 °C, slow braking), erythrocytes were lysed by addition of 4 x volume ACK buffer (acc. to the pellet). A colour change of the mixture from turbid light red to clear dark red indicated the lysis. Subsequently, the lysis reaction was stopped by addition of RPMI-1640 with 10 % FCS and the cells were centrifuged (1200 rpm for 10 min at 20 °C). Pelleted cells were resuspended in 20 ml of RPMI-1640 with 10 % FCS, counted and diluted to a concentration of 2 x 10^6 cells/ml.

3.1.3.4 *In vitro* expansion and culture of T lymphocytes

Activation of resting peripheral blood T lymphocytes was performed by using PHA. For this purpose isolated T cells were cultured at a concentration of 2 x 10^6 cells/ml in the presence of 1 µg/ml PHA for 16 h. Afterwards, activated T lymphocytes were washed three times with medium and cultured in RPMI-1640 supplemented with 10 % FCS and 25 U/ml IL2 for six days ("day 6") as described before [32, 254]. All experiments were performed with T cells isolated from at least two independent healthy donors.

3.2 Cell biology

3.2.1 *In vitro* stimulation of Jurkat and primary human T cells

One day before each experiment Jurkat T cells were diluted in fresh culture medium to obtain a concentration of 2–3 x 10^5 cells/ml on the day of the assay. For all experiments, cells were pelleted (1500 rpm, 10 min) and resuspended in fresh culture medium to a concentration of 5 x 10^5 cells/ml. Next, cells were stimulated with plate-bound anti-CD3 agonistic antibodies (OKT3) at a final concentration of 30 µg/ml. For this purpose, wells were coated over night at 4 °C with an appropriate volume of anti-CD3 solution. Alternatively, cells were treated with PMA (10 ng/ml) and Ionomycin (10 µM) or other stimuli (50 µg/ml CHX, 20 ng/ml TNFα, 25 µM LC, 250 g/ml APG101, 30 µM zVAD, 100 ng/ml Fc:CD95L, 20 mM NAC, 100 µM Trolox, 250 µg/ml ENBREL®, 5 µM SAHA). After stimulation for the indicated time periods, cells were harvested by transfer of the cell suspension into 15 ml tubes. Subsequently, cells were pelleted (1500 rpm for 10 min), the supernatant was removed and cells were lysed or stained depending on the performed experiment.

3.2.2 Cell lysis

Pelleted cells were lysed by addition of 100 µl ice-cold protein lysis buffer per 2 x 10^6 cells (addition of 1:100 Protease Inhibitor cocktail III prior to use) and incubated on ice for 30 min. Next, lysates were centrifuged in a table-top centrifuge at 13300 rpm and 4 °C for 30 min to clear protein lysates from debris. Subsequently, supernatants (whole cell lysates) were collected and protein concentration was assessed by BCA assay according to manufacturer's instructions. For gel electrophoresis, lysates were adjusted with protein

lysis buffer to equal volumes, mixed with reducing sample buffer (5 x) and heated to 95 °C for 5 min.

3.2.3 Cell death analysis

Cell death was analysed by AnnexinV-FITC/7AAD using flow cytometry. AnnexinV-FITC/7AAD staining of cells can be used to determine different modes of cell death (*e.g.* early and late apoptosis and necrosis). For cell death analysis performed in this thesis, all cell death modes were taken together to define "specific cell death". Briefly, cells were stimulated with plate-bound anti-CD3 agonistic antibodies (OKT3, 30 µg/ml) for 48 h. Following stimulation, cells were spun down at 1500 rpm and 4 °C for 10 min and stained with AnnexinV-FITC/7AAD (each 1:100 diluted in Annexin-binding-buffer) for 10 min on ice. Subsequently, cells were pelleted (1500 rpm for 10 min at 4 °C) and resuspended in Annexin-binding-buffer for flow cytometry analysis. Results are presented as percentage of specific cell death which was calculated according to the following formula (as described in [255]):

$$\text{Specific cell death } [\%] = \left[\frac{\text{dead cells } [\%] - \text{dead cells } [\%]_{\text{untreated control}}}{100 - \text{dead cells } [\%]_{\text{untreated control}}}\right] \times 100$$

3.2.4 Determination of ROS production

Intracellular status of ROS (H_2O_2 concentration) was analysed using H_2DCFDA, a molecule that becomes fluorescent upon oxidation. Cells were stained with H_2DCFDA by direct addition of the cell permeable dye to the cell suspension in a final concentration of 5 µM and incubated for 15 min at 37 °C. Next, cells were divided and stimulated with plate-bound anti-CD3 antibodies (OKT3, 30 µg/ml) for 1 h. Following incubation with the treatment, cells were pelleted by centrifugation at 1500 rpm and 4 °C for 10 min. Pelleted cells were finally resuspended in ice-cold PBS. ROS production was measured by assessing the fluorescent signal of processed H_2DCFDA (mean fluorescence intensity (MFI)) by flow cytometry. Results were calculated as % increase in H_2DCFDA MFI according to the following formula [256]:

$$\text{Increase in } H_2\text{DCFDA MFI } [\%] = \left[\frac{\text{MFI}_{\text{stimulated}} - \text{MFI}_{\text{unstimulated}}}{\text{MFI}_{\text{unstimulated}}}\right] \times 100$$

3.2.5 Cell proliferation analysis

On the one hand, cell proliferation was analysed using CFSE, a cell permeable and fluorescent dye. 1 x 10^6 cells were resuspended in PBS and incubated with an equal volume of CFSE solution (1 µM in PBS). Following 20 min incubation in the dark, the staining reaction was stopped by adding one volume of FCS. After 2 min at RT, the tube was filled up with ice cold RPMI-1640 with 10 % FCS and incubated for 5 min on ice. Finally, the cells were washed 2 times with RPMI-1640 with 10 % FCS. Proliferation was measured by assessing the fluorescent signal of intracellular CFSE.

On the other hand, cell proliferation was analysed using CellTiter 96® AQ_{ueous} One Solution Cell Proliferation Assay according to manufacturer's instructions. Briefly, 5.000 cells per well were seeded in a 96-well plate for the indicated time periods. Then, 20 µl CellTiter 96® AQ_{ueous} One Solution was added into each well and after 4 h of incubation, absorbance was recorded at 490 nm using a 96-well plate reader.

3.2.6 Trx activity assay

Trx activity was analysed using the fluorescence-based Trx activity assay kit according to manufacturer's instructions. In short, cells were lysed in protein lysis buffer and protein concentration was assessed by BCA assay according to manufacturer's instructions (see chapter 3.2.2). Measurement was conducted as triplicates in a 96-well format (black plates) using 20 µg total protein per sample. Increase of fluorescence within 1 h in a time period of 5 min was recorded using GloMax®-Multi+ Detection System. Trx activity was calculated in the linear range and displayed as % activity compared to control cells whose activity was set to 100 %.

3.2.7 Transfection of Jurkat cells using Amaxa technology

Using the Amaxa® Cell Line Nucleofactor™ Kit V, Jurkat cells were transfected by nucleofection according to manufacturer's instructions. In brief, 1 x 10^6 cells were resuspended in nucleofection solution containing either 300 nM siRNA or 1 or 2 µg plasmid DNA. Nucleofection was performed using programme X-01. 24 – 72 h after siRNA-mediated gene silencing, knockdown efficiency was assessed by western blot analysis.

3.2.8 Determination of CD3 and CD95 cell surface expression

Expression of surface molecules CD3 and CD95 was determined by immunofluorescence staining. First, cells were blocked in blocking buffer for 10 min on ice. Following blocking process, cells were incubated with fluorescence-conjugated anti-human CD3 or CD95 antibody (diluted 1:50 in blocking buffer) in a total volume of 100 µl per sample for 30 min on ice. Afterwards cells were washed once with PBS/10 % FCS and finally resuspended in PBS for flow cytometry analysis.

3.3 Biochemical methods

3.3.1 SDS-PAGE and Western blot

In order to separate proteins, Sodium dodecyl sulphate-polyacrylamide gel electrophoresis (SDS-PAGE) was conducted. For electrophoresis 10 % or 12 % polyacrylamide resolving gels and 5 % polyacrylamide stacking gels were prepared. Before loading on a gel, protein samples were denatured at 95 °C in reducing sample buffer for 5 min. Following denaturation, protein samples were subjected to SDS-PAGE (35 mA/gel). Subsequently, separated proteins were transferred onto a nitrocellulose membrane using a wet Blot-transfer system (90 V for 2 h at 4 °C). After blotting, membranes were blocked with 5 % milk powder or 5 % BSA in TBS-T for at least 30 min at RT. For protein detection, membranes were incubated with primary antibodies overnight at 4°C. On the next day, membranes were washed 3 times for 5 min with TBS-T and incubated for 1 h with a horseradish peroxidase (HRP)-conjugated secondary antibody at RT. Finally, the membrane was washed another 3 times 5 min with TBS-T and developed using ECL detection reagent (either Western Lightning Plus-ECL for β-Actin detection or Amersham ECL Select Western Blotting Detection Reagent for the detection of Trx1 and TXNIP) and recorded with the Chemi-Smart 5100 System. Analysis of β-Actin protein expression was used as loading control for each blot and if necessary, signal intensities were quantified using GelQuant.NET.

3.3.2 mRNA quantification

3.3.2.1 Isolation of RNA

RNA was extracted using the Qiagen RNeasy Mini Kit following manufacturer's protocol. Briefly, 1 - 5 x 10^6 cells were lysed in 350 µl RLT buffer. After adding 350 µl of 70 % absolute ethanol, the lysates were loaded on a provided silica column, centrifuged at 13000 rpm for 1 min and the flow-through was discarded. The columns were then washed once by applying 700 µl of RW1 wash buffer and discarding the flow-through. Subsequently, the column membranes were washed twice in the same manner with 500 µl of RPE buffer. The silica columns were then dried by centrifugation at 13000 rpm for 1 min and transferred to a clean RNAse-free elution tube. RNA was eluted by direct addition of 25 µl RNase free water to the membrane. The water was incubated for 1 min before centrifugation at 13000 rpm for 1 min. RNA concentration was determined by spectrophotometry and the eluted RNA was stored at -80 °C until use. All centrifugation steps were done in a table-top centrifuge at 4 °C.

3.3.2.2 Reverse transcription (RT) of RNA into cDNA

In order to perform gene expression analysis, 1000 ng RNA was reverse transcribed into cDNA by mixing 19,5 µl RNA solution with 20,5 µl mastermix as shown in Table 3.1. Next, RT-PCR was performed with the programme shown in Table 3.2. Synthesised cDNA was diluted 1:1 with water and stored at -20°C.

Table 3.1: RT-PCR 1x mastermix.

Component	Volume
$MgCl_2$ [25 mM]	8 µl
10 x PCR buffer	4 µl
dNTPs mix [10 mM]	4 µl
RNase inhibitor [20 U/µl]	2 µl
Oligo dT primer [100 pmol/µl]	2 µl
MuLV reverse transcriptase [200 U/µl]	0.5 µl

Table 3.2: RT-PCR reaction programme.

Temperature	Time
25°C	10 min
42 °C	45 min
95 °C	5 min
4 °C	∞

3.3.2.3 Quantitative Real Time-PCR (qRT-PCR)

For qRT-PCR analysis, synthesised cDNA (2 µl) was added to a mixture containing 12.5 µl Power SYBR® Green PCR Master Mix, 2 µl primer mix (25 µM stocks) and 8.5 µl ddH_2O. qRT-PCR was performed with the programme shown in Table 3.3 and each sample was measured in triplicate in a 96-well plate format with a final volume of 25 µl per reaction/well. Gene expression was evaluated using the ΔΔCT method and human GAPDH as reference gene.

Table 3.3: qRT-PCR reaction programme.

Temperature	Time	
50 °C	2 min	
60 °C	10 min	
95 °C	15 s	40 x
60 °C	1 min	

3.4 Microarray

In cooperation with the expression profiling service of the genomics and proteomics core facility (Dr. Melanie Bewerunge-Hudler, DKFZ) a genome-wide gene expression analysis was performed using Ilumina HT12 expression bead chip. Data analysis was carried out with the help of Dr. Thomas Hielscher (statistical department, DKFZ). Quantile-normalised expression values were log2 transformed. Differentially expressed clones were identified using the empirical Bayes approach [257] based on moderated t-statistics as implemented in the Bioconductor package limma [258]. Gene set enrichment analysis was performed using the camera test [259]. In case a gene was represented by multiple clones, the clone with the strongest effect was selected for pathway analysis. KEGG data base [260] and gene ontology [261] were used in pathways analysis. P-values were adjusted to control the false discovery rate using the Benjamini-Hochberg correction. Hierarchical clustering was performed using Euclidean distance and Ward linkage after gene-wise scaling. All analyses were performed with statistical software R 3.5 [262].

3.5 TXNIP KO induction by using the CRISPR/Cas9 technology

3.5.1 Cas9 nuclease construct and design of guideRNA oligonucleotides

In order to generate TXNIP KO Jurkat T cell clones the CRISPR/Cas9 technology was used. The utilised plasmid construct pSpCas9(BB)-2A-GFP (PX458) contains a Cas9 Nuclease coupled to GFP. Design of TXNIP-specific oligonucleotides (see chapter 2.7.1) which were applied as guideRNAs (gRNAs) was performed by using the following website (https://cm.jefferson.edu/Off-Spotter/). For annealing of oligonulceotides, 5 µl of each forward and reverse oligo (100 µM) were mixed with 10 µl annealing buffer (2 x). Annealing was performed using the programme shown in Table 3.4. Subsequently, annealed oligonucleotides were phosphorylated for 30 min at 37 °C using a T4 Polynucleotide Kinase according to manufacturer's instructions. Detailed information concerning the plasmid construct and the cloning procedure are described in the following publications [263, 264].

Table 3.4: Annealing programme.

Time	Temperature	Cycles
1 min	98 °C	
5 s	98 - 88 °C (decrease 0.1 °C per cycle)	99 x
10 s	88 - 78 °C (decrease 0.1 °C per cycle)	99 x
10 s	78 - 68 °C (decrease 0.1 °C per cycle)	99 x
10 s	68 - 58 °C (decrease 0.1 °C per cycle)	99 x
10 s	58 - 48 °C (decrease 0.1 °C per cycle)	99 x
10 s	48 - 38 °C (decrease 0.1 °C per cycle)	99 x
10 s	38 - 18 °C (decrease 0.2 °C per cycle)	99 x
forever	18 °C	

3.5.2 Ligation reaction

Before ligation of the annealed and phosphorylated gRNAs into the PX458 vector, the nucleotides were diluted tenfold in ddH_2O and the vector was digested using BbsI. Parameters for digestion were adjusted according to manufacturer's instructions. In general, a total volume of 20 µl was used for a digest reaction. In reactions for preparative scale, total reaction volume (40 µl) and DNA input (4 µg) were increased. Digestion of the

vector was followed by a clean-up and elution (in 30 µl ddH_2O) of the construct using the QIAquick PCR Purification Kit according to manufacturer's instructions. Ligation was conducted using the T4 DNA ligase according to manufacturer's instructions. For the ligation reaction, a molecular ratio of 1:4,5 vector to insert DNA was used.

3.5.3 Bacterial transformation by heat shock

For the amplification of plasmids, chemically competent DH5α bacteria were transformed using heat shock. In brief, competent bacteria were thawed on ice and subsequently incubated for 10 min with 5 µl ligation product on ice. Next, uptake of plasmid DNA was induced by a 30 sec heat pulse at 42 °C. Afterwards, bacteria were incubated for 2 min on ice, supplemented with LB medium without antibiotics and incubated on a shaker at 37 °C for at least 30 min. Finally, transformed bacteria were spread on LB plates containing ampicillin (100 µg/ml) and cultivated at 37 °C overnight. On the next day, single bacteria colonies were picked and used for inoculation of LB medium supplemented with ampicillin (100 µg/ml). LB plates with bacteria colonies were stored at 4 °C.

3.5.4 Plasmid purification (Mini- and Maxiprep)

Bacteria from a single culture were used to inoculate 2 ml (Mini-preparation, analytical scale) or 250 ml (Maxi-preparation, preparative scale) ampicillin-supplemented LB medium. Bacterial cultures grew overnight at 37 °C in a rotary shaker and plasmid DNA was isolated using the Qiagen® Plasmid Mini kit or the Qiagen® Plasmid Maxi kit, respectively. DNA purification was performed according to manufacturer's instructions and the isolated DNA was eluted in 30 µl (Mini) or 400 µl (Maxi) of ddH_2O and stored at -20 °C. DNA concentration was determined by spectrophotometry.

3.5.5 DNA sequencing

Correct ligation of the TXNIP-specific gRNAs into the PX458 vector was confirmed by sequencing. For analysis of cloned plasmid or genomic DNA, a mixture of 5 µl template DNA (80 – 100 ng/µl) and 5 µl (5 µM) of a U6 or a selected sequencing primer (TXNIP-specific, see chapter 2.7.1) were sent to GATC Biotech company (Constance, Germany).

GATC Biotech company makes use of the di-deoxy chain termination sequencing method [265].

3.5.6 Generation of TXNIP KO Jurkat cells

Jurkat J16 T cells were transfected *via* nucleofection with the CRISPR/Cas9 plasmid PX458 containing one of the two TXNIP-specific gRNAs (see chapter 3.2.7). 24 h after transfection GFP-positive cells were sorted as single cells into 96 well plates. In parallel, empty vector (EV) Jurkat single cell clones were equally generated using Cas9-GFP-plasmids without a TXNIP- sequence specific gRNA. As soon as EV and TXNIP KO single cell clones were grown, genomic DNA was isolated (using the GeneArt® Genomic Cleavage Detection Kit) and sequenced (see chapter 3.5.5). An overview of the generation of TXNIP KO Jurkat clones *via* CRISR/Cas9 is shown in Figure 3.1.

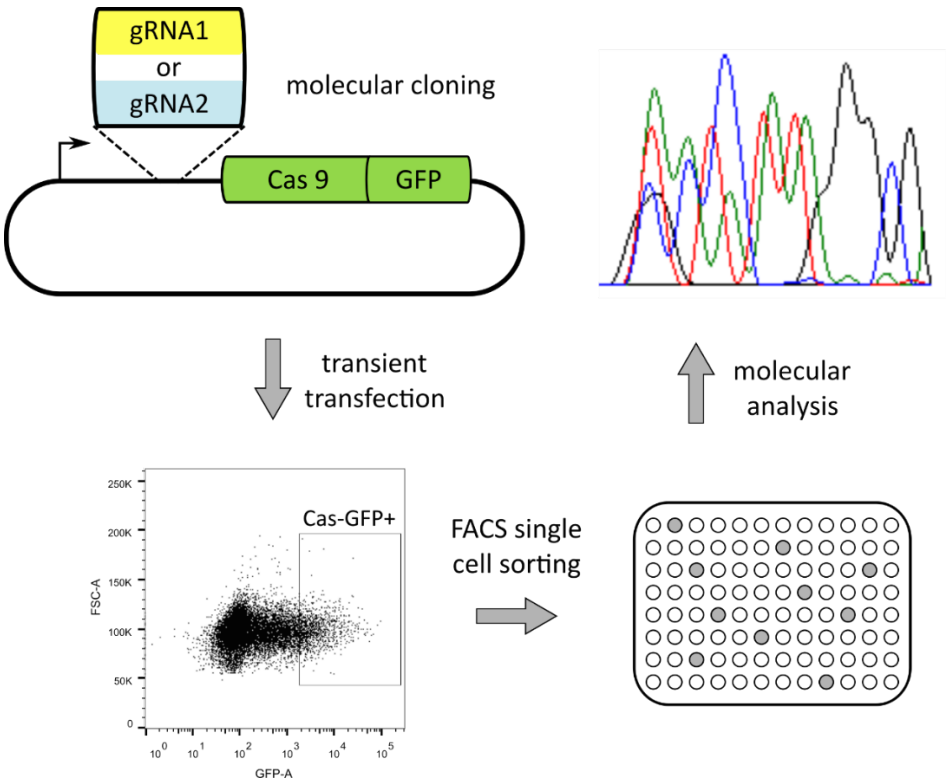

Figure 3.1: Scheme showing the generation process of CRISPR-Cas9-mediated KO of TXNIP in Jurkat T cells.
For the generation of CRISPR-Cas9-mediated TXNIP KO Jurkat single cell clones a TXNIP-sequence specific gRNA was cloned into a plasmid bearing Cas9 coupled to GFP allowing single cell sorting of transfected, Cas9-GFP positive Jurkat T cell clones. In parallel, EV Jurkat single cell clones were equally generated using Cas9-GFP-plasmids without a TXNIP-sequence specific gRNA. Sequence as well as protein expression analysis were performed to confirm WT sequence of TXNIP in EV as well as frameshift mutations in TXNIP KO Jurkat single cell clones.

4 Results

4.1 TCR restimulation leads to production of ROS and induction of AICD

Since Jurkat T cells act like an activated T cell, they represent an optimal model to analyse TCR restimulation. Comparable to activated T cells, TCR stimulation of Jurkat cells results in AICD. AICD is mediated by CD95L which expression dependents on ROS production [32, 266]. In order to confirm the role of the oxidative signal in TCR signalling in this study, we aimed to validate the regulation of CD95L-mediated AICD by ROS.

ROS production upon TCR stimulation of Jurkat T cells was determined using H_2DCFDA, a molecule that becomes fluorescent upon oxidation. Following stimulation of Jurkat T cells with plate-bound anti-CD3 antibodies, a specific increase in ROS generation of up to 45 % was observed (Figure 4.1A). Since activation-induced oxidative signalling is crucial for expression of CD95L [32, 33], CD95L mRNA level was analysed using RT-qPCR. As shown in Figure 4.1B, CD3 stimulation of Jurkat T cells resulted in a rise of CD95L mRNA expression levels over time. Addition of the ROS scavenger NAC reduced the oxidative signal to not determinable levels (data not shown) [32] and as anticipated, co-administration of NAC also significantly decreased expression of CD95L mRNA (Figure 4.1B). In line with the observed increase of CD95L gene expression, stimulation of Jurkat T cells with anti-CD3 antibodies increased cell death by 33 % compared to untreated cells (Figure 4.1C). This TCR stimulation-induced cell death was significantly reduced upon inhibition of the oxidative signal by NAC or upon abrogation of caspase activity by zVAD (Figure 4.1C). These results are in accordance with data showing that activation–induced ROS are important for CD95L mRNA expression in a model of AICD [32, 33, 44, 53, 266].

Pre-activated primary human T cells (“day 6” T cells) were used to verify the relevance of the oxidative signal in CD95L-mediated AICD in a more physiological setting. *In vitro* expanded human T cells were restimulated with anti-CD3 antibodies and induction of ROS production (Figure 4.2A), CD95L mRNA level (Figure 4.2B) as well as AICD (Figure 4.2C) were observed to be similar to the results obtained in Jurkat T cells (Figure 4.1). Furthermore, the importance of ROS generation for signal transduction upon TCR

stimulation was confirmed in “day 6” T cells as illustrated by the reduction of CD95L mRNA expression (Figure 4.2B) and AICD (Figure 4.2C) by the ROS scavenger NAC. Taken together, these results underline the relevance of the oxidative signal in TCR signalling leading to CD95L-mediated AICD in Jurkat and primary human T cells.

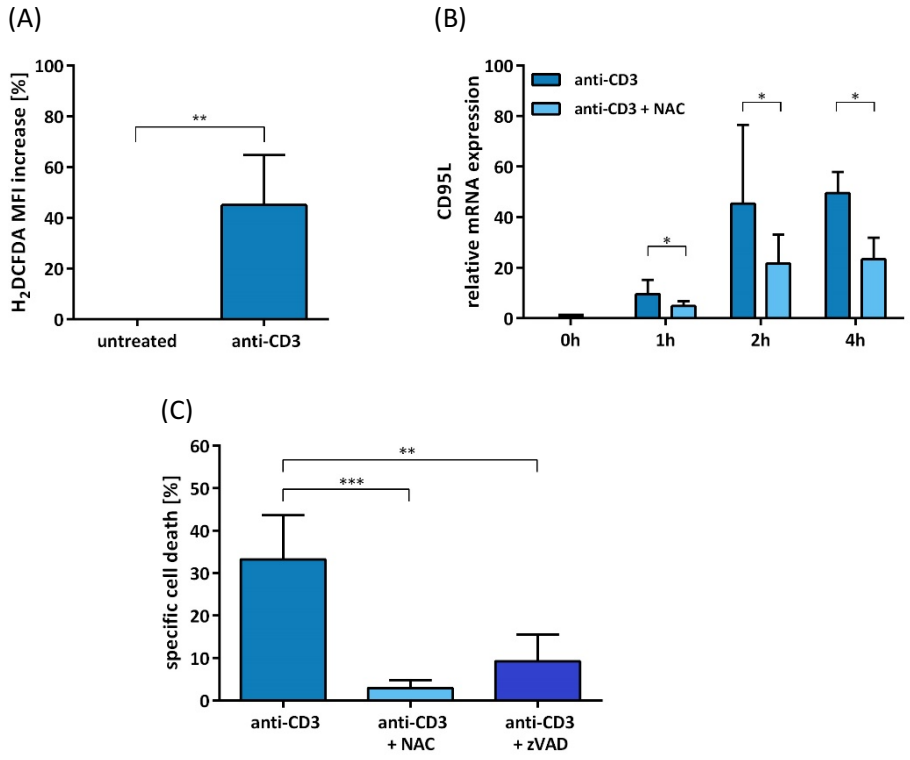

Figure 4.1: TCR stimulation induces ROS production, CD95L mRNA expression and AICD in Jurkat T cells.

(A) Jurkat T cells were incubated for 15 min with H_2DCFDA. Subsequently, cells were left untreated or stimulated with plate-bound anti-CD3 agonistic antibodies for 1 h. Mean ROS production is shown as percent increase in H_2DCFDA MFI compared to untreated cells (n = 4). (B) Jurkat T cells were pre-treated with or without NAC for 15 min and stimulated with anti-CD3 antibodies for the indicated time periods. CD95L gene expression was analysed by qRT-PCR and compared to untreated cells (0 h) (n = 3). (C) Jurkat T cells were pre-treated with or without NAC or zVAD for 15 min and then restimulated with anti-CD3 antibodies for 48 h to induce AICD. Cell death was assessed by flow cytometry using AnxV-FITC and 7AAD and calculated as “specific cell death” normalised to untreated cells (n = 5). Statistical significance was calculated using paired t-test (mean and standard deviation (SD), *p<0.05, **p<0.01, ***p<0.001).

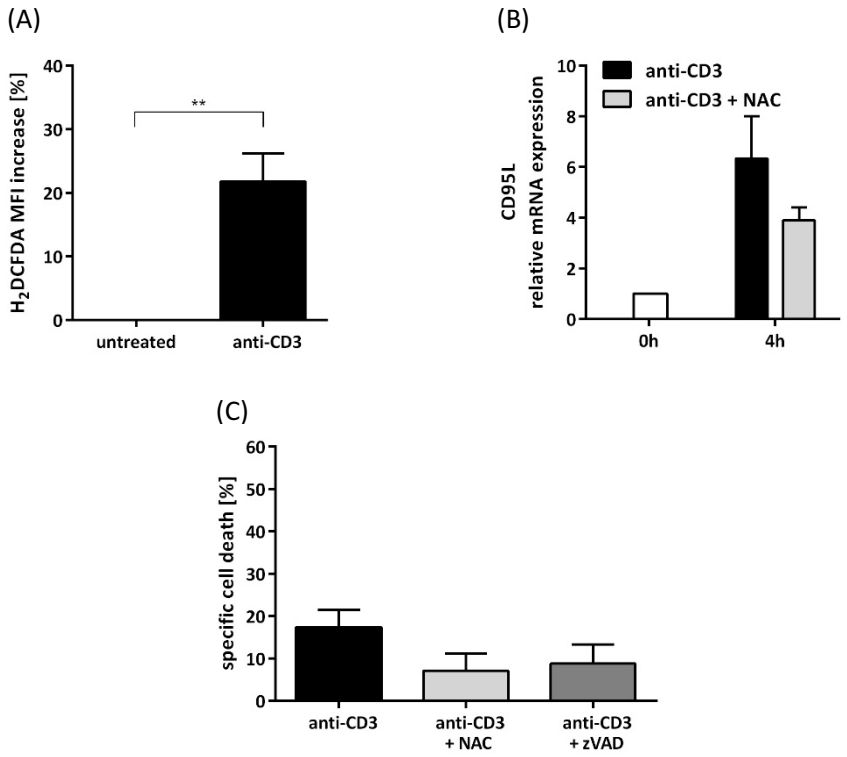

Figure 4.2: ROS generation, CD95L mRNA expression and AICD is induced upon TCR restimulation of human T cells.

(A) Pre-activated T cells ("day 6") were stained with H_2DCFDA for 15 min prior to CD3 stimulation for 1 h. Mean ROS production was calculated as increase in H_2DCFDA MFI compared to untreated cells. Statistical significance was calculated using paired t-test (**$p<0.01$). (B) In vitro expanded human T cells were treated with or without NAC for 15 min and then stimulated with anti-CD3 antibodies. Expression of CD95L was analysed by qRT-PCR and compared to untreated cells (0 h) of the same donor. (C) Human T cells "day 6" were treated with or without NAC or zVAD for 15 min and restimulated with anti-CD3 antibodies for 48 h to induce AICD. Cell death was assessed by flow cytometry using AnxV-FITC and 7AAD and calculated as "specific cell death" normalised to non-stimulated cells of the same donor. Bars represent mean values and SD of two independent donors.

4.2 Effects of T cell stimulation on Trx activity and TXNIP expression

TCR stimulation is characterised by alterations of the redox balance by transient production of ROS which serve as second messenger to mediate gene expression and, hence, regulate activation, proliferation and cell death [37, 44, 55]. However, since accumulation of ROS can also have toxic effects, ROS production needs to be tightly controlled by antioxidative systems *e.g.* the Trx system [175]. Thus, we investigated whether TCR stimulation which relies on production of ROS, affects activity of Trx as well as expression of TXNIP.

A fluorescence-based insulin reduction assay was used to evaluate whether TCR stimulation influences the activity of Trx. CD3 stimulation of Jurkat T cells significantly increased Trx activity by 42 % in comparison to untreated cells (Figure 4.3A). Since it has been reported that TXNIP binding to Trx inhibits the activity of Trx [222, 223], mRNA as well as protein expression of TXNIP was investigated. As illustrated in Figure 4.3B – C, TCR stimulation with anti-CD3 antibodies resulted in decreased TXNIP mRNA and protein levels. Similarly, TXNIP expression levels were reduced when Jurkat cells were treated with PMA/Iono which is a pharmacologic alternative to mimic TCR signalling (Figure 4.3D – E). Despite alterations of Trx activity are associated with changes of Trx levels [223], protein expression of Trx1 remained unchanged upon TCR stimulation (Figure 4.3 C, E). Thus, a TCR-induced rise of Trx reducing activity could be associated with the reduction of TXNIP level.

Furthermore, regulation of TXNIP expression upon TCR stimulation was evaluated and confirmed in a more physiological setting using pre-activated primary human T cells (Figure 4.4). In summary, TCR stimulation affects the Trx system by suppressing TXNIP mRNA and protein expression in Jurkat as well as in primary T cells which results in the enhancement of Trx reducing activity.

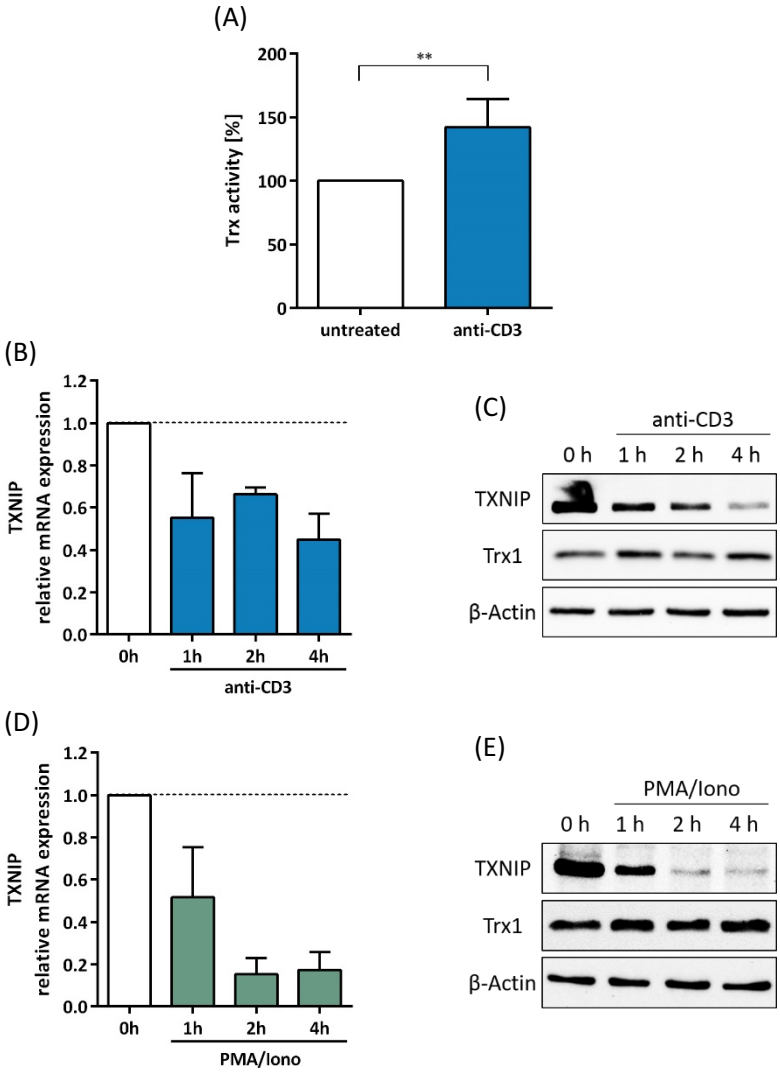

Figure 4.3: Increase of Trx activity and suppression of TXNIP mRNA as well as protein expression following TCR stimulation of Jurkat T cells.
(A) Jurkat T cells were stimulated with anti-CD3 antibodies for 4 h, lysed and subsequently, Trx activity was measured using an insulin reduction assay (Fk-TRX-04). Trx activity was normalised to activity in untreated cells (set to 100 %). Statistical significance was calculated using paired t-test (mean and SD, n = 5, **p<0.01) (B-E) Jurkat T cells were stimulated with anti-CD3 antibodies (B and C) or PMA/Iono (D and E) for the indicated time periods. (B and D) TXNIP gene expression was analysed by qRT-PCR and compared to untreated cells (0 h). Bars represent mean values and SD of at least four independent experiments. (C and E) TXNIP as well as Trx1 protein expression was determined by Western blot. The panels show a representative blot of at least four independent experiments.

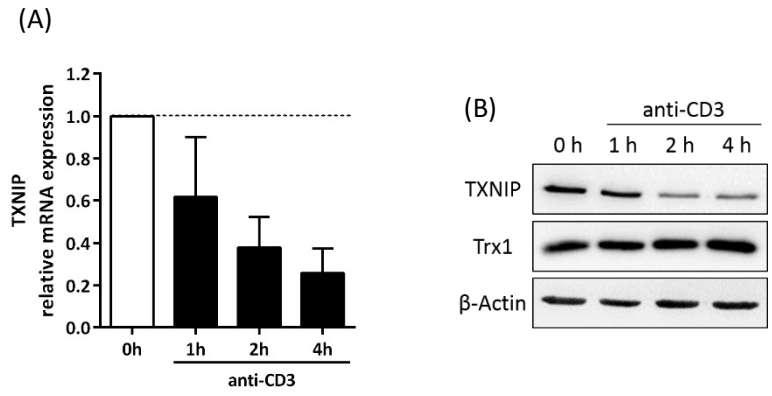

Figure 4.4: Downregulation of TXNIP expression upon TCR restimulation of human T cells.
Pre-activated primary human T cells "day 6" were restimulated with anti-CD3 antibodies for the indicated time points. (A) Gene expression of TXNIP was analysed by qRT-PCR and compared to untreated cells (0 h) of the same donor. Bars represent mean values and SD of four independent donors. (B) TXNIP as well as Trx1 protein expression was determined by Western blot. The panel shows a representative blot of four independent donors.

4.3 Effect of activation-induced ROS production on TXNIP expression

Since ROS suppress TXNIP expression which in turn enhance Trx activity in primary rat cardiomyocytes as well as human aortic smooth muscle cells, TXNIP is considered to function as a sensor of ROS which regulates redox-dependent processes *via* Trx [267, 268]. Thus, we hypothesised that the observed suppression of TXNIP is caused by ROS generation following TCR stimulation.

However, as illustrated in Figure 4.5, co-administration of the ROS scavengers NAC or Trolox did not affect TCR-induced suppression of TXNIP mRNA and protein level in Jurkat T cells. This observation indicates a ROS-independent TXNIP downregulation upon TCR stimulation. To further evaluate that TXNIP regulation is not ROS-mediated, Jurkat T cells were treated with TNFα which is known to trigger intracellular ROS production [269, 270]. Despite TNF receptor stimulation resulted in a similar production of ROS compared to TCR stimulation by anti-CD3 antibodies (Figure 4.6A), no change of TXNIP protein expression was observed upon TNFα treatment over time (Figure 4.6B). Taken together, Figure 4.5 and 4.6 demonstrate that suppression of TXNIP expression upon TCR engagement is not ROS-mediated in Jurkat T cells.

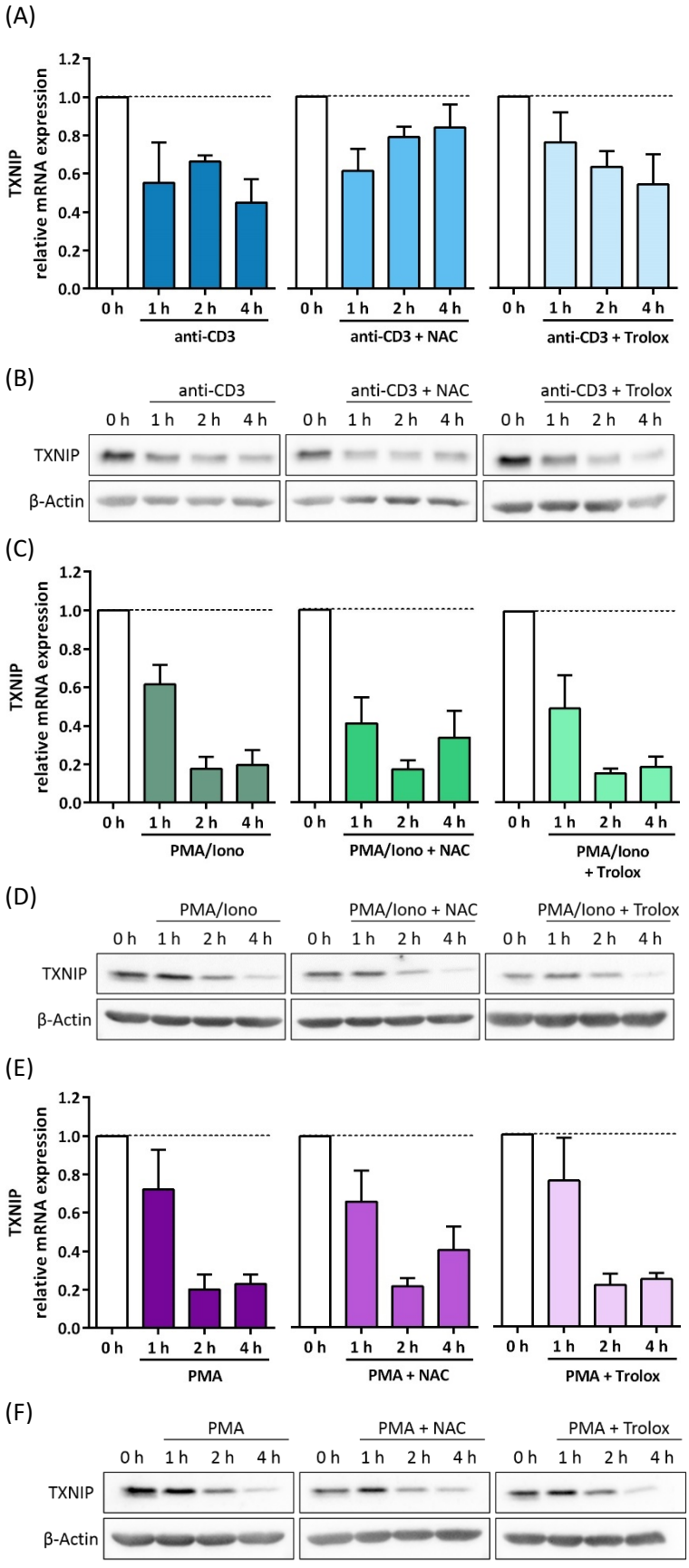

Figure 4.5: TCR-induced TXNIP suppression is not affected by antioxidant treatment.
Jurkat T cells were stimulated with anti-CD3 antibodies (A and B), PMA/Iono (C and D) or PMA (E and F) for the indicated time periods. (A, C and E) TXNIP gene expression was analysed by qRT-PCR and compared to untreated cells (0 h). Bars represent mean values and SD of four independent experiments. (B, D and F) TXNIP protein expression was determined by Western blot. The panels show a representative blot of four independent experiments.

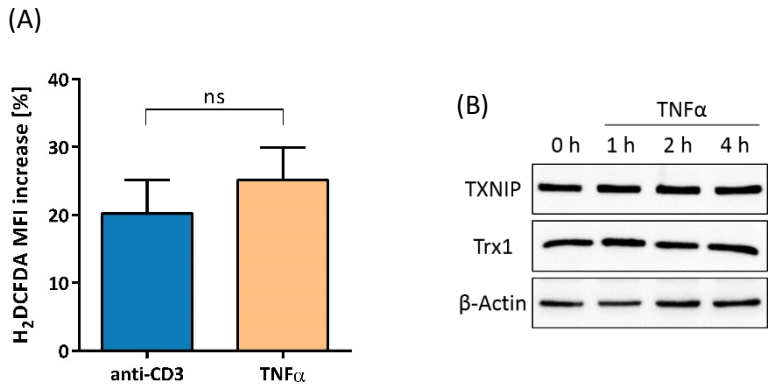

Figure 4.6: TXNIP protein level is not influenced by TNFα-induced ROS production.
(A) Jurkat T cells were incubated for 15 min with H_2DCFDA and subsequently, left untreated or stimulated with either anti-CD3 antibodies or TNFα for 1 h before ROS production was analysed. Statistical significance was calculated using paired t-test (mean and SD, n = 4, not significant (ns): p> 0.05). (B) Jurkat T cells were stimulated with TNFα for the indicated time periods and TXNIP as well as Trx1 protein expression was determined by Western blot. The panel shows a representative blot of three independent experiments.

4.4 Regulation of TXNIP expression by proteasomal degradation and altered protein synthesis

TCR stimulation of Jurkat and primary human T cells resulted in reduced TXNIP levels but the kinetics and underlying regulatory mechanisms are yet to be determined.

A time-dependent decline of TXNIP mRNA and protein level after anti-CD3 stimulation of Jurkat T cells was observed and resulted in a strong reduction of TXNIP mRNA as well as protein expression 4 h after TCR engagement (Figure 4.7A – C, 4.3B – C).

To further analyse mechanisms involved in TCR-induced TXNIP downregulation, protein synthesis was blocked using the translation inhibitor CHX. CHX treatment of Jurkat T cells induced rapid reduction and complete abolishment of TXNIP protein level after 2 h (Figure 4.8A) pointing to a regulation of TXNIP by proteasomal degradation. Co-administration of CHX and CD3 stimulation lead to accelerated reduction of pre-existing TXNIP protein (Figure 4.8B – C) suggesting that TCR engagement enhanced degradation of TXNIP. Regulation of TXNIP protein by proteasomal degradation was verified using the proteasome inhibitor LC which resulted in an accumulation of basal TXNIP protein (Figure 4.8E). However, less TXNIP protein accumulation was observed in Jurkat T cells treated with LC prior to CD3 stimulation compared to LC treatment alone (Figure 4.8D –

E) indicating that TCR engagement mediates suppression of TXNIP protein synthesis. These results indicate that TXNIP downregulation upon TCR stimulation is regulated by acceleration of proteasomal degradation as well as reduction of protein synthesis.

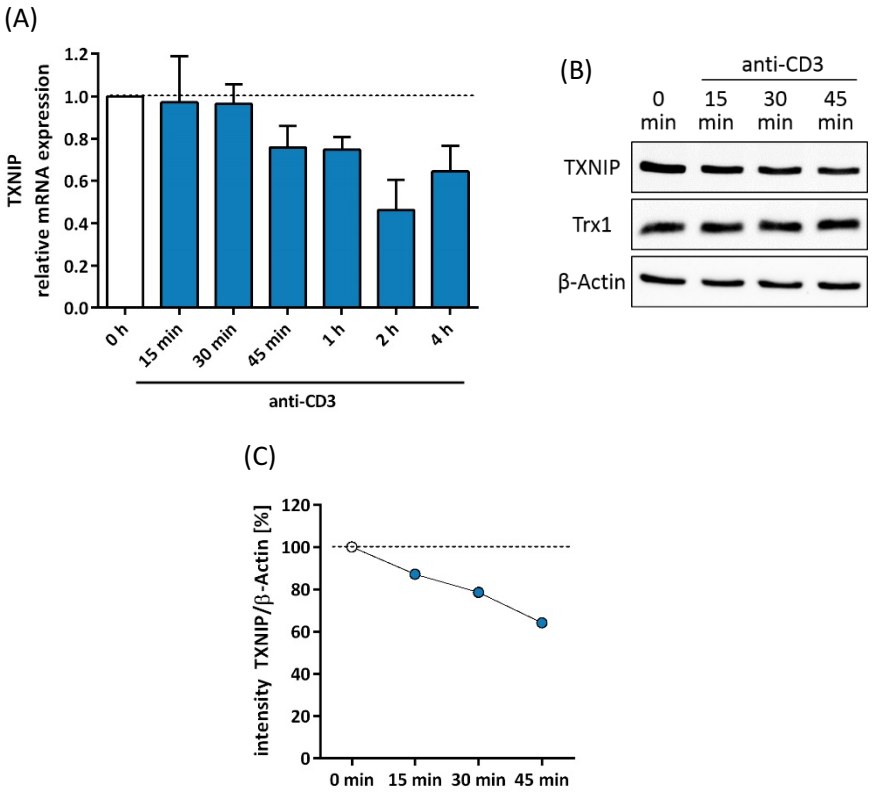

Figure 4.7: TXNIP downregulation following TCR stimulation is regulated on protein as well as on mRNA level.
Jurkat T cells were stimulated with anti-CD3 antibodies for the indicated time periods. (A) TXNIP gene expression was analysed by qRT-PCR and compared to untreated cells (0 h). Bars represent mean values and SD of four independent experiments. (B) TXNIP and Trx1 protein expression was determined by Western blot. The panels show a representative blot of four independent experiments. (C) Quantification of Western blot results of (B). TXNIP signal intensity was divided by the respective β-Actin signal intensity. The value of untreated cells (0 min) was set to 100 %.

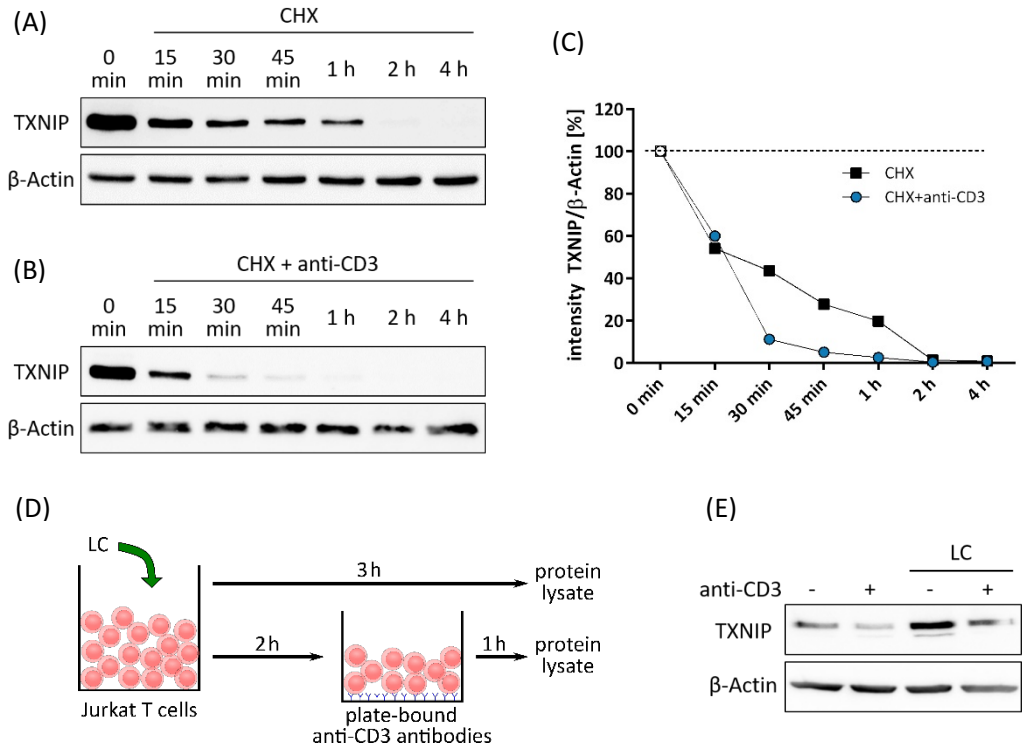

Figure 4.8: Impact of proteasomal degradation as well as protein synthesis on TXNIP expression. (A and B) Jurkat T cells were treated with CHX and stimulated with or without anti-CD3 antibodies for the indicated time periods. TXNIP protein expression was determined by Western blot. The panels show a representative blot of three independent experiments. (C) Quantification of CHX (A) and CHX + anti-CD3 (B) Western blot results. TXNIP signal intensity was divided by the respective β-Actin signal intensity. The value of untreated cells (0 min) was set to 100 %. (D) Jurkat T cells were treated with LC for 2 h or left untreated. Then, cells were either left untreated further on or transferred on plates coated with anti-CD3 antibodies and stimulated for 1 h with or without LC. (E) TXNIP protein expression was determined by Western blot. The panel shows a representative blot of three independent experiments.

4.5 Generation and characterisation of CRISPR-Cas9-mediated KO of TXNIP in Jurkat T cells

In section 4.2, TXNIP expression was demonstrated to be reduced upon TCR stimulation. In order to investigate whether reduced TXNIP in turn has an effect on TCR downstream signalling, a TXNIP KO was introduced to Jurkat T cells using the CRISPR-Cas9 system.

4.5.1 Generation of EV and TXNIP KO Jurkat single cell clones

Details about the generation and validation of the CRISPR-Cas9-mediated KO of TXNIP are described in section 3.5. Sequence analysis of the TXNIP gene of three single cell-sorted EV and three KO clones confirmed TXNIP wild type (WT) sequence and identified CRISPR-Cas9-induced frameshift mutations (Figure 4.9A – C). CRISPR-Cas9-mediated nucleotide insertions or deletions (letters depicted in red or crossed out with a red line, respectively) as well as the resulting premature stop codons (bold and underlined letters) in the TXNIP gene sequence of each TXNIP KO clone are summarised in Figure 4.9A – C.

In order to confirm the CRISPR-Cas9-induced KO of TXNIP, protein expression was determined. As illustrated in Figure 4.9D, TXNIP protein expression in KO clones was completely abolished compared to EV clones which exhibited protein levels comparable to WT Jurkat T cells. In summary, Figure 4.9 demonstrates that CRISPR-Cas9-mediated frameshift mutations resulted in abrogation of TXNIP protein expression in the KO clones whereas the TXNIP WT sequence as well as protein expression in EV clones was not affected.

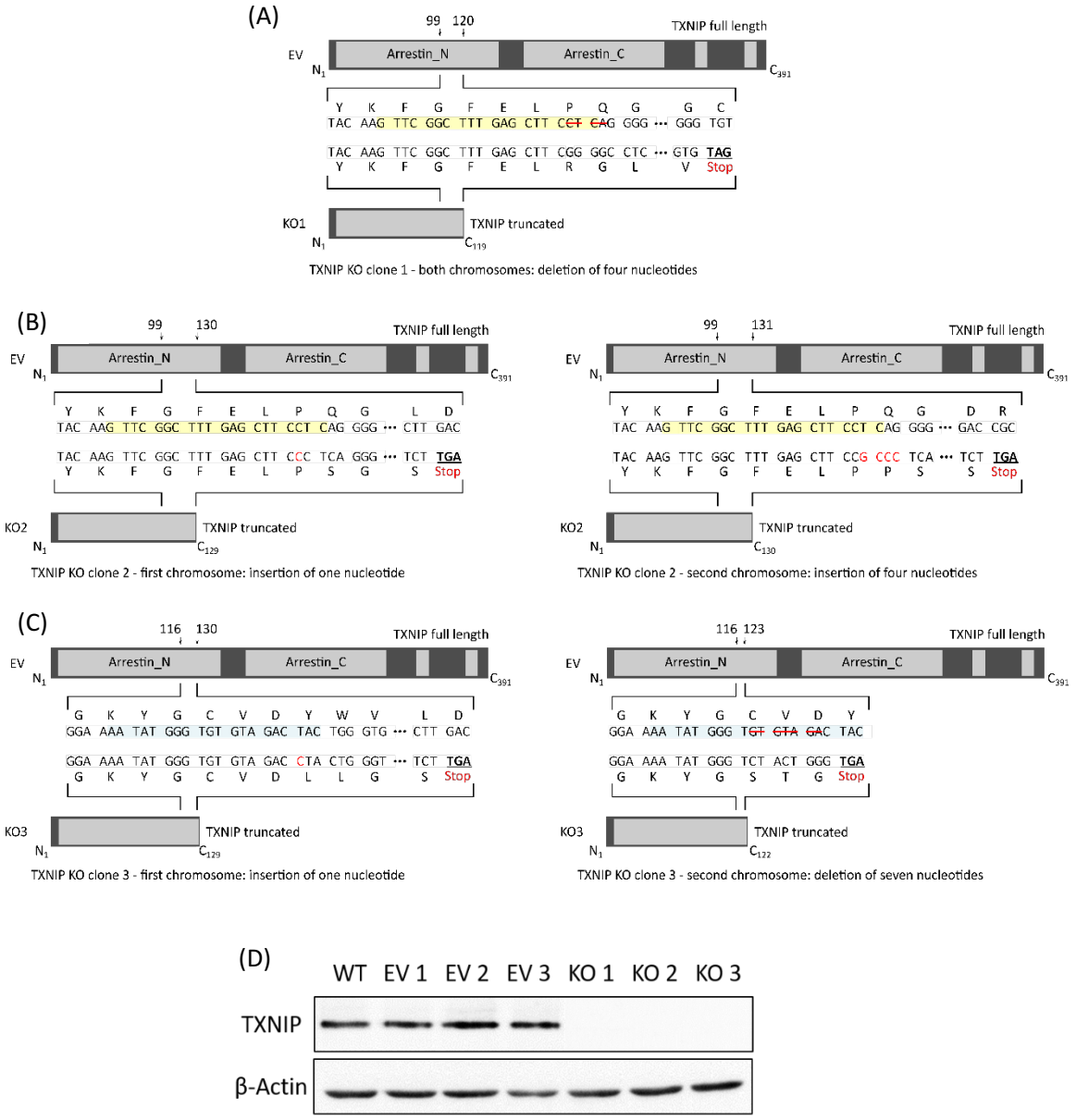

Figure 4.9: Analysis of CRISPR-Cas9-mediated KO of TXNIP in Jurkat T cells.
(A-C) Sanger sequencing of EV and TXNIP KO Jurkat single cell clones revealed TXNIP WT sequence or frameshift mutations, respectively. Schematic diagrams showing Cas9-mediated nucleotide insertions or deletions in TXNIP KO clone 1 (A), clone 2 (B) or clone 3 (C) in comparison to EV (WT) TXNIP sequence. The sequence of the two guide RNAs are highlighted in yellow and blue, respectively. (D) WT Jurkat T cells as well as EV and TXNIP KO clones were analysed for basal TXNIP protein expression by Western blot. The panel shows a representative blot of three independent experiments.

4.5.2 Surface expression analysis of CD3 and CD95 on EV and TXNIP KO clones

This study use Jurkat T cells as a model for TCR signalling in terms of CD95L-mediated AICD which is a readout for TCR stimulation *e.g.* by anti-CD3 antibodies. Hence, verification of CD3 and CD95 expression on EV and KO Jurkat single cell clones is a prerequisite for their usage in further experiments. As shown in Figure 4.10, surface expression of CD3 and CD95 on EV and KO clones was comparable to the expression levels on WT Jurkat T cells. Thus, EV and TXNIP KO clones are suitable for TCR signalling experiments based on the CD95L-mediated AICD model.

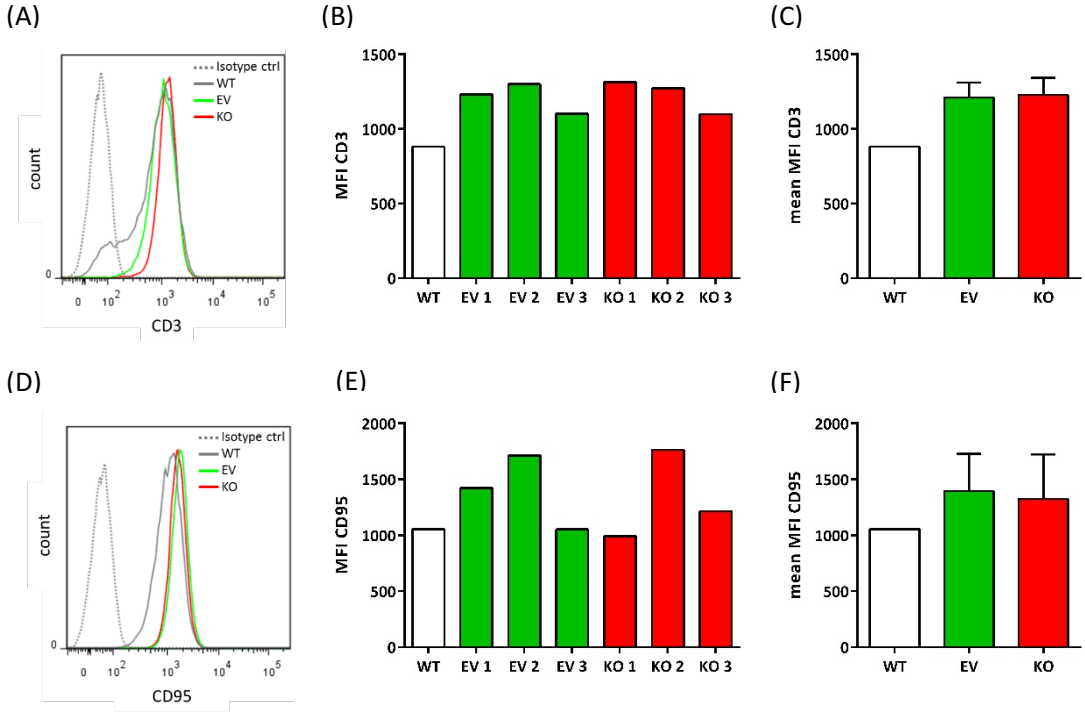

Figure 4.10: CD3 and CD95 surface expression in EV and TXNIP KO Jurkat single cell clones. The different types of Jurkat T cells were stained for CD3 or CD95 and analysed by flow cytometry. MFI of one representative example is shown. (A and D) Representative FACS profiles of CD3 or CD95 surface expression, respectively. Scattered grey profiles show isotype control, grey profiles represent WT Jurkat T cells, green profiles show EV and red profiles depict TXNIP KO clones. (B and E) Bars represent MFI of CD3 or CD95 of one representative experiment and (C and F) MFI of CD3 or CD95 as a mean of the three EV or KO clones.

4.6 Impact of TXNIP KO on basal Trx activity and TCR-induced ROS production

Since TXNIP suppression in turn mediated enhanced Trx activity (Figure 4.3), TXNIP might regulate redox-dependent processes *via* Trx. Hence, we hypothesised that increased Trx activity influences ROS production upon TCR stimulation.

First, the impact of TXNIP KO on basal Trx activity was analysed using a fluorescence-based insulin reduction assay. TXNIP KO clones had a significant increase of basal Trx activity compared to EV clones (Figure 4.11A) whereas Trx protein expression remained unchanged in unstimulated as well as anti-CD3 stimulated EV and TXNIP KO clones (Figure 4.11 B) verifying the impact of TXNIP downregulation on Trx activity observed in Figure 4.3A. Next, the contribution of enhanced Trx activity on activation-induced ROS release was determined in TXNIP KO clones. CD3 stimulation resulted in comparable production of ROS in EV and KO clones (Figure 4.11C). These results demonstrate that the rise of basal Trx reducing activity in TXNIP KO clones had no impact on TCR stimulation-induced ROS generation.

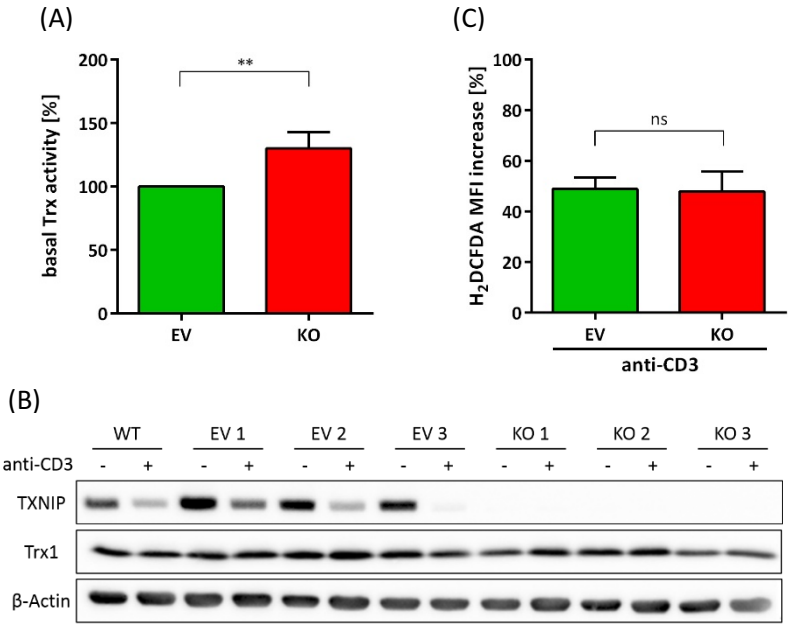

Figure 4.11: TXNIP KO clones exhibit increased basal Trx activity and similar TCR-induced ROS production compared to EV clones.

(A) Basal Trx activity was measured using an insulin reduction assay (Fk-TRX-04) and is displayed as percent Trx activity normalised to untreated EV clones (set to 100 %). Bars represent mean values of the three EV and TXNIP KO clones of five independent experiments (n = 5). (B) Cell clones were left untreated or stimulated with anti-CD3 antibodies for 4 h and TXNIP as well as Trx1 protein expression were determined by Western blot. The panel shows a representative blot of

three independent experiments. (C) Cell clones were analysed for ROS production 1 h after anti-CD3 stimulation and percent increase in H_2DCFDA MFI was normalised to untreated cells. Bars represent mean values of the three EV and TXNIP KO clones of four independent experiments (n = 4). (A and C) Statistical significance of was calculated using unpaired t-test (mean and SD, ns: p> 0.05, **p<0.01).

4.7 Effect of TXNIP KO on activation-induced gene expression

Trx1 plays a critical role in the activation of redox-sensitive transcription factors *e.g.* NFκB and AP1 [64, 76, 113] which are mandatory for TCR stimulation-induced gene expression [34–36, 55]. Thus, we investigated whether enhanced Trx activity of TXNIP KO clones affects gene expression upon TCR stimulation by using a genome-wide gene expression analysis.

Although not significant, this analysis revealed enhanced expression of early growth response 2 (EGR2), granzyme B (GZMB), CD95L, tumour necrosis factor alpha (TNFA), granulocyte-macrophage colony-stimulating factor (GMCSF), interferon gamma (IFNG) and IL2 genes upon CD3 stimulation of TXNIP KO compared to EV clones whereas no difference was observed comparing unstimulated EV and TXNIP KO clones (Figure 4.12). These genes were selected for further analysis due to their involvement in T cell activation, differentiation, cytokine signalling as well as cell death.

To verify the impact of TXNIP on activation-induced gene expression, mRNA expression analysis of the selected genes mapped in Figure 4.12 was performed using RT-qPCR. As shown in Figure 4.13, CD3 stimulation resulted in the induction of CD95L, GMCSF, GZMB, IFNG, IL2, TNFA and EGR2 mRNA expression which was increased in TXNIP KO compared to EV clones. In summary, TXNIP deficiency mediates enhanced gene expression upon TCR stimulation suggesting that TXNIP acts as a transcriptional inhibitor.

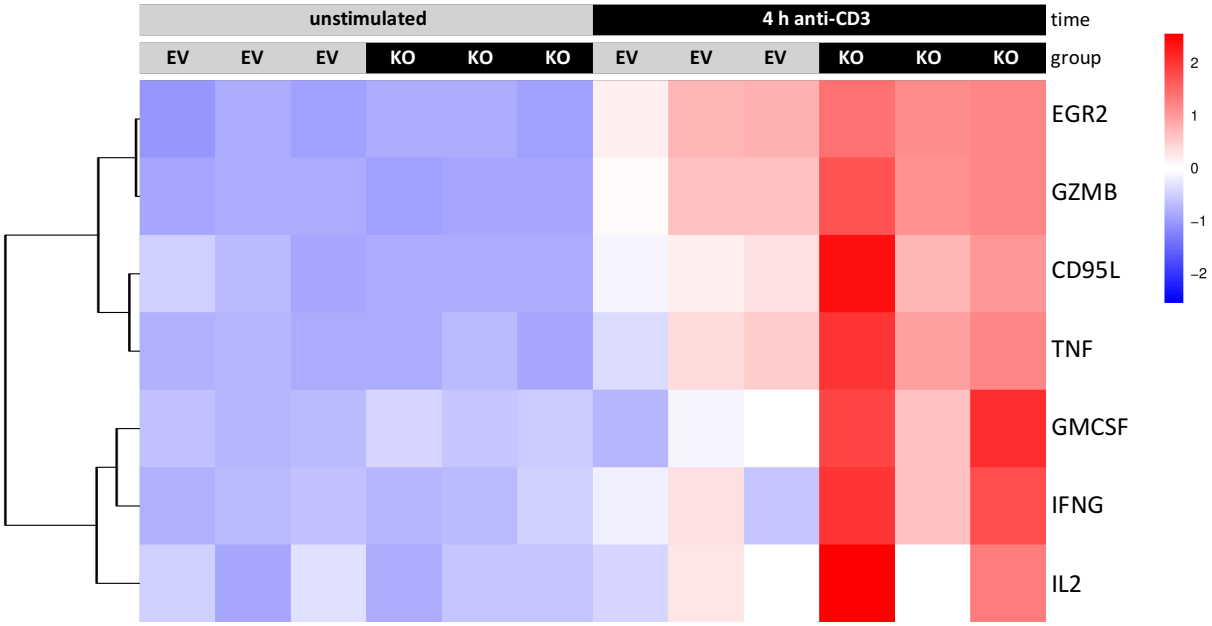

Figure 4.12: Illumina whole-genome gene expression analysis in EV and TXNIP KO clones.
EV and TXNIP KO clones were stimulated for 4 h with anti-CD3 antibodies or left untreated before mRNA was analysed by Illumina HT12 bead chip. Expression of selected genes, involved in TCR signalling, is depicted in a heat map (red indicates upregulation and blue downregulation according to the spectrum on the right). The entire data of the microarray analysis are filed on a hard disk and available at the division of Immunogenetics (D030) of Prof. Dr. Peter H. Krammer at the DKFZ in Heidelberg.

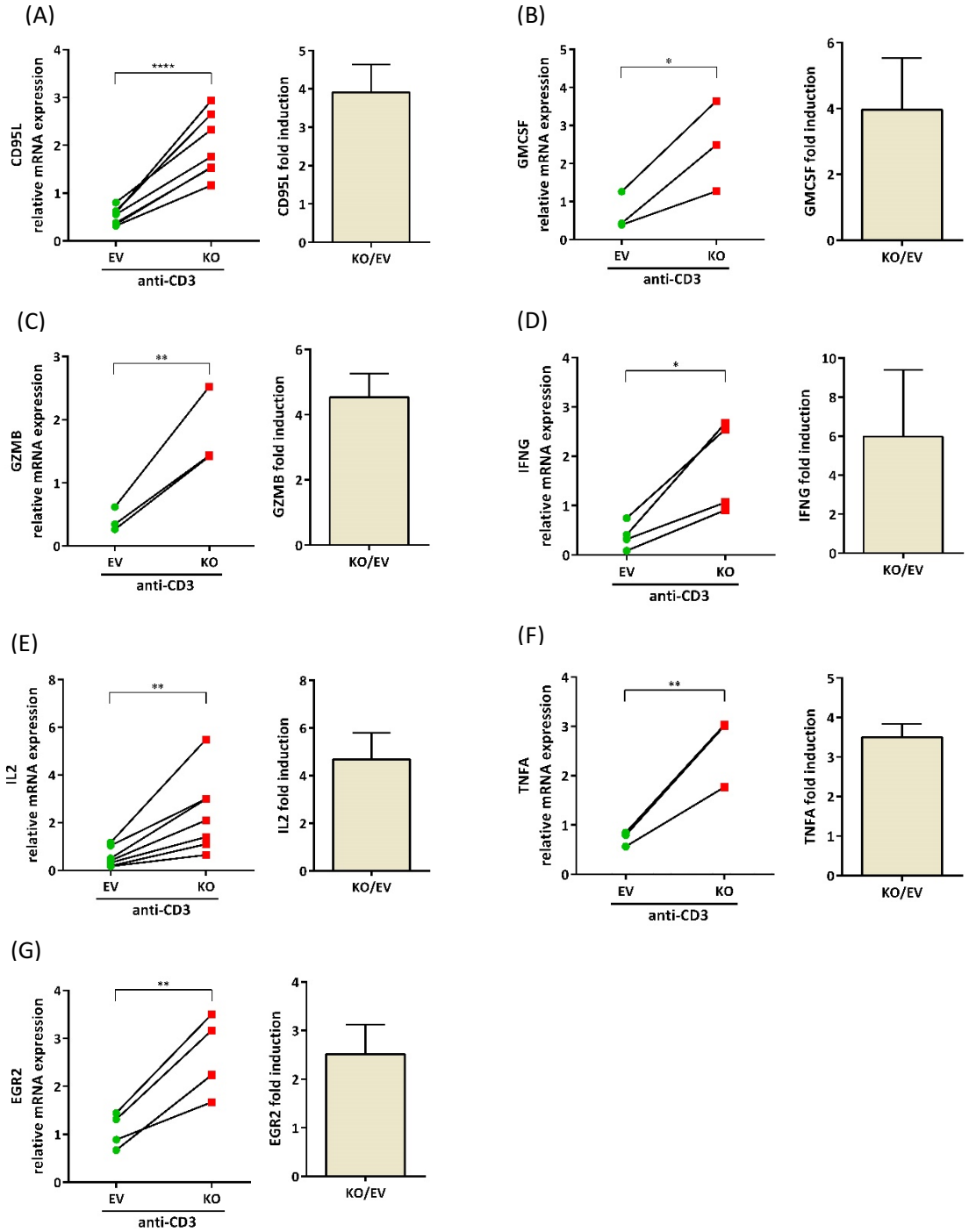

Figure 4.13: TXNIP KO clones exhibit enforced CD95L, GMCSF, GZMB, IFNG, IL2, TNFA, and EGR2 mRNA expression following TCR stimulation.

EV and TXNIP KO clones were stimulated with anti-CD3 antibodies for 4 h before (A) CD95L, (B) GMCSF, (C) GZMB, (D) IFNG, (E) IL2, (F) TNFA and (G) EGR2 mRNA expression was analysed by qRT-PCR. The indicated values represent mean activation-induced mRNA expression of three EV (green dot) and three TXNIP KO clones (red square) which was calculated compared to anti-CD3 stimulated WT Jurkat T cells (untreated values were not taken into account). Stimulation-induced mRNA expression of WT Jurkat cells was used as reference point ("1") to illustrate variabilities of individual EV and KO measurements (data not shown). Bars represent mean ratio of KO to EV stimulation-induced mRNA expression of indicated measurements. Statistical significance of at least three independent experiments was calculated using unpaired t-test (mean and SD, *p<0.05, **p<0.01, ****p<0.0001).

4.8 Impact of CD95L mRNA expression on AICD in TXNIP KO Jurkat T cells

Since the Jurkat T cell line is a model for TCR-induced CD95L-mediated AICD [32, 266], we hypothesised that elevated CD95L mRNA expression in TXNIP KO clones influence AICD. In line with the increased CD95L gene expression in TXNIP KO clones (Figure 4.13A), CD3 stimulation resulted in a significantly enhanced induction of AICD in TXNIP KO compared to EV single cell clones (Figure 4.14A) while basal cell death was unchanged (Figure 4.14B). The TCR-induced specific cell death was reduced by blocking CD95L using a human CD95-Fc fusion protein (APG101) or by using the pan-caspase inhibitor zVAD (Figure 4.14C). In addition, stimulation with a human CD95L-Fc fusion protein (Fc:CD95L) resulted in a similar induction of specific cell death in EV and TXNIP KO clones (Figure 4.14D – G) suggesting that basic CD95 signalling pathway is not affected by TXNIP KO. In summary, TXNIP deficiency sensitises Jurkat T cell to AICD by enhanced mRNA expression of the CD95L gene.

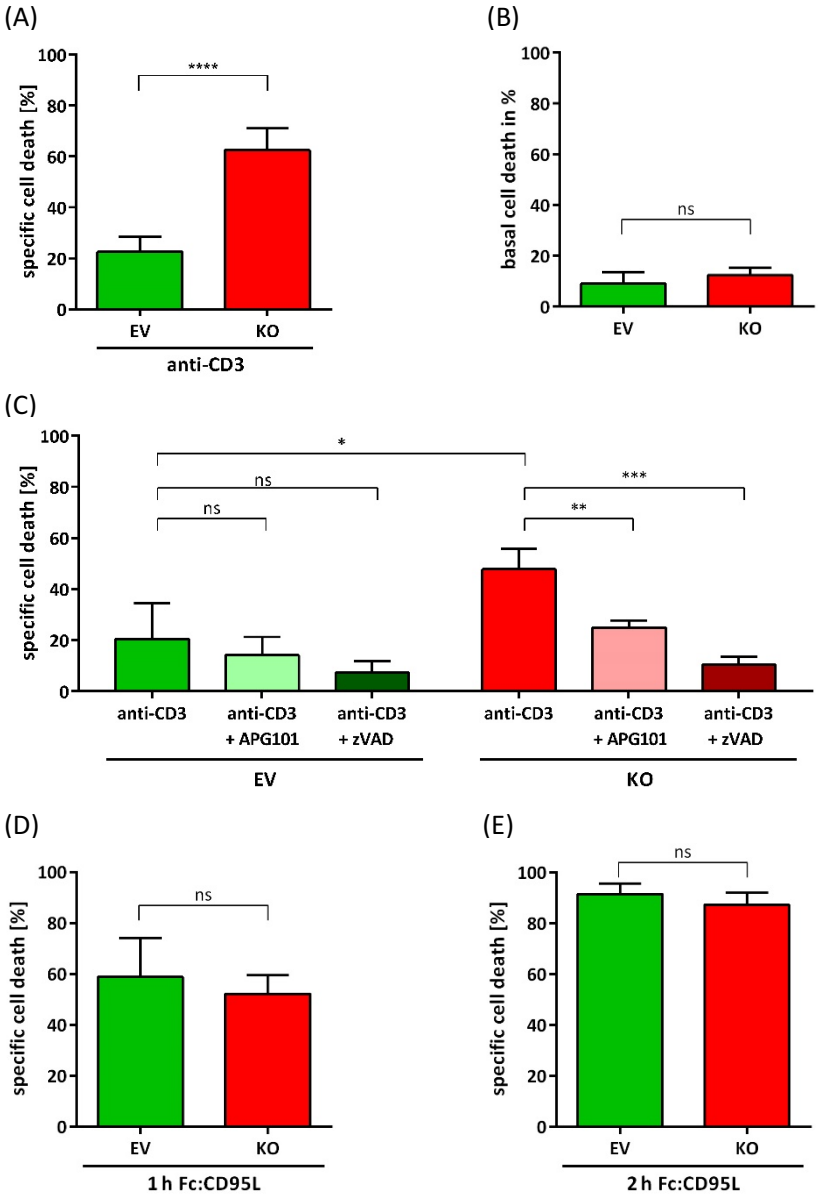

Figure 4.14: TXNIP KO Jurkat single cell clones exhibit enforced AICD compared to EV clones.
(A) Cell clones were stimulated with anti-CD3 antibodies for 48 h to induce AICD. Cell death was assessed by flow cytometry using AnxV-FITC and 7AAD and calculated as "specific cell death" normalised to untreated cells (n = 5). (B) "Basal cell death" of untreated cells from (A). (C) EV and TXNIP KO clones were pre-treated with or without NAC or APG101 for 15 min and then restimulated with anti-CD3 antibodies for 48 h to induce AICD. Cell death was calculated as "specific cell death" normalised to untreated cells (n = 4). (D and E) Cell clones were treated with recombinant Fc:CD95L for 1 h (D) or 2 h (E). Cell death was calculated as "specific cell death" normalised to untreated cells. Bars represent "specific cell death" as a mean of the three EV and TXNIP KO clones of one representative of two experiments. (A – E) Statistical significance was calculated using unpaired t-test (mean and SD, ns: $p > 0.05$, $^{**}p < 0.01$, $^{***}p < 0.001$).

5 Discussion

In the past decades evidence accumulated that ROS play a key role as second messengers in many physiologic processes *e.g.* TCR signalling [32, 33, 40, 44, 51, 53]. Strict control of the TCR-induced oxidative signal is a prerequisite for its physiological function as well as for the protection of cells from damaging effects of ROS [40]. This is achieved by the action of a variety of cellular reductants or antioxidative systems [42, 43]. The Trx system plays a major role in maintaining intracellular redox balance and is composed of Trx, TrxR and TXNIP [271]. Trx can be naturally inhibited by TXNIP and as such the Trx-TXNIP-interaction is a regulatory mechanism of cellular redox processes [272]. In addition, TXNIP modulates transcription and contributes to glucose uptake as well as proliferation independent of the function of Trx [233]. Considering that TXNIP influences TCR signalling at different levels, we hypothesise that TXNIP is involved in the regulation of T cell immune responses. The Jurkat T cell line, a model for CD95L-mediated AICD, was used to analyse the impact of TCR stimulation on TXNIP as well as on Trx. The modulatory effects of TXNIP on TCR signalling were investigated using TXNIP KO clones.

5.1 TCR-induced oxidative signalling is mandatory for T cell responses

Production of H_2O_2 is a hallmark of TCR signalling and required for CD95L-mediated AICD. Previously, mitochondria were identified as the main source of H_2O_2 involved in AICD. Production of mitochondrial-derived H_2O_2 is indispensable for TCR-induced CD95L gene expression by regulating activity of redox-sensitive transcription factors such as NFκB and AP1 [32, 33, 44, 53–55, 266, 273]. In line with these reports, Figure 4.1 demonstrated that TCR-induced ROS production is essential for CD95L-mediated AICD in Jurkat T cells. We verified our results by eliciting a similar response in terms of AICD following TCR stimulation of pre-activated human T cells (Figure 4.2) and confirmed the usage of Jurkat T cells as a suitable model for further analysis regarding TCR signalling. Taken together, TCR-induced ROS production is mandatory for T cell immune responses by facilitating and amplifying the signals initiated by receptor engagement. However, since oxidative stress is implicated in the pathology of various diseases, strict control of ROS is a prerequisite for proper T cell functions [274].

5.2 The Trx system does not contribute to ROS regulation following TCR stimulation

The Trx system which consists of TrxR, the redox active protein Trx and its negative regulator TXNIP is one of the major cellular antioxidant systems implicated in the aforementioned regulation of ROS required for T cell responses [214, 274]. Since T cell activation enhances ROS level, we investigated whether it also affects Trx activity. Figure 4.3A illustrated that the activity of Trx is enhanced upon TCR engagement in Jurkat T cells suggesting that the Trx system is involved in the regulation of TCR-induced ROS.

5.2.1 Activation-induced TXNIP suppression mediates enhanced Trx activity

We examined the mechanism underlying regulation of Trx activity in TCR signalling. One possibility is the interaction of Trx with TXNIP. By binding to the redox active centre of Trx, TXNIP inhibits activity of Trx [222, 223]. Accordingly, activation-induced rise of Trx activity was paralleled by TXNIP downregulation (Figure 4.3B – E, 4.4).

By comprehensively quantifying the HeLa cell proteome, Bekker-Jensen et al. demonstrate a low copy number of TXNIP in comparison to Trx [275]. This unbalanced ratio of protein amounts implies that Trx activity is unlikely affected by regulation *via* TXNIP. Although a number of studies demonstrate TXNIP-mediated suppression of Trx activity, these studies use TXNIP overexpressing model systems which may exhibit higher than physiological TXNIP levels [198, 221, 223, 226, 268]. Hence, it can be questioned whether the observed TCR stimulation-induced TXNIP suppression contributes to enhanced Trx activity in the present study. However, other reports provide evidence that the regulation of Trx by TXNIP plays a major role in physiological settings [226, 268, 276, 277]. Ogata et al. show that reduced interaction of TXNIP with Trx, due to decreased TXNIP expression, is mandatory for nuclear localisation of Trx. Interestingly, the usage of HeLa cells in the study of Ogata et al. suggests that despite this cell line exhibits an excess of Trx comparable to TXNIP protein amounts, a relative minor proportion of Trx bound to TXNIP can have major signalling effects.

Besides the direct impact of TXNIP on Trx activity, Nishiyama et al. report that the regulation of Trx activity *via* TXNIP is accompanied by changes of Trx expression [223]. This indicates that TXNIP indirectly controls Trx activity by modulating Trx protein level.

Since Trx protein expression remained unchanged in the same experimental setting (Figure 4.3C and E), contribution of Trx protein level to enhanced Trx activity can be excluded.

In summary, this study illustrates that reduction of TXNIP-Trx interactions by TCR-induced TXNIP downregulation contributes to increased Trx activity and, thereby, underlines the physiological relevance of TXNIP as negative regulator of Trx.

Another regulator of Trx activity is TrxR which is to date the only enzyme known to reduce Trx [207]. It can be speculated that a rise of TrxR expression or TrxR activity contributes to the observed TCR-induced increase of Trx activity. Whether TrxR is involved in regulation of Trx activity needs to be further investigated *e.g.* by determining TrxR expression level and changes of TrxR activity upon TCR stimulation.

5.2.2 Regulation of TXNIP suppression upon TCR stimulation

Here we show that enhanced Trx activity upon TCR stimulation is mediated by TXNIP suppression (Figure 4.3) and we further investigated the effector mechanism involved in TCR-induced TXNIP downregulation.

Since ROS suppress TXNIP expression in primary rat cardiomyocytes as well as human aortic smooth muscle cells [267, 268], we hypothesised that the observed suppression of TXNIP is caused by ROS produced upon TCR stimulation. In contrast to the literature [267, 268], Figure 4.5 and 4.6 illustrated that TXNIP downregulation upon TCR engagement is not ROS-mediated in Jurkat T cells. This difference can be explained by the use of distinct cell types from different species and by the use of distinct ROS sources. The studies by Schulze et al. and Wang et al. use mainly H_2O_2 treatment as oxidative stress stimulus whereas our study utilised TCR stimulation which indirectly leads to H_2O_2 production in rather low concentration with the potential to act as second messenger. Nonetheless, the results obtained in the present study are in accordance with a report describing that LPS-induced TXNIP suppression is not affected by antioxidant treatment in a murine macrophage cell line [278]. Thus, the present study demonstrates that TCR-induced TXNIP suppression is ROS-independent in Jurkat T cells but the effector mechanism involved remains elusive.

In general, TXNIP is considered as an early response gene due to fast changes in its expression upon induction of neuronal apoptosis [279] and its expression is regulated at

the level of protein synthesis and protein stability [246, 280, 281]. In line with these reports, this study showed rapid activation-induced TXNIP downregulation (Figure 4.7) mediated by accelerated proteasomal degradation as well as reduced protein synthesis (Figure 4.8).

Protein destruction is carried out by the ubiquitin-proteasome pathway. Specificity of ubiquitination is achieved by E3 ubiquitin ligases which transfer ubiquitin to the target protein resulting in its degradation by the proteasome [282]. The E3 ubiquitin ligase Itch is involved in the regulation of T cell activation, differentiation and tolerance induction [283]. Since Itch mediates poly-ubiquitination of TXNIP in 293T as well as U2OS cells [281], we assumed that Itch is involved in activation-induced degradation of TXNIP. However, knocking down Itch in Jurkat T cells could not confirm the reported Itch-mediated TXNIP degradation (Supplementary Figure 1).

Besides regulation of TXNIP level *via* accelerated proteasomal degradation, TXNIP mRNA expression was reduced upon TCR stimulation (Figure 4.3B and D, 4.4A, 4.7A) indicating the involvement of transcriptional regulators. TXNIP is a transcriptional target of the dimeric transcription factor MondoA:Mlx which negatively controls glucose uptake *via* TXNIP regulation [244]. It can be supposed that activation-induced changes in intracellular glucose level [53] influence MondoA:Mlx activity resulting in suppression of TXNIP transcription. However, this hypothesis needs to be further investigated *e.g.* by using chromatin immunoprecipitation (ChIP) assays and by introducing a knockdown of MondoA and/or Mlx.

Another modulator of TXNIP mRNA expression might be the transcription factor forkhead box protein O1 (FOXO1) which is a phosphatidylinositol 3 kinase (PI3K)-downstream effector and implicated in the regulation of T cell immune responses [284, 285]. Activation of the PI3K/Akt signalling pathway mediates FOXO1 dissociation from the TXNIP promotor as well as its nuclear export resulting in inhibition of TXNIP transcription in a model of synaptic activity [286]. Accordingly, other studies demonstrate that PI3K/Akt activation regulates TXNIP expression [287, 288]. Whether the FOXO1-PI3K/Akt axis contributes to TCR-induced TXNIP downregulation in Jurkat T cells observed in the present study was not validated yet and needs to be further analysed *e.g.* by using inhibitors of PI3K or knockdown of FOXO1. However, it should be noticed that Jurkat T cells exhibit constitutive PI3K/Akt activation due to the deficiency of the lipid phosphatase PTEN which is the

natural inhibitor of the PI3K/Akt pathway [289, 290]. Whether defective PTEN expression in Jurkat T cells may alter their response to TCR stimulation remains unclear. Thus, analysis concerning the impact of PI3K/Akt signalling on activation-induced TXNIP suppression in Jurkat T cells should be considered with caution and obtained results need to be validated with other model systems *e.g.* primary human T cells.

In general, gene expression is regulated by various mechanisms including reversible protein acetylation which is mediated by HATs and HDACs. Acetylation of transcription factors or histones results in enhanced whereas deacetylation of these proteins mediates reduced gene expression [227–229]. In pancreatic beta cells, glucose-induced TXNIP expression is mediated by transcription factor carbohydrate response element binding protein (ChREBP) which forms a complex with HAT p300 [291] pointing towards an involvement of protein acetylation in transcriptional regulation of TXNIP. Accordingly, treatment with the HDAC inhibitor SAHA enhance TXNIP protein level in different cancer cell lines [219] and our study further showed that SAHA treatment caused TXNIP accumulation in Jurkat T cells (Supplementary Figure 2). A rise of histone or transcription factor acetylation might mediate an increase of TXNIP transcription in this setting [229, 292]. Alternatively, enhanced acetylation of TXNIP might mask ubiquitination sites resulting in reduced proteasomal degradation [293]. Nevertheless, SAHA-mediated accumulation of TXNIP was not sufficient to overcome TCR stimulation-induced TXNIP suppression (Supplementary Figure 2) indicating that further regulatory mechanisms besides acetylation are involved in TXNIP regulation.

In summary, here we show that TCR engagement induced rapid TXNIP suppression by accelerating proteasomal degradation as well as reducing protein synthesis in Jurkat T cells. Whereas ROS-mediated suppression of TXNIP during TCR signalling can be excluded, the underlying effector mechanisms remain unknown. Knockdown experiments as well as the usage of specific kinases or pathway inhibitors could help to identify transcription factors or signalling pathways necessary for TCR stimulation-induced TXNIP suppression in Jurkat T cells.

5.2.3 Enhanced Trx activity does not regulate TCR-induced oxidative signal

Since activation-induced suppression of TXNIP resulted in enhanced Trx activity (Figure 4.3), TXNIP might regulate redox-mediated processes *via* Trx in Jurkat T cells. Hence, we hypothesised that the obtained rise of Trx activity contributes to ROS regulation upon TCR stimulation.

In order to test this hypothesis, we mimicked TCR-induced TXNIP suppression by introducing a CRIPSR-Cas9-mediated KO of TXNIP in Jurkat T cells (chapter 4.5). Similar to increased Trx activity observed upon activation-induced TXNIP downregulation (Figure 4.3), basal Trx activity was significantly enhanced due to TXNIP deficiency and not affected by changes of Trx expression (Figure 4.11A – B). This data verifies the role of TXNIP as negative regulator of Trx activity. In contrast to these results, TXNIP deficient mice exhibit no change of Trx activity [239, 241]. This discrepancy can be explained by different assay procedures (*e.g.* incubation time, readout in terms of optical density and increase of fluorescence) and/or by the use of different samples from distinct species (liver homogenates from mice and human T cell line). Nonetheless, the inhibitory effect of TXNIP on Trx activity has been demonstrated in various cell lines whereas the regulatory role of TXNIP was not consistently confirmed *in vivo* [294].

By using the generated TXNIP KO clones as a model system for activation-induced TXNIP suppression, we investigated whether increased Trx activity influences ROS level in TCR signalling. Contrary the hypothesis that enhanced Trx activity scavenges ROS, Figure 4.11C illustrated similar activation-induced ROS production in EV and TXNIP KO suggesting that other intracellular antioxidants contribute to ROS regulation upon TCR signalling. It is feasible that the GSH system which is the most abundant antioxidant system in cells [295, 296], is important for the regulation of the TCR-induced oxidative signal [297]. Although the GSH and the Trx system have many overlapping functions [298], the GSH system cannot compensate for all activities of the Trx system. For instance, the function of the Trx system is indispensable for nucleotide biosynthesis since it provides electrons to the RNR during activation-induced T cell proliferation [211]. In summary, this study showed that downregulation of TXNIP increases Trx activity which does not contribute to ROS regulation upon TCR stimulation.

5.3 TXNIP regulates activation-induced gene expression

Besides its function as antioxidant, Trx regulates DNA binding of redox-sensitive transcription factors *e.g.* NFκB and AP1 [64, 76, 113, 267] which are mandatory for TCR-induced gene expression [34–36]. Thus, we investigated whether enhanced Trx activity, mediated by TXNIP suppression, affects gene transcription in T cells. TCR stimulation resulted in increased expression of genes involved in T cell activation, differentiation, cytokine signalling as well as death in TXNIP KO compared to EV clones (Figure 4.12 and 4.13) indicating that TXNIP functions as a transcriptional inhibitor. Interestingly, TXNIP is identified as a component of transcriptional corepressor complexes which are associated with HDACs and facilitate suppression of gene expression *via* protein deacetylation [230–232]. This suggests that TXNIP regulates transcription in stimulated Jurkat T cells by modulation of Trx activity, by influencing protein acetylation or by a combination of both mechanisms. Further experiments including the usage of Trx inhibitors or protein complex immunoprecipitation (Co-IP), to uncover TXNIP-HDAC interactions, are needed to specify which mechanism caused altered gene expression. In general, the results obtained in TXNIP KO clones should be further confirmed by rescuing TXNIP expression in these KO cells. Although transduction experiments in TXNIP KO clones were performed, a rescue was not achieved so far and further experiments are needed. Nonetheless, Minn et al. report that TXNIP overexpression downregulates several genes in pancreatic beta cells [299] which underlines the inhibitory role of TXNIP on transcription. Consistent to the present study, the authors could not rule out whether TXNIP contributes to suppressed gene expression by interacting with HDACs, *via* Trx or whether a combination of both mechanisms is involved.

This study demonstrated that TXNIP functions as a transcriptional repressor in TCR signalling but the downstream mechanism involved in transcriptional regulation remains elusive. NFκB is a major regulator of gene expression and amongst others associated with the transcriptional response during T cell activation, proliferation as well as cell death [59, 60]. NFκB activation is regulated by several posttranslational modifications including Trx-mediated control of p50 thiol redox status [64, 65, 202] as well as acetylation status of p65 by transcriptional corepressors/coactivators [300, 301]. TXNIP is a component of corepressor complexes which mediate p65 deacetylation resulting in suppressed NFκB

activity [231, 232]. Since TXNIP as well as activity of Trx are implicated in activation of NFκB, we hypothesised that the rise of TCR-induced gene expression in TXNIP KO clones relies on regulation *via* NFκB. In line with our hypothesis, all genes upregulated by TXNIP deficiency following TCR stimulation (Figure 4.12) are designated as NFκB target genes [302–304]. Whether NFκB activity is controlled by TXNIP needs to be further investigated *e.g.* by assessing NFκB activity using luciferase assays or enzyme-linked immunosorbent assays (ELISAs).

In general, TCR stimulation results in activation of a plethora of transcription factors including NFκB, AP1 as well as NFAT which have distinct but also overlapping signal requirements and act in concert to achieve transcription of *e.g.* the CD95L or IL2 gene [32, 34, 35, 305]. The rise of activation-induced CD95L and IL2 gene expression in TXNIP KO clones (Figure 4.13A and E) indicates that TXNIP regulates activation of several transcription factors.

Similar to regulation of NFκB activity, AP1 transcriptional activity is determined by its redox status which is controlled by Trx and Ref-1 [76, 306] as well as by its acetylation status [307, 308]. This suggests that TXNIP can influence AP1-induced transcription. Accordingly, the differentially regulated genes identified (Figure 4.12 and 4.13) are also described as AP1 target genes [302]. However, it should be noticed that in this setting EGR2 and GZMB are only depicted as AP1 target genes in mouse.

In contrast to NFκB and AP1, transcriptional control of NFAT does not rely on Trx-regulated redox status. Regulation of NFAT activity depends on the intracellular Ca^{2+} level [309] which is not associated with the TXNIP-Trx axis so far. However, as described for NFκB and AP1, acetylation contributes to NFAT activation [310, 311] indicating that NFAT represents another possible target of TXNIP-containing transcriptional corepressor complexes. Accordingly, the observed activation-induced differentially expressed genes in TXNIP KO clones, namely EGR2 [312], GMCSF [313], TNFA [314], IFNG [315, 316], GZMB [317] as well as the above-mentioned CD95L and IL2 are all reported to be controlled by NFAT.

Taken together, TXNIP acts as a transcriptional repressor and impacts gene transcription most likely by controlling activity of several transcription factors including NFκB, AP1 as well as NFAT. The influence of TXNIP on the activity of these transcription factors needs to be verified *e.g.* by using a ChIP or an electrophoretic mobility shift assay (EMSA).

5.4 TXNIP regulates CD95L-mediated AICD

Restimulation of T cells leads to AICD which is commonly known to involve the CD95-CD95L system [153, 318, 319]. Since TCR engagement of TXNIP KO clones resulted in a rise of CD95L transcription (Figure 4.13A), we hypothesised that TXNIP influences AICD. As shown in Figure 4.14A, AICD was significantly enhanced in TXNIP KO clones and the impact of CD95L on AICD was verified by blocking CD95L leading to a substantial inhibition of AICD (Figure 4.14C). In addition, induction of similar cell death in EV and TXNIP KO clones using recombinant CD95L (Figure 4.14 D and E) revealed no alterations of the basic CD95 signalling pathway due to TXNIP deficiency which confirmed the link between CD95L transcription and AICD.

In line with previous reports [318, 320], inhibition of AICD by neutralising CD95L was in the range of 50 % (Figure 4.14C) indicating that CD95-independent mechanisms also contribute to AICD in Jurkat T cells. For instance, TNFα might be involved but its role is controversial. While TNFα and TNFR deficient mice show normal AICD [321], others report that blocking of TNF decreases TCR-induced cell death [322]. Since TNFA mRNA expression is elevated in TCR-stimulated TXNIP KO clones (Figure 4.13F), it can be assumed that TNFα is involved in AICD of Jurkat T cells. Despite these indications for a role of TNFα, we found no alteration in AICD of TXNIP KO clones in the presence of TNFα blockade (Supplementary Figure 3). While Zheng et al. report AICD of $CD8^+$ T cells following TNFR stimulation, our data as well as data from Dhein et al. and Lawrence et al. suggest that TNFα has no major impact on AICD in $CD4^+$ Jurkat T cells [318, 323].

Another death ligand involved in AICD of Jurkat T cells is TRAIL [323, 324]. However, since microarray analysis revealed no altered TRAIL transcription in TXNIP KO clones (data not shown), its contribution to AICD of Jurkat T cells seems unlikely. Nevertheless, an impact of TRAIL on AICD in this study cannot completely be excluded and should be further evaluated *e.g.* by using neutralising TRAIL antibodies.

Besides its regulation *via* death receptors, AICD can be induced by GZMB [325, 326]. In accordance with Huang et al. who illustrate that Jurkat T cells upregulate GZMB expression following activation [327], TCR-induced GZMB mRNA expression was enhanced in TXNIP KO clones (Figure 4.13C). Whether GZMB contributes to AICD in this study has yet to be confirmed.

Taken together, these results underline the major role of CD95L for AICD and illustrate that TXNIP regulates AICD by controlling CD95L expression in Jurkat T cells. However, another TXNIP-mediated mechanism seems to be involved in AICD, most likely a GZMB-dependent pathway.

AICD is controlled by expression of CD95L [328] which is restricted to particular cell types including activated T cells [153, 154]. Accordingly, upregulation of CD95L mRNA expression coincides with a rise of AICD following TCR stimulation of Jurkat T cells (Figure 4.1B and 4.13A). As discussed in section 5.3, TCR-induced CD95L gene expression is influenced by TXNIP and controlled by several transcription factors including NFκB, AP1 and NFAT which act cooperatively to induce its transcription [35, 305].

In addition to the direct effects of these transcription factors, they also support transcription of other factors that favour CD95L expression. For instance, NFAT mediates expression of Egr2 which binds to the CD95L promotor [329, 330]. TCR-induced rise of EGR2 transcription in TXNIP KO clones (Figure 4.13G) indicates that CD95L mRNA expression might be indirectly influenced by NFAT-Egr2 axis. Likewise, IFNγ initiates CD95L mRNA expression [331–333] and its gene expression was found to be increased in TCR-stimulated TXNIP KO clones (Figure 4.13D). Whether Egr2 or IFNγ contribute to the control of CD95L transcription needs to be further investigated *e.g.* by ChIP assay, EMSA or IFNγ blockage.

In summary, TXNIP deficiency sensitises Jurkat T cells to AICD by enforcing CD95L mRNA expression and, thereby, underlines the role of TXNIP as transcriptional inhibitor as well as its impact on the regulation of T cell immune responses.

5.5 Impact of TXNIP on glucose uptake and proliferation

We showed that TXNIP is a negative regulator of activation-induced gene expression and, thus, T cell immune responses. Induction of immune responses is a substantial metabolic challenge. Meeting the energetic and biosynthetic requirements for transcriptional and translational programmes that promote TCR-induced growth, proliferation and effector functions relies on metabolic reprogramming from oxidative phosphorylation to aerobic glycolysis. The latter is accompanied by increased glucose uptake as well as enhanced glycolytic flux [53, 248, 249]. Since TXNIP is considered as a negative regulator of glucose

uptake [334, 335], it can be assumed that activation-induced TXNIP suppression promotes acquisition of glucose to fuel aerobic glycolysis. In line, Elgort et al. report that TXNIP downregulation coincides with enhanced uptake of glucose in activated murine T lymphocytes [247]. As discussed in 5.2.2, activity of the dimeric transcription factor MondoA:Mlx controls TXNIP expression and is inhibited by an increased glycolytic flux [244]. Whether MondoA:Mlx controls TXNIP suppression which in turn promotes glucose uptake to fuel aerobic glycolysis upon TCR stimulation of Jurkat T cells needs to be analysed in future studies *e.g.* by examining glucose uptake in TXNIP KO clones.

Besides its role as negative regulator of glucose uptake, TXNIP controls cell proliferation. By regulating Trx activity, TXNIP affects the function of Trx as an autocrine growth factor [336]. Trx promotes cell proliferation *e.g.* by activating transcription factors [40] or providing reducing equivalents for nucleotide biosynthesis [211]. TXNIP inhibits cell division indirectly by suppressing Trx function and directly by influencing the activity of cyclins which are important regulators of cell cycle progression [230, 337]. Thus, we investigated whether TXNIP expression influences proliferation of Jurkat T cells. TXNIP KO clones exhibited no change of basal proliferation (Supplementary Figure 4). Contrary to these results, Nishinaka et al. report that TXNIP overexpression suppresses T cell growth [338]. This discrepancy may be due to the use of different T cell lines. Nishinaka et al. use human T-lymphotropic virus type 1 (HTLV-I) transformed human T-cell leukemia cells whereas we utilised Jurkat T cells. It should be considered, that Jurkat cells are cancer cells which may already proliferate at a high rate. Hence, analysis concerning the impact of TXNIP on proliferation should be validated in another model system *e.g.* primary human T cells.

In addition to its role as a transcriptional inhibitor, TXNIP may contribute to induction of T cell immune responses by controlling glucose uptake as well as proliferation following TCR stimulation of Jurkat T cells. Thus, future studies should address whether TXNIP affects TCR signalling by regulating glucose uptake and cell growth.

5.6 Conclusion

The present study shows that TXNIP is involved in regulation of TCR signalling. TXNIP expression was downregulated due to increased proteasomal degradation as well as reduced protein synthesis upon TCR stimulation. Blocking activation-induced ROS production did not affect TXNIP level. Additional studies are needed to identify the contributing effector mechanism leading to the reduction of TXNIP upon TCR engagement.

Activation-induced downregulation of TXNIP resulted in a rise of Trx activity. Despite its well-known function as antioxidant, enhanced Trx activity did not contribute to ROS regulation in the setting of TCR stimulation.

However, this study revealed that rather than controlling activation-induced ROS level, TXNIP influences gene expression by acting as a transcriptional inhibitor. Expression of genes involved in T cell activation, differentiation, cytokine signalling as well as cell death was affected by TXNIP following TCR engagement. Whether TXNIP contributes to stimulation-induced transcription by influencing protein acetylation, by modulating Trx activity or if a combination of both mechanisms is involved remains to be investigated. Regardless of the underlying mechanism, TXNIP might control gene expression by regulating the activity of one or various transcription factors including NFκB, AP1 and NFAT which act in concert to induce specific transcriptional programmes. Figure 5.1 illustrates a model for TXNIP-mediated regulation of stimulation-induced gene expression.

The role of TXNIP as negative regulator of transcription was underlined by using CD95L-mediated AICD as a readout for the impact of TXNIP on activation-induced CD95L expression. Deficiency of TXNIP lead to increased CD95L transcription upon TCR engagement which in turn resulted in a rise of AICD.

Although the underlying mechanisms remain to be elucidated, this study demonstrates that TXNIP is involved in the regulation of TCR signalling by acting as transcriptional inhibitor. Therefore, TXNIP might be considered as a potential therapeutic target to manipulate T cell responses *e.g.* in autoimmune or tumour diseases.

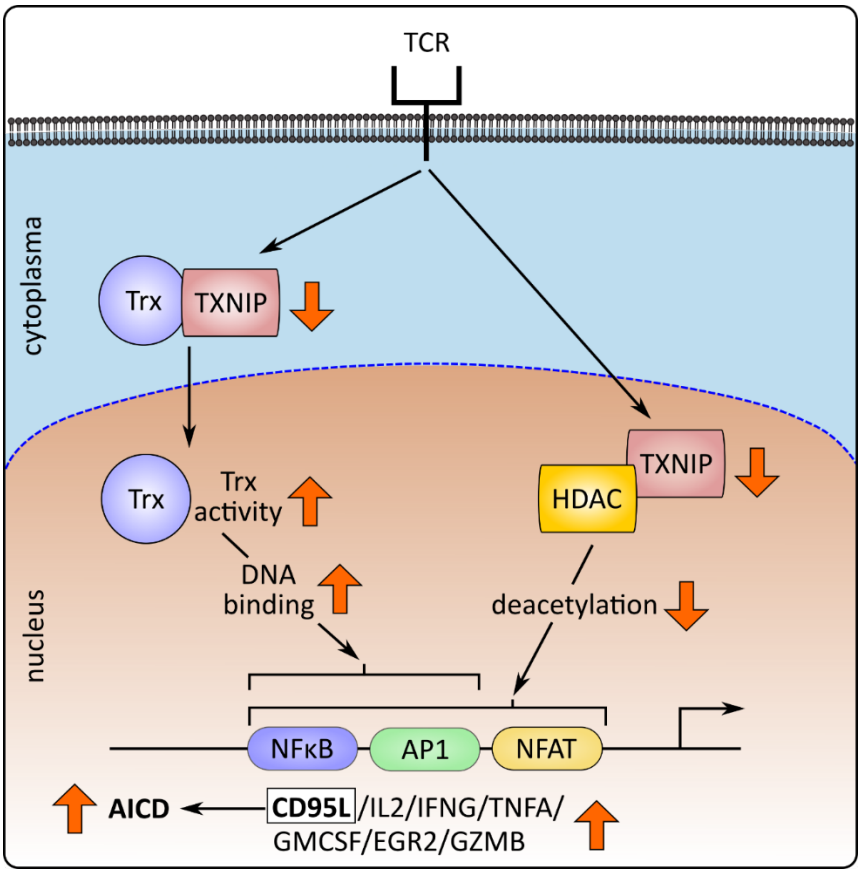

Figure 5.1: Scheme of TXNIP-mediated regulation of activation-induced gene expression in T cells.

TXNIP is a natural inhibitor of Trx. Therefore, stimulation-induced downregulation of TXNIP results in a rise of Trx activity. Increased Trx activity in turn can enhance DNA binding of redox-sensitive transcription factors such as NFκB and AP1. In addition, TXNIP can interact with HDACs which facilitate suppression of gene expression *via* protein deacetylation. Thus, TXNIP reduction following TCR stimulation might result in diminished association with HDACs. This in turn would lead to increased acetylation which mediates *e.g.* activation of transcription factors such as NFκB, AP1 and NFAT. TCR-induced TXNIP downregulation contributes to activation-induced transcription either by one of these or a combination of both mechanisms. TXNIP-mediated stimulation-induced gene expression includes transcription of CD95L mediating AICD in apoptosis-sensitive T cells.

References

1. Janeway CA (1992) The immune system evolved to discriminate infectious nonself from noninfectious self. Immunology Today 13:11–16

2. Janeway CA, Medzhitov R (2002) Innate Immune Recognition. Annual Review of Immunology 20:197–216

3. Cooper MD, Alder MN (2006) The evolution of adaptive immune systems. Cell 124:815–822

4. Markert ML, Boeck A, Hale LP, et al (1999) Transplantation of thymus tissue in complete DiGeorge syndrome. N Engl J Med 341:1180–1189

5. Miller JF (1961) Immunological function of the thymus. Lancet 2:748–749

6. Donskoy E, Goldschneider I (1992) Thymocytopoiesis is maintained by blood-borne precursors throughout postnatal life. A study in parabiotic mice. J Immunol 148:1604–1612

7. Tonegawa S, Steinberg C, Dube S, Bernardini A (1974) Evidence for Somatic Generation of Antibody Diversity. Proc Natl Acad Sci U S A 71:4027–4031

8. Klein L, Kyewski B, Allen PM, Hogquist KA (2014) Positive and negative selection of the T cell repertoire: what thymocytes see (and don't see). Nat Rev Immunol 14:377–391

9. Starr TK, Jameson SC, Hogquist KA (2003) Positive and negative selection of T cells. Annu Rev Immunol 21:139–176

10. Green DR, Droin N, Pinkoski M (2003) Activation-induced cell death in T cells. Immunol Rev 193:70–81

11. Kabelitz D, Janssen O (1997) Antigen-induced death of T-lymphocytes. Front Biosci 2:d61-77

12. Medzhitov R, Janeway CA (1997) Innate immunity: impact on the adaptive immune response. Current Opinion in Immunology 9:4–9

13. Blumberg RS, Ley S, Sancho J, Lonberg N, Lacy E, McDermott F, Schad V, Greenstein JL, Terhorst C (1990) Structure of the T-cell antigen receptor: evidence for two CD3 epsilon subunits in the T-cell receptor-CD3 complex. Proc Natl Acad Sci USA 87:7220–7224

14. Clevers H, Alarcon B, Wileman T, Terhorst C (1988) The T cell receptor/CD3 complex: a dynamic protein ensemble. Annu Rev Immunol 6:629–662

15. Koning F, Maloy WL, Coligan JE (1990) The implications of subunit interactions for the structure of the T cell receptor-CD3 complex. Eur J Immunol 20:299–305

16. Weiss A, Imboden J, Hardy K, Manger B, Terhorst C, Stobo J (1986) The role of the T3/antigen receptor complex in T-cell activation. Annu Rev Immunol 4:593–619

17. Cambier JC (1995) New nomenclature for the Reth motif (or ARH1/TAM/ARAM/YXXL). Immunol Today 16:110

18. Letourneur F, Klausner RD (1992) Activation of T cells by a tyrosine kinase activation domain in the cytoplasmic tail of CD3 epsilon. Science 255:79–82

19. Reth M (1989) Antigen receptor tail clue. Nature 338:383–384

20. Wegener AM, Letourneur F, Hoeveler A, Brocker T, Luton F, Malissen B (1992) The T cell receptor/CD3 complex is composed of at least two autonomous transduction modules. Cell 68:83–95

21. Weiss A, Littman DR (1994) Signal transduction by lymphocyte antigen receptors. Cell 76:263–274

22. van Oers NS, Weiss A (1995) The Syk/ZAP-70 protein tyrosine kinase connection to antigen receptor signalling processes. Semin Immunol 7:227–236

23. Iwashima M, Irving BA, van Oers NS, Chan AC, Weiss A (1994) Sequential interactions of the TCR with two distinct cytoplasmic tyrosine kinases. Science 263:1136–1139

24. Clements JL, Boerth NJ, Lee JR, Koretzky GA (1999) Integration of T cell receptor-dependent signaling pathways by adapter proteins. Annu Rev Immunol 17:89–108

25. Zhang W, Sloan-Lancaster J, Kitchen J, Trible RP, Samelson LE (1998) LAT: the ZAP-70 tyrosine kinase substrate that links T cell receptor to cellular activation. Cell 92:83–92

26. Cockcroft S, Thomas GM (1992) Inositol-lipid-specific phospholipase C isoenzymes and their differential regulation by receptors. Biochem J 288 (Pt 1):1–14

27. Lewis RS (2001) Calcium signaling mechanisms in T lymphocytes. Annu Rev Immunol 19:497–521

28. Crabtree GR (1999) Generic signals and specific outcomes: signaling through Ca2+, calcineurin, and NF-AT. Cell 96:611–614

29. Cantrell D (1996) T cell antigen receptor signal transduction pathways. Annu Rev Immunol 14:259–274

30. Werlen G, Jacinto E, Xia Y, Karin M (1998) Calcineurin preferentially synergizes with PKC-theta to activate JNK and IL-2 promoter in T lymphocytes. EMBO J 17:3101–3111

31. Isakov N, Altman A (2002) Protein kinase C(theta) in T cell activation. Annu Rev Immunol 20:761–794

32. Gülow K, Kaminski M, Darvas K, Süss D, Li-Weber M, Krammer PH (2005) HIV-1 trans-activator of transcription substitutes for oxidative signaling in activation-induced T cell death. J Immunol 174:5249–5260

33. Kaminski M, Kiessling M, Süss D, Krammer PH, Gülow K (2007) Novel role for mitochondria: protein kinase C theta-dependent oxidative signaling organelles in activation-induced T-cell death. Mol Cell Biol 27:3625–3639

34. Katsiari CG, Tsokos GC (2006) Transcriptional repression of interleukin-2 in human systemic lupus erythematosus. Autoimmun Rev 5:118–121

35. Li-Weber M, Krammer PH (2003) Function and regulation of the CD95 (APO-1/Fas) ligand in the immune system. Semin Immunol 15:145–157

36. Li-Weber M, Krammer PH (2003) Regulation of IL4 gene expression by T cells and therapeutic perspectives. Nat Rev Immunol 3:534–543

37. Kamiński MM, Röth D, Krammer PH, Gülow K (2013) Mitochondria as oxidative signaling organelles in T-cell activation: physiological role and pathological implications. Arch Immunol Ther Exp (Warsz) 61:367–384

38. Truneh A, Albert F, Golstein P, Schmitt-Verhulst AM (1985) Early steps of lymphocyte activation bypassed by synergy between calcium ionophores and phorbol ester. Nature 313:318–320

39. Tsoukas CD, Landgraf B, Bentin J, Valentine M, Lotz M, Vaughan JH, Carson DA (1985) Activation of resting T lymphocytes by anti-CD3 (T3) antibodies in the absence of monocytes. The Journal of Immunology 135:1719–1723

40. Dröge W (2002) Free radicals in the physiological control of cell function. Physiol Rev 82:47–95

41. Reth M (2002) Hydrogen peroxide as second messenger in lymphocyte activation. Nat Immunol 3:1129–1134

42. Paget MSB, Buttner MJ (2003) Thiol-based regulatory switches. Annu Rev Genet 37:91–121

43. Rhee SG, Bae YS, Lee SR, Kwon J (2000) Hydrogen peroxide: a key messenger that modulates protein phosphorylation through cysteine oxidation. Sci STKE 2000:pe1

44. Devadas S, Zaritskaya L, Rhee SG, Oberley L, Williams MS (2002) Discrete generation of superoxide and hydrogen peroxide by T cell receptor stimulation: selective regulation of mitogen-activated protein kinase activation and fas ligand expression. J Exp Med 195:59–70

45. Bauer MK, Vogt M, Los M, Siegel J, Wesselborg S, Schulze-Osthoff K (1998) Role of reactive oxygen intermediates in activation-induced CD95 (APO-1/Fas) ligand expression. J Biol Chem 273:8048–8055

46. Chaudhri G, Clark IA, Hunt NH, Cowden WB, Ceredig R (1986) Effect of antioxidants on primary alloantigen-induced T cell activation and proliferation. J Immunol 137:2646–2652

47. Chaudhri G, Hunt NH, Clark IA, Ceredig R (1988) Antioxidants inhibit proliferation and cell surface expression of receptors for interleukin-2 and transferrin in T lymphocytes stimulated with phorbol myristate acetate and ionomycin. Cell Immunol 115:204–213

48. Sandstrom PA, Mannie MD, Buttke TM (1994) Inhibition of activation-induced death in T cell hybridomas by thiol antioxidants: oxidative stress as a mediator of apoptosis. J Leukoc Biol 55:221–226

49. Yi JS, Holbrook BC, Michalek RD, Laniewski NG, Grayson JM (2006) Electron transport complex I is required for CD8+ T cell function. J Immunol 177:852–862

50. Los M, Schenk H, Hexel K, Baeuerle PA, Dröge W, Schulze-Osthoff K (1995) IL-2 gene expression and NF-kappa B activation through CD28 requires reactive oxygen production by 5-lipoxygenase. EMBO J 14:3731–3740

51. Jackson SH, Devadas S, Kwon J, Pinto LA, Williams MS (2004) T cells express a phagocyte-type NADPH oxidase that is activated after T cell receptor stimulation. Nat Immunol 5:818–827

52. Kwon J, Shatynski KE, Chen H, Morand S, de Deken X, Miot F, Leto TL, Williams MS (2010) The nonphagocytic NADPH oxidase Duox1 mediates a positive feedback loop during T cell receptor signaling. Sci Signal 3:ra59

53. Kamiński MM, Sauer SW, Kamiński M, Opp S, Ruppert T, Grigaravičius P, Grudnik P, Gröne H-J, Krammer PH, Gülow K (2012) T cell activation is driven by an ADP-dependent glucokinase linking enhanced glycolysis with mitochondrial reactive oxygen species generation. Cell Rep 2:1300–1315

54. Röth D, Krammer PH, Gülow K (2014) Dynamin related protein 1-dependent mitochondrial fission regulates oxidative signalling in T cells. FEBS Lett 588:1749–1754

55. Kaminski MM, Sauer SW, Klemke C-D, Süss D, Okun JG, Krammer PH, Gülow K (2010) Mitochondrial reactive oxygen species control T cell activation by regulating IL-2 and IL-4 expression: mechanism of ciprofloxacin-mediated immunosuppression. J Immunol 184:4827–4841

56. Knorre DG, Kudryashova NV, Godovikova TS (2009) Chemical and functional aspects of posttranslational modification of proteins. Acta Naturae 1:29–51

57. Caselli A, Marzocchini R, Camici G, Manao G, Moneti G, Pieraccini G, Ramponi G (1998) The inactivation mechanism of low molecular weight phosphotyrosine-protein phosphatase by H2O2. J Biol Chem 273:32554–32560

58. Kwon J, Qu C-K, Maeng J-S, Falahati R, Lee C, Williams MS (2005) Receptor-stimulated oxidation of SHP-2 promotes T-cell adhesion through SLP-76-ADAP. EMBO J 24:2331–2341

59. Gerondakis S, Siebenlist U (2010) Roles of the NF-κB Pathway in Lymphocyte Development and Function. Cold Spring Harb Perspect Biol. doi: 10.1101/cshperspect.a000182

60. Oh H, Ghosh S (2013) NF-κB: Roles and Regulation In Different CD4+ T cell subsets. Immunol Rev 252:41–51

61. Ghosh S, May MJ, Kopp EB (1998) NF-kappa B and Rel proteins: evolutionarily conserved mediators of immune responses. Annu Rev Immunol 16:225–260

62. Gloire G, Piette J (2009) Redox regulation of nuclear post-translational modifications during NF-kappaB activation. Antioxid Redox Signal 11:2209–2222

63. Kabe Y, Ando K, Hirao S, Yoshida M, Handa H (2005) Redox regulation of NF-kappaB activation: distinct redox regulation between the cytoplasm and the nucleus. Antioxid Redox Signal 7:395–403

64. Matthews JR, Wakasugi N, Virelizier JL, Yodoi J, Hay RT (1992) Thioredoxin regulates the DNA binding activity of NF-kappa B by reduction of a disulphide bond involving cysteine 62. Nucleic Acids Res 20:3821–3830

65. Nishi T, Shimizu N, Hiramoto M, et al (2002) Spatial redox regulation of a critical cysteine residue of NF-kappa B in vivo. J Biol Chem 277:44548–44556

66. Okamoto T, Ogiwara H, Hayashi T, Mitsui A, Kawabe T, Yodoi J (1992) Human thioredoxin/adult T cell leukemia-derived factor activates the enhancer binding protein of human immunodeficiency virus type 1 by thiol redox control mechanism. Int Immunol 4:811–819

67. Toledano MB, Leonard WJ (1991) Modulation of transcription factor NF-kappa B binding activity by

oxidation-reduction in vitro. Proc Natl Acad Sci U S A 88:4328–4332

68. Israël N, Gougerot-Pocidalo MA, Aillet F, Virelizier JL (1992) Redox status of cells influences constitutive or induced NF-kappa B translocation and HIV long terminal repeat activity in human T and monocytic cell lines. The Journal of Immunology 149:3386–3393

69. Schreck R, Rieber P, Baeuerle PA (1991) Reactive oxygen intermediates as apparently widely used messengers in the activation of the NF-kappa B transcription factor and HIV-1. EMBO J 10:2247–2258

70. Abate C, Patel L, Rauscher FJ, Curran T (1990) Redox regulation of fos and jun DNA-binding activity in vitro. Science 249:1157–1161

71. Rincón M, Flavell RA (1994) AP-1 transcriptional activity requires both T-cell receptor-mediated and co-stimulatory signals in primary T lymphocytes. EMBO J 13:4370–4381

72. Karin M, Liu Z g, Zandi E (1997) AP-1 function and regulation. Curr Opin Cell Biol 9:240–246

73. Angel P, Karin M (1991) The role of Jun, Fos and the AP-1 complex in cell-proliferation and transformation. Biochim Biophys Acta 1072:129–157

74. Karin M, Smeal T (1992) Control of transcription factors by signal transduction pathways: the beginning of the end. Trends Biochem Sci 17:418–422

75. Filomeni G, Rotilio G, Ciriolo MR (2005) Disulfide relays and phosphorylative cascades: partners in redox-mediated signaling pathways. Cell Death Differ 12:1555–1563

76. Hirota K, Matsui M, Iwata S, Nishiyama A, Mori K, Yodoi J (1997) AP-1 transcriptional activity is regulated by a direct association between thioredoxin and Ref-1. Proc Natl Acad Sci USA 94:3633–3638

77. Xanthoudakis S, Miao G, Wang F, Pan YC, Curran T (1992) Redox activation of Fos-Jun DNA binding activity is mediated by a DNA repair enzyme. EMBO J 11:3323–3335

78. Krammer PH (2000) CD95's deadly mission in the immune system. Nature 407:789–795

79. Algeciras-Schimnich A, Griffith TS, Lynch DH, Paya CV (1999) Cell cycle-dependent regulation of FLIP levels and susceptibility to Fas-mediated apoptosis. J Immunol 162:5205–5211

80. Lenardo MJ (1991) Interleukin-2 programs mouse alpha beta T lymphocytes for apoptosis. Nature 353:858–861

81. Refaeli Y, Van Parijs L, London CA, Tschopp J, Abbas AK (1998) Biochemical mechanisms of IL-2-regulated Fas-mediated T cell apoptosis. Immunity 8:615–623

82. Xiao S, Matsui K, Fine A, Zhu B, Marshak-Rothstein A, Widom RL, Ju ST (1999) FasL promoter activation by IL-2 through SP1 and NFAT but not Egr-2 and Egr-3. Eur J Immunol 29:3456–3465

83. Cookson BT, Brennan MA (2001) Pro-inflammatory programmed cell death. Trends Microbiol 9:113–114

84. Fietta P (2006) Many ways to die: passive and active cell death styles. Riv Biol 99:69–83

85. Galluzzi L, Vicencio JM, Kepp O, Tasdemir E, Maiuri MC, Kroemer G (2008) To die or not to die: that is the

autophagic question. Curr Mol Med 8:78–91

86. Tait SWG, Ichim G, Green DR (2014) Die another way--non-apoptotic mechanisms of cell death. J Cell Sci 127:2135–2144

87. Vandenabeele P, Galluzzi L, Vanden Berghe T, Kroemer G (2010) Molecular mechanisms of necroptosis: an ordered cellular explosion. Nat Rev Mol Cell Biol 11:700–714

88. Elmore S (2007) Apoptosis: a review of programmed cell death. Toxicol Pathol 35:495–516

89. Kerr JF, Wyllie AH, Currie AR (1972) Apoptosis: a basic biological phenomenon with wide-ranging implications in tissue kinetics. Br J Cancer 26:239–257

90. Savill J, Fadok V, Henson P, Haslett C (1993) Phagocyte recognition of cells undergoing apoptosis. Immunol Today 14:131–136

91. Pellettieri J, Alvarado AS (2007) Cell Turnover and Adult Tissue Homeostasis: From Humans to Planarians. Annual Review of Genetics 41:83–105

92. Ravichandran KS (2010) Find-me and eat-me signals in apoptotic cell clearance: progress and conundrums. J Exp Med 207:1807–1817

93. Owen JJ, Jenkinson EJ (1992) Apoptosis and T-cell repertoire selection in the thymus. Ann N Y Acad Sci 663:305–310

94. Surh CD, Sprent J (1994) T-cell apoptosis detected in situ during positive and negative selection in the thymus. Nature 372:100–103

95. Akbar AN, Salmon M (1997) Cellular environments and apoptosis: tissue microenvironments control activated T-cell death. Immunology Today 18:72–76

96. Gronski MA, Weinem M (2006) Death Pathways in T Cell Homeostasis and Their Role in Autoimmune Diabetes. Rev Diabet Stud 3:88–95

97. Thompson CB (1995) Apoptosis in the pathogenesis and treatment of disease. Science 267:1456–1462

98. Kawasaki E (2014) Type 1 Diabetes and Autoimmunity. Clin Pediatr Endocrinol 23:99–105

99. Mountz JD, Wu J, Cheng J, Zhou T (1994) Autoimmune disease. A problem of defective apoptosis. Arthritis Rheum 37:1415–1420

100. Badley AD, Pilon AA, Landay A, Lynch DH (2000) Mechanisms of HIV-associated lymphocyte apoptosis. Blood 96:2951–2964

101. Finkel TH, Tudor-Williams G, Banda NK, Cotton MF, Curiel T, Monks C, Baba TW, Ruprecht RM, Kupfer A (1995) Apoptosis occurs predominantly in bystander cells and not in productively infected cells of HIV- and SIV-infected lymph nodes. Nat Med 1:129–134

102. Gougeon ML, Lecoeur H, Dulioust A, Enouf MG, Crouvoiser M, Goujard C, Debord T, Montagnier L (1996) Programmed cell death in peripheral lymphocytes from HIV-infected persons: increased susceptibility to apoptosis of CD4 and CD8 T cells correlates with lymphocyte activation and with disease progression. J Immunol 156:3509–3520

103. Earnshaw WC, Martins LM, Kaufmann SH (1999) Mammalian Caspases: Structure, Activation,

Substrates, and Functions During Apoptosis. Annual Review of Biochemistry 68:383–424

104. Hengartner MO (2000) The biochemistry of apoptosis. Nature 407:770–776

105. Thornberry NA, Lazebnik Y (1998) Caspases: enemies within. Science 281:1312–1316

106. Igney FH, Krammer PH (2002) Death and anti-death: tumour resistance to apoptosis. Nat Rev Cancer 2:277–288

107. Cory S, Adams JM (2002) The Bcl2 family: regulators of the cellular life-or-death switch. Nat Rev Cancer 2:647–656

108. Erlacher M, Michalak EM, Kelly PN, Labi V, Niederegger H, Coultas L, Adams JM, Strasser A, Villunger A (2005) BH3-only proteins Puma and Bim are rate-limiting for gamma-radiation- and glucocorticoid-induced apoptosis of lymphoid cells in vivo. Blood 106:4131–4138

109. Acehan D, Jiang X, Morgan DG, Heuser JE, Wang X, Akey CW (2002) Three-dimensional structure of the apoptosome: implications for assembly, procaspase-9 binding, and activation. Mol Cell 9:423–432

110. Lorenzo HK, Susin SA (2004) Mitochondrial effectors in caspase-independent cell death. FEBS Lett 557:14–20

111. Bouillet P, O'Reilly LA (2009) CD95, BIM and T cell homeostasis. Nat Rev Immunol 9:514–519

112. Du C, Fang M, Li Y, Li L, Wang X (2000) Smac, a mitochondrial protein that promotes cytochrome c-dependent caspase activation by eliminating IAP inhibition. Cell 102:33–42

113. Schroeder A, Warnken U, Röth D, et al (2017) Targeting Thioredoxin-1 by dimethyl fumarate induces ripoptosome-mediated cell death. Sci Rep 7:43168

114. Suzuki Y, Imai Y, Nakayama H, Takahashi K, Takio K, Takahashi R (2001) A serine protease, HtrA2, is released from the mitochondria and interacts with XIAP, inducing cell death. Mol Cell 8:613–621

115. Candé C, Cecconi F, Dessen P, Kroemer G (2002) Apoptosis-inducing factor (AIF): key to the conserved caspase-independent pathways of cell death? J Cell Sci 115:4727–4734

116. Li LY, Luo X, Wang X (2001) Endonuclease G is an apoptotic DNase when released from mitochondria. Nature 412:95–99

117. Schulze-Osthoff K, Ferrari D, Los M, Wesselborg S, Peter ME (1998) Apoptosis signaling by death receptors. Eur J Biochem 254:439–459

118. Smith CA, Farrah T, Goodwin RG (1994) The TNF receptor superfamily of cellular and viral proteins: activation, costimulation, and death. Cell 76:959–962

119. Itoh N, Yonehara S, Ishii A, Yonehara M, Mizushima S, Sameshima M, Hase A, Seto Y, Nagata S (1991) The polypeptide encoded by the cDNA for human cell surface antigen Fas can mediate apoptosis. Cell 66:233–243

120. Oehm A, Behrmann I, Falk W, Pawlita M, Maier G, Klas C, Li-Weber M, Richards S, Dhein J, Trauth BC (1992) Purification and molecular cloning of the APO-1 cell surface antigen, a member of the tumor necrosis factor/nerve growth factor receptor

superfamily. Sequence identity with the Fas antigen. J Biol Chem 267:10709–10715

121. Trauth BC, Klas C, Peters AM, Matzku S, Möller P, Falk W, Debatin KM, Krammer PH (1989) Monoclonal antibody-mediated tumor regression by induction of apoptosis. Science 245:301–305

122. French LE, Tschopp J (2003) Protein-based therapeutic approaches targeting death receptors. Cell Death Differ 10:117–123

123. Wajant H (2003) Death receptors. Essays Biochem 39:53–71

124. Ashkenazi A, Dixit VM (1999) Apoptosis control by death and decoy receptors. Curr Opin Cell Biol 11:255–260

125. Sheridan JP, Marsters SA, Pitti RM, et al (1997) Control of TRAIL-induced apoptosis by a family of signaling and decoy receptors. Science 277:818–821

126. Gruss HJ, Dower SK (1995) Tumor necrosis factor ligand superfamily: involvement in the pathology of malignant lymphomas. Blood 85:3378–3404

127. Carswell EA, Old LJ, Kassel RL, Green S, Fiore N, Williamson B (1975) An endotoxin-induced serum factor that causes necrosis of tumors. Proc Natl Acad Sci USA 72:3666–3670

128. Lavrik I, Golks A, Krammer PH (2005) Death receptor signaling. J Cell Sci 118:265–267

129. Migone TS, Zhang J, Luo X, et al (2002) TL1A is a TNF-like ligand for DR3 and TR6/DcR3 and functions as a T cell costimulator. Immunity 16:479–492

130. Suda T, Takahashi T, Golstein P, Nagata S (1993) Molecular cloning and expression of the Fas ligand, a novel member of the tumor necrosis factor family. Cell 75:1169–1178

131. Wiley SR, Schooley K, Smolak PJ, Din WS, Huang CP, Nicholl JK, Sutherland GR, Smith TD, Rauch C, Smith CA (1995) Identification and characterization of a new member of the TNF family that induces apoptosis. Immunity 3:673–682

132. Krueger A, Fas SC, Baumann S, Krammer PH (2003) The role of CD95 in the regulation of peripheral T-cell apoptosis. Immunol Rev 193:58–69

133. Schulte M, Reiss K, Lettau M, Maretzky T, Ludwig A, Hartmann D, de Strooper B, Janssen O, Saftig P (2007) ADAM10 regulates FasL cell surface expression and modulates FasL-induced cytotoxicity and activation-induced cell death. Cell Death Differ 14:1040–1049

134. Wallach D, Varfolomeev EE, Malinin NL, Goltsev YV, Kovalenko AV, Boldin MP (1999) TUMOR NECROSIS FACTOR RECEPTOR AND Fas SIGNALING MECHANISMS. Annual Review of Immunology 17:331–367

135. Kischkel FC, Hellbardt S, Behrmann I, Germer M, Pawlita M, Krammer PH, Peter ME (1995) Cytotoxicity-dependent APO-1 (Fas/CD95)-associated proteins form a death-inducing signaling complex (DISC) with the receptor. EMBO J 14:5579–5588

136. Boldin MP, Goncharov TM, Goltsev YV, Wallach D (1996) Involvement of MACH, a novel MORT1/FADD-interacting protease, in Fas/APO-1- and TNF receptor-induced cell death. Cell 85:803–815

137. Chinnaiyan AM, O'Rourke K, Tewari M, Dixit VM (1995) FADD, a novel death domain-containing protein, interacts with the death domain of Fas and initiates apoptosis. Cell 81:505–512

138. Muzio M, Chinnaiyan AM, Kischkel FC, et al (1996) FLICE, a novel FADD-homologous ICE/CED-3-like protease, is recruited to the CD95 (Fas/APO-1) death--inducing signaling complex. Cell 85:817–827

139. Muzio M, Stockwell BR, Stennicke HR, Salvesen GS, Dixit VM (1998) An induced proximity model for caspase-8 activation. J Biol Chem 273:2926–2930

140. Yang X, Chang HY, Baltimore D (1998) Autoproteolytic activation of pro-caspases by oligomerization. Mol Cell 1:319–325

141. Medema JP, Scaffidi C, Kischkel FC, Shevchenko A, Mann M, Krammer PH, Peter ME (1997) FLICE is activated by association with the CD95 death-inducing signaling complex (DISC). EMBO J 16:2794–2804

142. Li H, Zhu H, Xu CJ, Yuan J (1998) Cleavage of BID by caspase 8 mediates the mitochondrial damage in the Fas pathway of apoptosis. Cell 94:491–501

143. Luo X, Budihardjo I, Zou H, Slaughter C, Wang X (1998) Bid, a Bcl2 Interacting Protein, Mediates Cytochrome c Release from Mitochondria in Response to Activation of Cell Surface Death Receptors. Cell 94:481–490

144. Scaffidi C, Fulda S, Srinivasan A, Friesen C, Li F, Tomaselli KJ, Debatin KM, Krammer PH, Peter ME (1998) Two CD95 (APO-1/Fas) signaling pathways. EMBO J 17:1675–1687

145. Chang DW, Xing Z, Pan Y, Algeciras-Schimnich A, Barnhart BC, Yaish-Ohad S, Peter ME, Yang X (2002) c-FLIPL is a dual function regulator for caspase-8 activation and CD95-mediated apoptosis. EMBO J 21:3704–3714

146. Golks A, Brenner D, Fritsch C, Krammer PH, Lavrik IN (2005) c-FLIPR, a new regulator of death receptor-induced apoptosis. J Biol Chem 280:14507–14513

147. Irmler M, Thome M, Hahne M, et al (1997) Inhibition of death receptor signals by cellular FLIP. Nature 388:190–195

148. Krueger A, Baumann S, Krammer PH, Kirchhoff S (2001) FLICE-Inhibitory Proteins: Regulators of Death Receptor-Mediated Apoptosis. Mol Cell Biol 21:8247–8254

149. Kovalenko A, Wallach D (2006) If the Prophet Does Not Come to the Mountain: Dynamics of Signaling Complexes in NF-κB Activation. Molecular Cell 22:433–436

150. Micheau O, Tschopp J (2003) Induction of TNF receptor I-mediated apoptosis via two sequential signaling complexes. Cell 114:181–190

151. Hildeman DA, Zhu Y, Mitchell TC, Kappler J, Marrack P (2002) Molecular mechanisms of activated T cell death in vivo. Curr Opin Immunol 14:354–359

152. Leithäuser F, Dhein J, Mechtersheimer G, Koretz K, Brüderlein S, Henne C, Schmidt A, Debatin KM, Krammer PH, Möller P (1993) Constitutive and induced expression of APO-1, a new member of the nerve growth factor/tumor necrosis factor receptor superfamily,

in normal and neoplastic cells. Lab Invest 69:415–429

153. Brunner T, Mogil RJ, LaFace D, Yoo NJ, Mahboubi A, Echeverri F, Martin SJ, Force WR, Lynch DH, Ware CF (1995) Cell-autonomous Fas (CD95)/Fas-ligand interaction mediates activation-induced apoptosis in T-cell hybridomas. Nature 373:441–444

154. Nagata S (1999) Fas Ligand-Induced Apoptosis. Annual Review of Genetics 33:29–55

155. Yamada A, Arakaki R, Saito M, Kudo Y, Ishimaru N (2017) Dual Role of Fas/FasL-Mediated Signal in Peripheral Immune Tolerance. Front Immunol. doi: 10.3389/fimmu.2017.00403

156. Forrester JV, Xu H, Lambe T, Cornall R (2008) Immune privilege or privileged immunity? Mucosal Immunol 1:372–381

157. Griffith TS, Brunner T, Fletcher SM, Green DR, Ferguson TA (1995) Fas ligand-induced apoptosis as a mechanism of immune privilege. Science 270:1189–1192

158. Hong S, Van Kaer L (1999) Immune Privilege. J Exp Med 190:1197–1200

159. Kobayashi S, Hirano T, Kakinuma M, Uede T (1993) Transcriptional repression and differential splicing of Fas mRNA by early transposon (ETn) insertion in autoimmune lpr mice. Biochem Biophys Res Commun 191:617–624

160. Wu J, Zhou T, He J, Mountz JD (1993) Autoimmune disease in mice due to integration of an endogenous retrovirus in an apoptosis gene. J Exp Med 178:461–468

161. Mariani SM, Matiba B, Armandola EA, Krammer PH (1994) The APO-1/Fas (CD95) receptor is expressed in homozygous MRL/lpr mice. Eur J Immunol 24:3119–3123

162. Nagata S, Suda T (1995) Fas and Fas ligand: lpr and gld mutations. Immunol Today 16:39–43

163. Ramsdell F, Seaman MS, Miller RE, Tough TW, Alderson MR, Lynch DH (1994) gld/gld mice are unable to express a functional ligand for Fas. Eur J Immunol 24:928–933

164. Takahashi T, Tanaka M, Brannan CI, Jenkins NA, Copeland NG, Suda T, Nagata S (1994) Generalized lymphoproliferative disease in mice, caused by a point mutation in the Fas ligand. Cell 76:969–976

165. Adachi M, Suematsu S, Suda T, Watanabe D, Fukuyama H, Ogasawara J, Tanaka T, Yoshida N, Nagata S (1996) Enhanced and accelerated lymphoproliferation in Fas-null mice. Proc Natl Acad Sci U S A 93:2131–2136

166. Chun HJ, Lenardo MJ (2001) Autoimmune lymphoproliferative syndrome: types I, II and beyond. Adv Exp Med Biol 490:49–57

167. Rieux-Laucat F, Le Deist F, Fischer A (2003) Autoimmune lymphoproliferative syndromes: genetic defects of apoptosis pathways. Cell Death Differ 10:124–133

168. Brenner D, Krammer PH, Arnold R (2008) Concepts of activated T cell death. Crit Rev Oncol Hematol 66:52–64

169. Lohman BL, Razvi ES, Welsh RM (1996) T-lymphocyte downregulation after acute viral infection is not dependent on CD95 (Fas) receptor-

ligand interactions. Journal of Virology 70:8199–8203

170. Cao K, Wang G, Li W, et al (2015) Histone deacetylase inhibitors prevent activation-induced cell death and promote anti-tumor immunity. Oncogene 34:5960–5970

171. Chappell DB, Restifo NP (1998) T cell–tumor cell: a fatal interaction? Cancer Immunol Immunother 47:65–71

172. Pai C-CS, Huang JT, Lu X, et al (2019) Clonal Deletion of Tumor-Specific T Cells by Interferon-γ Confers Therapeutic Resistance to Combination Immune Checkpoint Blockade. Immunity 50:477-492.e8

173. Saff RR, Spanjaard ES, Hohlbaum AM, Marshak-Rothstein A (2004) Activation-induced cell death limits effector function of CD4 tumor-specific T cells. J Immunol 172:6598–6606

174. Künkele A, Johnson AJ, Rolczynski LS, Chang CA, Hoglund V, Kelly-Spratt KS, Jensen MC (2015) Functional Tuning of CARs Reveals Signaling Threshold above Which CD8+ CTL Antitumor Potency Is Attenuated due to Cell Fas–FasL-Dependent AICD. Cancer Immunol Res 3:368–379

175. Halliwell B, Gutteridge JMC (2015) Free Radicals in Biology and Medicine, Fifth Edition. Oxford University Press, Oxford, New York

176. Fridovich I (1970) Quantitative Aspects of the Production of Superoxide Anion Radical by Milk Xanthine Oxidase. J Biol Chem 245:4053–4057

177. Keisari Y, Braun L, Flescher E (1983) The oxidative burst and related phenomena in mouse macrophages elicited by different sterile inflammatory stimuli. Immunobiology 165:78–89

178. Nathan CF, Root RK (1977) Hydrogen peroxide release from mouse peritoneal macrophages: dependence on sequential activation and triggering. J Exp Med 146:1648–1662

179. Segal AW, Shatwell KP (1997) The NADPH oxidase of phagocytic leukocytes. Ann N Y Acad Sci 832:215–222

180. Rashba-Step J, Turro NJ, Cederbaum AI (1993) Increased NADPH- and NADH-dependent production of superoxide and hydroxyl radical by microsomes after chronic ethanol treatment. Arch Biochem Biophys 300:401–408

181. Sies H (1977) Peroxisomal enzymes and oxygen metabolism in liver. Adv Exp Med Biol 78:51–60

182. Nicholls, Ferguson (2002) Bioenergetics 3. Biochemistry (Moscow) 69:818–819

183. Chance B, Sies H, Boveris A (1979) Hydroperoxide metabolism in mammalian organs. Physiol Rev 59:527–605

184. Kovacic P, Pozos RS, Somanathan R, Shangari N, O'Brien PJ (2005) Mechanism of mitochondrial uncouplers, inhibitors, and toxins: focus on electron transfer, free radicals, and structure-activity relationships. Curr Med Chem 12:2601–2623

185. McLennan HR, Esposti MD (2000) The Contribution of Mitochondrial Respiratory Complexes to the Production of Reactive Oxygen Species. J Bioenerg Biomembr 32:153–162

186. Balaban RS, Nemoto S, Finkel T (2005) Mitochondria, oxidants, and aging. Cell 120:483–495

187. Sena LA, Li S, Jairaman A, et al (2013) Mitochondria are required for antigen-specific T cell activation through reactive oxygen species signaling. Immunity 38:225–236

188. Fridovich I (1995) Superoxide radical and superoxide dismutases. Annu Rev Biochem 64:97–112

189. Zamocky M, Furtmüller PG, Obinger C (2008) Evolution of catalases from bacteria to humans. Antioxid Redox Signal 10:1527–1548

190. Holmgren A (1989) Thioredoxin and glutaredoxin systems. J Biol Chem 264:13963–13966

191. Deneke SM, Fanburg BL (1989) Regulation of cellular glutathione. Am J Physiol 257:L163-173

192. Holmgren A (1988) Thioredoxin and glutaredoxin: small multi-functional redox proteins with active-site disulphide bonds. Biochem Soc Trans 16:95–96

193. Bondareva AA, Capecchi MR, Iverson SV, et al (2007) Effects of thioredoxin reductase-1 deletion on embryogenesis and transcriptome. Free Radic Biol Med 43:911–923

194. Jakupoglu C, Przemeck GKH, Schneider M, et al (2005) Cytoplasmic thioredoxin reductase is essential for embryogenesis but dispensable for cardiac development. Mol Cell Biol 25:1980–1988

195. Matsui M, Oshima M, Oshima H, Takaku K, Maruyama T, Yodoi J, Taketo MM (1996) Early embryonic lethality caused by targeted disruption of the mouse thioredoxin gene. Dev Biol 178:179–185

196. Nordberg J, Arnér ES (2001) Reactive oxygen species, antioxidants, and the mammalian thioredoxin system. Free Radic Biol Med 31:1287–1312

197. Karlenius TC, Tonissen KF (2010) Thioredoxin and Cancer: A Role for Thioredoxin in all States of Tumor Oxygenation. Cancers (Basel) 2:209–232

198. Patwari P, Higgins LJ, Chutkow WA, Yoshioka J, Lee RT (2006) The Interaction of Thioredoxin with Txnip: Evidence for Formation of a Mixed Disulfide by Disulfide Exchange. J Biol Chem 281:21884–21891

199. Kallis GB, Holmgren A (1980) Differential reactivity of the functional sulfhydryl groups of cysteine-32 and cysteine-35 present in the reduced form of thioredoxin from Escherichia coli. J Biol Chem 255:10261–10265

200. Watson WH, Jones DP (2003) Oxidation of nuclear thioredoxin during oxidative stress. FEBS Lett 543:144–147

201. Byrne BM, Welsh J (2005) Altered thioredoxin subcellular localization and redox status in MCF-7 cells following 1,25-dihydroxyvitamin D3 treatment. J Steroid Biochem Mol Biol 97:57–64

202. Hirota K, Murata M, Sachi Y, Nakamura H, Takeuchi J, Mori K, Yodoi J (1999) Distinct roles of thioredoxin in the cytoplasm and in the nucleus. A two-step mechanism of redox regulation of transcription factor NF-kappaB. J Biol Chem 274:27891–27897

203. Spyrou G, Enmark E, Miranda-Vizuete A, Gustafsson J-Å (1997) Cloning and Expression of a Novel

Mammalian Thioredoxin. J Biol Chem 272:2936–2941

204. Miranda-Vizuete A, Ljung J, Damdimopoulos AE, Gustafsson J-Å, Oko R, Pelto-Huikko M, Spyrou G (2001) Characterization of Sptrx, a Novel Member of the Thioredoxin Family Specifically Expressed in Human Spermatozoa. J Biol Chem 276:31567–31574

205. Miranda-Vizuete A, Damdimopoulos AE, Pedrajas JR, Gustafsson J-Å, Spyrou G (1999) Human mitochondrial thioredoxin reductase. European Journal of Biochemistry 261:405–412

206. Gladyshev VN, Jeang KT, Stadtman TC (1996) Selenocysteine, identified as the penultimate C-terminal residue in human T-cell thioredoxin reductase, corresponds to TGA in the human placental gene. Proc Natl Acad Sci USA 93:6146–6151

207. Mustacich D, Powis G (2000) Thioredoxin reductase. Biochem J 346 Pt 1:1–8

208. Butterfield LH, Merino A, Golub SH, Shau H (1999) From cytoprotection to tumor suppression: the multifactorial role of peroxiredoxins. Antioxid Redox Signal 1:385–402

209. Holmgren A, Björnstedt M (1995) Thioredoxin and thioredoxin reductase. Meth Enzymol 252:199–208

210. Lu J, Chew E-H, Holmgren A (2007) Targeting thioredoxin reductase is a basis for cancer therapy by arsenic trioxide. Proc Natl Acad Sci USA 104:12288–12293

211. Muri J, Heer S, Matsushita M, Pohlmeier L, Tortola L, Fuhrer T, Conrad M, Zamboni N, Kisielow J, Kopf M (2018) The thioredoxin-1 system is essential for fueling DNA synthesis during T-cell metabolic reprogramming and proliferation. Nature Communications 9:1851

212. Ichijo H, Nishida E, Irie K, ten Dijke P, Saitoh M, Moriguchi T, Takagi M, Matsumoto K, Miyazono K, Gotoh Y (1997) Induction of apoptosis by ASK1, a mammalian MAPKKK that activates SAPK/JNK and p38 signaling pathways. Science 275:90–94

213. Saitoh M, Nishitoh H, Fujii M, Takeda K, Tobiume K, Sawada Y, Kawabata M, Miyazono K, Ichijo H (1998) Mammalian thioredoxin is a direct inhibitor of apoptosis signal-regulating kinase (ASK) 1. EMBO J 17:2596–2606

214. Mahmood DFD, Abderrazak A, El Hadri K, Simmet T, Rouis M (2013) The thioredoxin system as a therapeutic target in human health and disease. Antioxid Redox Signal 19:1266–1303

215. Puca L, Brou C (2014) α-Arrestins – new players in Notch and GPCR signaling pathways in mammals. J Cell Sci 127:1359–1367

216. Spindel ON, World C, Berk BC (2012) Thioredoxin Interacting Protein: Redox Dependent and Independent Regulatory Mechanisms. Antioxid Redox Signal 16:587–596

217. Chen KS, DeLuca HF (1994) Isolation and characterization of a novel cDNA from HL-60 cells treated with 1,25-dihydroxyvitamin D-3. Biochim Biophys Acta 1219:26–32

218. Abu el Maaty MA, Almouhanna F, Wölfl S (2018) Expression of TXNIP in Cancer Cells and Regulation by 1,25(OH)2D3: Is It Really the Vitamin D3 Upregulated Protein? Int J Mol Sci. doi: 10.3390/ijms19030796

219. Butler LM, Zhou X, Xu W-S, Scher HI, Rifkind RA, Marks PA, Richon VM (2002) The histone deacetylase inhibitor SAHA arrests cancer cell growth, up-regulates thioredoxin-binding protein-2, and down-regulates thioredoxin. PNAS 99:11700–11705

220. Hirota T, Okano T, Kokame K, Shirotani-Ikejima H, Miyata T, Fukada Y (2002) Glucose Down-regulates Per1 and Per2mRNA Levels and Induces Circadian Gene Expression in Cultured Rat-1 Fibroblasts. J Biol Chem 277:44244–44251

221. Schulze PC, Yoshioka J, Takahashi T, He Z, King GL, Lee RT (2004) Hyperglycemia promotes oxidative stress through inhibition of thioredoxin function by thioredoxin-interacting protein. J Biol Chem 279:30369–30374

222. Junn E, Han SH, Im JY, et al (2000) Vitamin D3 up-regulated protein 1 mediates oxidative stress via suppressing the thioredoxin function. J Immunol 164:6287–6295

223. Nishiyama A, Matsui M, Iwata S, Hirota K, Masutani H, Nakamura H, Takagi Y, Sono H, Gon Y, Yodoi J (1999) Identification of Thioredoxin-binding Protein-2/Vitamin D3 Up-regulated Protein 1 as a Negative Regulator of Thioredoxin Function and Expression. J Biol Chem 274:21645–21650

224. Powis G, Montfort WR (2001) Properties and biological activities of thioredoxins. Annu Rev Pharmacol Toxicol 41:261–295

225. Devi TS, Hosoya K-I, Terasaki T, Singh LP (2013) Critical role of TXNIP in oxidative stress, DNA damage and retinal pericyte apoptosis under high glucose: Implications for diabetic retinopathy. Exp Cell Res 319:1001–1012

226. Oberacker T, Bajorat J, Ziola S, Schroeder A, Röth D, Kastl L, Edgar BA, Wagner W, Gülow K, Krammer PH (2018) Enhanced expression of thioredoxin-interacting-protein regulates oxidative DNA damage and aging. FEBS Lett 592:2297–2307

227. Verdone L, Agricola E, Caserta M, Di Mauro E (2006) Histone acetylation in gene regulation. Brief Funct Genomic Proteomic 5:209–221

228. Yang X-J, Seto E (2007) HATs and HDACs: from structure, function and regulation to novel strategies for therapy and prevention. Oncogene 26:5310–5318

229. Soutoglou E, Katrakili N, Talianidis I (2000) Acetylation regulates transcription factor activity at multiple levels. Mol Cell 5:745–751

230. Han SH, Jeon JH, Ju HR, et al (2003) VDUP1 upregulated by TGF-beta1 and 1,25-dihydorxyvitamin D3 inhibits tumor cell growth by blocking cell-cycle progression. Oncogene 22:4035–4046

231. Kim MJ, Kim WS, Kim DO, et al (2017) Macrophage migration inhibitory factor interacts with thioredoxin-interacting protein and induces NF-κB activity. Cell Signal 34:110–120

232. Kwon H-J, Won Y-S, Suh H-W, et al (2010) Vitamin D3 upregulated protein 1 suppresses TNF-α-induced NF-κB activation in hepatocarcinogenesis. J Immunol 185:3980–3989

233. Kim SY, Suh H-W, Chung JW, Yoon S-R, Choi I (2007) Diverse functions of VDUP1 in cell proliferation, differentiation, and diseases. Cell Mol Immunol 4:345–351

234. Dutta KK, Nishinaka Y, Masutani H, et al (2005) Two distinct mechanisms for loss of thioredoxin-binding protein-2 in oxidative stress-induced renal carcinogenesis. Lab Invest 85:798–807

235. Ikarashi M, Takahashi Y, Ishii Y, Nagata T, Asai S, Ishikawa K (2002) Vitamin D3 up-regulated protein 1 (VDUP1) expression in gastrointestinal cancer and its relation to stage of disease. Anticancer Res 22:4045–4048

236. Yang X, Young LH, Voigt JM (1998) Expression of a vitamin D-regulated gene (VDUP-1) in untreated- and MNU-treated rat mammary tissue. Breast Cancer Res Treat 48:33–44

237. Bodnar JS, Chatterjee A, Castellani LW, et al (2002) Positional cloning of the combined hyperlipidemia gene Hyplip1. Nat Genet 30:110–116

238. Donnelly KL, Margosian MR, Sheth SS, Lusis AJ, Parks EJ (2004) Increased lipogenesis and fatty acid reesterification contribute to hepatic triacylglycerol stores in hyperlipidemic Txnip-/- mice. J Nutr 134:1475–1480

239. Chutkow WA, Patwari P, Yoshioka J, Lee RT (2008) Thioredoxin-interacting protein (Txnip) is a critical regulator of hepatic glucose production. J Biol Chem 283:2397–2406

240. Oka S, Liu W, Masutani H, Hirata H, Shinkai Y, Yamada S, Yoshida T, Nakamura H, Yodoi J (2006) Impaired fatty acid utilization in thioredoxin binding protein-2 (TBP-2)-deficient mice: a unique animal model of Reye syndrome. FASEB J 20:121–123

241. Sheth SS, Castellani LW, Chari S, Wagg C, Thipphavong CK, Bodnar JS, Tontonoz P, Attie AD, Lopaschuk GD, Lusis AJ (2005) Thioredoxin-interacting protein deficiency disrupts the fasting-feeding metabolic transition. J Lipid Res 46:123–134

242. Minn AH, Hafele C, Shalev A (2005) Thioredoxin-interacting protein is stimulated by glucose through a carbohydrate response element and induces beta-cell apoptosis. Endocrinology 146:2397–2405

243. Yu F-X, Luo Y (2009) Tandem ChoRE and CCAAT Motifs and Associated Factors Regulate Txnip Expression in Response to Glucose or Adenosine-Containing Molecules. PLOS ONE 4:e8397

244. Stoltzman CA, Peterson CW, Breen KT, Muoio DM, Billin AN, Ayer DE (2008) Glucose sensing by MondoA:Mlx complexes: a role for hexokinases and direct regulation of thioredoxin-interacting protein expression. Proc Natl Acad Sci USA 105:6912–6917

245. Wu N, Zheng B, Shaywitz A, et al (2013) AMPK-Dependent Degradation of TXNIP upon Energy Stress Leads to Enhanced Glucose Uptake via GLUT1. Molecular Cell 49:1167–1175

246. Yu F-X, Chai TF, He H, Hagen T, Luo Y (2010) Thioredoxin-interacting protein (Txnip) gene expression: sensing oxidative phosphorylation status and glycolytic rate. J Biol Chem 285:25822–25830

247. Elgort MG, O'Shea JM, Jiang Y, Ayer DE (2010) Transcriptional and Translational Downregulation of Thioredoxin Interacting Protein Is Required for Metabolic Reprogramming during G(1). Genes Cancer 1:893–907

248. Frauwirth KA, Thompson CB (2004) Regulation of T Lymphocyte Metabolism. The Journal of Immunology 172:4661–4665

249. Wang T, Marquardt C, Foker J (1976) Aerobic glycolysis during lymphocyte proliferation. Nature 261:702–705

250. Lee KN, Kang H-S, Jeon J-H, et al (2005) VDUP1 is required for the development of natural killer cells. Immunity 22:195–208

251. Son A, Nakamura H, Okuyama H, et al (2008) Dendritic cells derived from TBP-2-deficient mice are defective in inducing T cell responses. Eur J Immunol 38:1358–1367

252. Zhou R, Tardivel A, Thorens B, Choi I, Tschopp J (2010) Thioredoxin-interacting protein links oxidative stress to inflammasome activation. Nat Immunol 11:136–140

253. Tepper AD, Cock JG, de Vries E, Borst J, van Blitterswijk WJ (1997) CD95/Fas-induced ceramide formation proceeds with slow kinetics and is not blocked by caspase-3/CPP32 inhibition. J Biol Chem 272:24308–24312

254. Klas C, Debatin KM, Jonker RR, Krammer PH (1993) Activation interferes with the APO-1 pathway in mature human T cells. Int Immunol 5:625–630

255. Sprick MR, Weigand MA, Rieser E, Rauch CT, Juo P, Blenis J, Krammer PH, Walczak H (2000) FADD/MORT1 and caspase-8 are recruited to TRAIL receptors 1 and 2 and are essential for apoptosis mediated by TRAIL receptor 2. Immunity 12:599–609

256. Devadas S, Zaritskaya L, Rhee SG, Oberley L, Williams MS (2002) Discrete generation of superoxide and hydrogen peroxide by T cell receptor stimulation: selective regulation of mitogen-activated protein kinase activation and fas ligand expression. J Exp Med 195:59–70

257. Smyth GK (2004) Linear models and empirical bayes methods for assessing differential expression in microarray experiments. Stat Appl Genet Mol Biol 3:Article3

258. Smyth GK (2005) limma: Linear Models for Microarray Data. In: Gentleman R, Carey VJ, Huber W, Irizarry RA, Dudoit S (eds) Bioinformatics and Computational Biology Solutions Using R and Bioconductor. Springer-Verlag, New York, pp 397–420

259. Wu D, Smyth GK (2012) Camera: a competitive gene set test accounting for inter-gene correlation. Nucleic Acids Res 40:e133–e133

260. Kanehisa M, Goto S (2000) KEGG: kyoto encyclopedia of genes and genomes. Nucleic Acids Res 28:27–30

261. GO Consortium (2017) Expansion of the Gene Ontology knowledgebase and resources. Nucleic Acids Res 45:D331–D338

262. R Core Team (2018) R: A language and environment for statistical computing. R Foundation for Statistical Computing.

263. Ran FA, Hsu PD, Wright J, Agarwala V, Scott DA, Zhang F (2013) Genome engineering using the CRISPR-Cas9 system. Nat Protoc 8:2281–2308

264. Bauer DE, Canver MC, Orkin SH (2015) Generation of genomic deletions in mammalian cell lines via CRISPR/Cas9. J Vis Exp e52118

265. Sanger F, Nicklen S, Coulson AR (1977) DNA sequencing with chain-

terminating inhibitors. Proc Natl Acad Sci USA 74:5463–5467

266. Kamiński MM, Röth D, Sass S, Sauer SW, Krammer PH, Gülow K (2012) Manganese superoxide dismutase: a regulator of T cell activation-induced oxidative signaling and cell death. Biochim Biophys Acta 1823:1041–1052

267. Schulze PC, De Keulenaer GW, Yoshioka J, Kassik KA, Lee RT (2002) Vitamin D3-upregulated protein-1 (VDUP-1) regulates redox-dependent vascular smooth muscle cell proliferation through interaction with thioredoxin. Circ Res 91:689–695

268. Wang Y, Keulenaer GWD, Lee RT (2002) Vitamin D3-up-regulated Protein-1 Is a Stress-responsive Gene That Regulates Cardiomyocyte Viability through Interaction with Thioredoxin. J Biol Chem 277:26496–26500

269. Garg AK, Aggarwal BB (2002) Reactive oxygen intermediates in TNF signaling. Mol Immunol 39:509–517

270. Shen H-M, Pervaiz S (2006) TNF receptor superfamily-induced cell death: redox-dependent execution. The FASEB Journal. doi: 10.1096/fj.05-5603rev

271. Arnér ES, Holmgren A (2000) Physiological functions of thioredoxin and thioredoxin reductase. Eur J Biochem 267:6102–6109

272. Chung JW, Jeon J-H, Yoon S-R, Choi I (2006) Vitamin D3 upregulated protein 1 (VDUP1) is a regulator for redox signaling and stress-mediated diseases. J Dermatol 33:662–669

273. Kießling MK, Linke B, Brechmann M, Süss D, Krammer PH, Gülow K (2010) Inhibition of NF-κB induces a switch from CD95L-dependent to CD95L-independent and JNK-mediated apoptosis in T cells. FEBS Letters 584:4679–4688

274. Kesarwani P, Murali AK, Al-Khami AA, Mehrotra S (2013) Redox regulation of T-cell function: from molecular mechanisms to significance in human health and disease. Antioxid Redox Signal 18:1497–1534

275. Bekker-Jensen DB, Kelstrup CD, Batth TS, et al (2017) An Optimized Shotgun Strategy for the Rapid Generation of Comprehensive Human Proteomes. Cell Syst 4:587-599.e4

276. Ogata FT, Batista WL, Sartori A, Gesteira TF, Masutani H, Arai RJ, Yodoi J, Stern A, Monteiro HP (2013) Nitrosative/Oxidative Stress Conditions Regulate Thioredoxin-Interacting Protein (TXNIP) Expression and Thioredoxin-1 (TRX-1) Nuclear Localization. PLOS ONE 8:e84588

277. World C, Spindel ON, Berk BC (2011) Thioredoxin-interacting protein mediates TRX1 translocation to the plasma membrane in response to tumor necrosis factor-α: a key mechanism for vascular endothelial growth factor receptor-2 transactivation by reactive oxygen species. Arterioscler Thromb Vasc Biol 31:1890–1897

278. Kanari Y, Sato Y, Aoyama S, Muta T (2013) Thioredoxin-Interacting Protein Gene Expression via MondoA Is Rapidly and Transiently Suppressed during Inflammatory Responses. PLOS ONE 8:e59026

279. Saitoh T, Tanaka S, Koike T (2001) Rapid induction and Ca(2+) influx-mediated suppression of vitamin D3 up-regulated protein 1 (VDUP1)

mRNA in cerebellar granule neurons undergoing apoptosis. J Neurochem 78:1267–1276

280. Shao W, Yu Z, Fantus IG, Jin T (2010) Cyclic AMP signaling stimulates proteasome degradation of thioredoxin interacting protein (TxNIP) in pancreatic beta-cells. Cell Signal 22:1240–1246

281. Zhang P, Wang C, Gao K, et al (2010) The ubiquitin ligase itch regulates apoptosis by targeting thioredoxin-interacting protein for ubiquitin-dependent degradation. J Biol Chem 285:8869–8879

282. Hershko A, Ciechanover A (1998) The Ubiquitin System. Annual Review of Biochemistry 67:425–479

283. Liu Y-C (2007) The E3 ubiquitin ligase Itch in T cell activation, differentiation, and tolerance. Semin Immunol 19:197–205

284. Carrette F, Fabre S, Bismuth G (2009) FOXO1, T-cell trafficking and immune responses. Adv Exp Med Biol 665:3–16

285. Hedrick SM, Michelini RH, Doedens AL, Goldrath AW, Stone EL (2012) FOXO transcription factors throughout T cell biology. Nat Rev Immunol. doi: 10.1038/nri3278

286. Papadia S, Soriano FX, Léveillé F, et al (2008) Synaptic NMDA receptor activity boosts intrinsic antioxidant defenses. Nat Neurosci 11:476–487

287. Hong SY, Yu F-X, Luo Y, Hagen T (2016) Oncogenic activation of the PI3K/Akt pathway promotes cellular glucose uptake by downregulating the expression of thioredoxin-interacting protein. Cell Signal 28:377–383

288. Zaragoza-Campillo MA, Morán J (2017) Reactive Oxygen Species Evoked by Potassium Deprivation and Staurosporine Inactivate Akt and Induce the Expression of TXNIP in Cerebellar Granule Neurons. Oxid Med Cell Longev 2017:8930406

289. Astoul E, Edmunds C, Cantrell DA, Ward SG (2001) PI 3-K and T-cell activation: limitations of T-leukemic cell lines as signaling models. Trends Immunol 22:490–496

290. Shan X, Czar MJ, Bunnell SC, Liu P, Liu Y, Schwartzberg PL, Wange RL (2000) Deficiency of PTEN in Jurkat T Cells Causes Constitutive Localization of Itk to the Plasma Membrane and Hyperresponsiveness to CD3 Stimulation. Mol Cell Biol 20:6945–6957

291. Cha-Molstad H, Saxena G, Chen J, Shalev A (2009) Glucose-stimulated Expression of Txnip Is Mediated by Carbohydrate Response Element-binding Protein, p300, and Histone H4 Acetylation in Pancreatic Beta Cells. J Biol Chem 284:16898–16905

292. Kuo MH, Allis CD (1998) Roles of histone acetyltransferases and deacetylases in gene regulation. Bioessays 20:615–626

293. Loosdregt J van, Vercoulen Y, Guichelaar T, et al (2010) Regulation of Treg functionality by acetylation-mediated Foxp3 protein stabilization. Blood 115:965–974

294. Dunn LL, Buckle AM, Cooke JP, Ng MKC (2010) THE EMERGING ROLE OF THE THIOREDOXIN SYSTEM IN ANGIOGENESIS. Arterioscler Thromb Vasc Biol 30:2089–2098

295. Circu ML, Aw TY (2008) Glutathione and apoptosis. Free Radic Res 42:689–706

296. Lu SC (2013) GLUTATHIONE SYNTHESIS. Biochim Biophys Acta 1830:3143–3153

297. Won HY, Sohn JH, Min HJ, Lee K, Woo HA, Ho Y-S, Park JW, Rhee S-G, Hwang ES (2010) Glutathione peroxidase 1 deficiency attenuates allergen-induced airway inflammation by suppressing Th2 and Th17 cell development. Antioxid Redox Signal 13:575–587

298. Lillig CH, Holmgren A (2007) Thioredoxin and related molecules--from biology to health and disease. Antioxid Redox Signal 9:25–47

299. Minn AH, Pise-Masison CA, Radonovich M, Brady JN, Wang P, Kendziorski C, Shalev A (2005) Gene expression profiling in INS-1 cells overexpressing thioredoxin-interacting protein. Biochem Biophys Res Commun 336:770–778

300. Ashburner BP, Westerheide SD, Baldwin AS (2001) The p65 (RelA) Subunit of NF-κB Interacts with the Histone Deacetylase (HDAC) Corepressors HDAC1 and HDAC2 To Negatively Regulate Gene Expression. Mol Cell Biol 21:7065–7077

301. Chen null, Fischle W, Verdin E, Greene WC (2001) Duration of nuclear NF-kappaB action regulated by reversible acetylation. Science 293:1653–1657

302. Jiang C, Xuan Z, Zhao F, Zhang MQ (2007) TRED: a transcriptional regulatory element database, new entries and other development. Nucleic Acids Res 35:D137–D140

303. Pahl HL (1999) Activators and target genes of Rel/NF-kappaB transcription factors. Oncogene 18:6853–6866

304. Yang Y, Wu J, Wang J (2016) A database and functional annotation of NF-κB target genes. Int J Clin Exp Med 9:7986–95

305. Krammer PH, Kamiński M, Kiessling M, Gülow K (2007) No life without death. Adv Cancer Res 97:111–138

306. Schenk H, Klein M, Erdbrügger W, Dröge W, Schulze-Osthoff K (1994) Distinct effects of thioredoxin and antioxidants on the activation of transcription factors NF-kappa B and AP-1. Proc Natl Acad Sci U S A 91:1672–1676

307. Wang W-M, Wu S-Y, Lee A-Y, Chiang C-M (2011) Binding site specificity and factor redundancy in activator protein-1-driven human papillomavirus chromatin-dependent transcription. J Biol Chem 286:40974–40986

308. Yang C-M, Chen Y-W, Chi P-L, Lin C-C, Hsiao L-D (2017) Resveratrol inhibits BK-induced COX-2 transcription by suppressing acetylation of AP-1 and NF-κB in human rheumatoid arthritis synovial fibroblasts. Biochem Pharmacol 132:77–91

309. Rao A, Luo C, Hogan PG (1997) TRANSCRIPTION FACTORS OF THE NFAT FAMILY:Regulation and Function. Annual Review of Immunology 15:707–747

310. Kim JH, Kim K, Youn BU, Jin HM, Kim J-Y, Moon JB, Ko A, Seo S-B, Lee K-Y, Kim N (2011) RANKL induces NFATc1 acetylation and stability via histone acetyltransferases during osteoclast differentiation. Biochem J 436:253–262

311. Sarikhani M, Maity S, Mishra S, et al (2018) SIRT2 deacetylase represses NFAT transcription factor to maintain cardiac homeostasis. J Biol Chem 293:5281–5294

312. Lazarevic V, Zullo AJ, Schweitzer MN, Staton TL, Gallo EM, Crabtree GR, Glimcher LH (2009) The gene encoding early growth response 2, a target of the transcription factor NFAT, is required for the development and maturation of natural killer T cells. Nat Immunol 10:306–313

313. Brettingham-Moore KH, Rao S, Juelich T, Shannon MF, Holloway AF (2005) GM-CSF promoter chromatin remodelling and gene transcription display distinct signal and transcription factor requirements. Nucleic Acids Res 33:225–234

314. Falvo JV, Tsytsykova AV, Goldfeld AE (2010) Transcriptional Control of the TNF Gene. Curr Dir Autoimmun 11:27–60

315. Kiani A, García-Cózar FJ, Habermann I, Laforsch S, Aebischer T, Ehninger G, Rao A (2001) Regulation of interferon-gamma gene expression by nuclear factor of activated T cells. Blood 98:1480–1488

316. Sica A, Dorman L, Viggiano V, Cippitelli M, Ghosh P, Rice N, Young HA (1997) Interaction of NF-κB and NFAT with the Interferon-γ Promoter. J Biol Chem 272:30412–30420

317. Klein-Hessling S, Muhammad K, Klein M, et al (2017) NFATc1 controls the cytotoxicity of CD8+ T cells. Nat Commun. doi: 10.1038/s41467-017-00612-6

318. Dhein J, Walczak H, Bäumler C, Debatin KM, Krammer PH (1995) Autocrine T-cell suicide mediated by APO-1/(Fas/CD95). Nature 373:438–441

319. Ju ST, Panka DJ, Cui H, Ettinger R, el-Khatib M, Sherr DH, Stanger BZ, Marshak-Rothstein A (1995) Fas(CD95)/FasL interactions required for programmed cell death after T-cell activation. Nature 373:444–448

320. Daniel PT, Kroidl A, Cayeux S, Bargou R, Blankenstein T, Dörken B (1997) Costimulatory signals through B7.1/CD28 prevent T cell apoptosis during target cell lysis. J Immunol 159:3808–3815

321. Sytwu HK, Liblau RS, McDevitt HO (1996) The roles of Fas/APO-1 (CD95) and TNF in antigen-induced programmed cell death in T cell receptor transgenic mice. Immunity 5:17–30

322. Zheng L, Fisher G, Miller RE, Peschon J, Lynch DH, Lenardo MJ (1995) Induction of apoptosis in mature T cells by tumour necrosis factor. Nature 377:348–351

323. Lawrence CP, Chow SC (2005) FADD deficiency sensitises Jurkat T cells to TNF-α-dependent necrosis during activation-induced cell death. FEBS Letters 579:6465–6472

324. Martínez-Lorenzo MJ, Alava MA, Gamen S, Kim KJ, Chuntharapai A, Piñeiro A, Naval J, Anel A (1998) Involvement of APO2 ligand/TRAIL in activation-induced death of Jurkat and human peripheral blood T cells. Eur J Immunol 28:2714–2725

325. Devadas S, Das J, Liu C, Zhang L, Roberts AI, Pan Z, Moore PA, Das G, Shi Y (2006) Granzyme B is critical for T cell receptor-induced cell death of type 2 helper T cells. Immunity 25:237–247

326. Gorak-Stolinska P, Truman J-P, Kemeny DM, Noble A (2001) Activation-induced cell death of human T-cell subsets is mediated by Fas and granzyme B but is independent of TNF-α. Journal of Leukocyte Biology 70:756–766

327. Huang C, Bi E, Hu Y, Deng W, Tian Z, Dong C, Hu Y, Sun B (2006) A Novel NF-κB Binding Site Controls Human Granzyme B Gene Transcription. The Journal of Immunology 176:4173–4181

328. Zhang J, Xu X, Liu Y (2004) Activation-induced cell death in T cells and autoimmunity. Cell Mol Immunol 1:186–192

329. Mittelstadt PR, Ashwell JD (1999) Role of Egr-2 in Up-regulation of Fas Ligand in Normal T Cells and Aberrant Double-negative lpr and gld T Cells. J Biol Chem 274:3222–3227

330. Rengarajan J, Mittelstadt PR, Mages HW, Gerth AJ, Kroczek RA, Ashwell JD, Glimcher LH (2000) Sequential involvement of NFAT and Egr transcription factors in FasL regulation. Immunity 12:293–300

331. Chow WA, Fang JJ, Yee JK (2000) The IFN regulatory factor family participates in regulation of Fas ligand gene expression in T cells. J Immunol 164:3512–3518

332. Kirchhoff S, Sebens T, Baumann S, Krueger A, Zawatzky R, Li-Weber M, Meinl E, Neipel F, Fleckenstein B, Krammer PH (2002) Viral IFN-regulatory factors inhibit activation-induced cell death via two positive regulatory IFN-regulatory factor 1-dependent domains in the CD95 ligand promoter. J Immunol 168:1226–1234

333. Refaeli Y, Parijs LV, Alexander SI, Abbas AK (2002) Interferon γ Is Required for Activation-induced Death of T Lymphocytes. Journal of Experimental Medicine 196:999–1005

334. Patwari P, Chutkow WA, Cummings K, Verstraeten VLRM, Lammerding J, Schreiter ER, Lee RT (2009) Thioredoxin-independent Regulation of Metabolism by the α-Arrestin Proteins. J Biol Chem 284:24996–25003

335. Yoshioka, Imahashi, Kenichi, Gabel, Scott A., et al (2007) Targeted Deletion of Thioredoxin-Interacting Protein Regulates Cardiac Dysfunction in Response to Pressure Overload. Circulation Research 101:1328–1338

336. Wakasugi N, Tagaya Y, Wakasugi H, Mitsui A, Maeda M, Yodoi J, Tursz T (1990) Adult T-cell leukemia-derived factor/thioredoxin, produced by both human T-lymphotropic virus type I-and Epstein-Barr virus-transformed lymphocytes, acts as an autocrine growth factor and synergizes with interleukin 1 and interleukin 2. Proc Natl Acad Sci USA 87:8282–8286

337. Jeon J-H, Lee K-N, Hwang CY, Kwon K-S, You K-H, Choi I (2005) Tumor Suppressor VDUP1 Increases p27kip1 Stability by Inhibiting JAB1. Cancer Res 65:4485–4489

338. Nishinaka Y, Nishiyama A, Masutani H, Oka S, Ahsan KM, Nakayama Y, Ishii Y, Nakamura H, Maeda M, Yodoi J (2004) Loss of thioredoxin-binding protein-2/vitamin D3 up-regulated protein 1 in human T-cell leukemia virus type I-dependent T-cell transformation: implications for adult T-cell leukemia leukemogenesis. Cancer Res 64:1287–1292

Supplementary results

Impact of Itch on TCR-induced proteasomal degradation of TXNIP

The E3 ubiquitin ligase Itch mediates poly-ubiquitination of TXNIP in 293T as well as U2OS cells [281]. Since Itch is involved in the regulation of T cell immune responses [283], we investigated whether Itch mediates degradation of TXNIP following TCR stimulation. However, as illustrated in Supplementary Figure 1, knocking down Itch did not alter TXNIP protein levels. This observation indicates Itch-independent proteasomal degradation of TXNIP upon TCR stimulation.

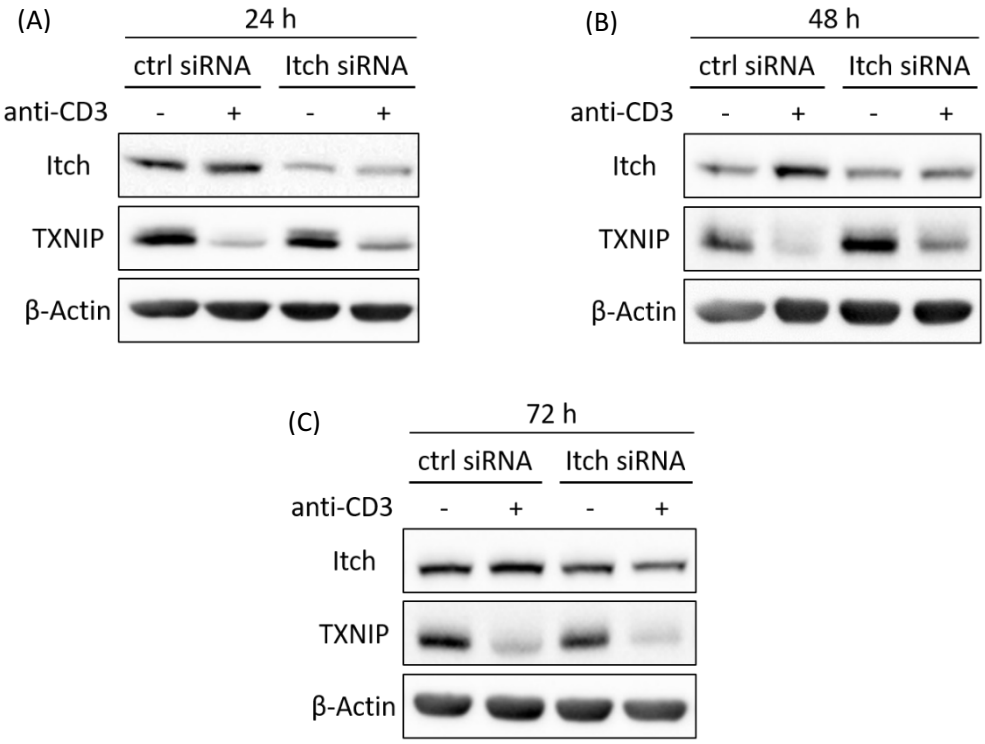

Supplementary Figure 1: Effect of Itch-knockdown on TCR-induced TXNIP protein degradation. (A – C) Jurkat T cells were transiently transfected with control (ctrl) or Itch siRNA oligonucleotides. After the indicated time periods, cells were left untreated or stimulated with anti-CD3 antibodies for 4 h, lysed and subsequently, Itch as well as TXNIP protein expression was determined by Western blot. The panels show a representative blot of three independent experiments.

Effect of SAHA on TXNIP protein level

Since Butler et al. demonstrate that treatment with the HDAC inhibitor SAHA enhances TXNIP protein level in different cancer cell lines [219], we investigated whether acetylation also affects TXNIP protein expression in Jurkat T cells. SAHA treatment of Jurkat T cells mediated accumulation of TXNIP protein (Supplementary Figure 2). However, simultaneous stimulation of cells with anti-CD3 antibodies abolished the SAHA-induced effect on TXNIP protein level (Supplementary Figure 2). Taken together, SAHA treatment cause TXNIP accumulation in Jurkat T cells but it is not sufficient to overcome TCR-induced TXNIP suppression.

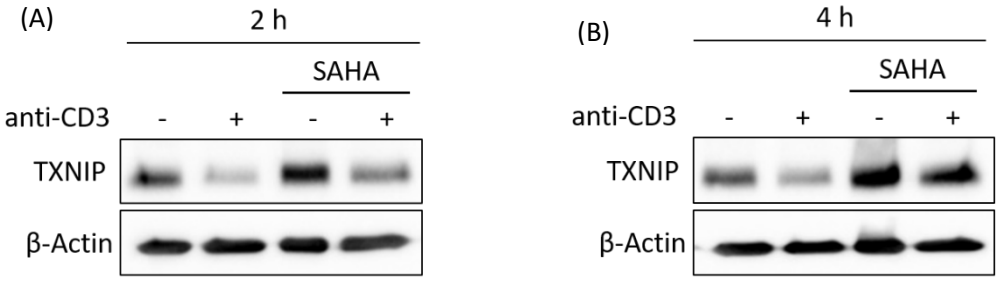

Supplementary Figure 2: Impact of SAHA on TXNIP protein expression.
(A and B) Jurkat T cells were treated with SAHA and stimulated with or without anti-CD3 antibodies for the indicated time periods. TXNIP protein expression was determined by Western blot. The panels show a representative blot of three independent experiments.

Impact of TNFα mRNA expression on AICD in TXNIP knockout Jurkat T cells

Inhibition of AICD by neutralising CD95L was in the range of 50 % (Figure 4.14C) indicating that CD95-independent mechanisms also contribute to AICD in Jurkat T cells. Another death ligand described to influence TCR-induced cell death is TNFα [322]. Since TNFA mRNA expression is increased in TCR-stimulated TXNIP KO clones (Figure 4.13F), we examined whether TNFα is involved in AICD of Jurkat T cells. As shown in Supplementary Figure 3, blockage of TNFα did not alter AICD of EV and TXNIP KO clones suggesting that other TXNIP-mediated mechanisms lead to AICD of Jurkat T cells.

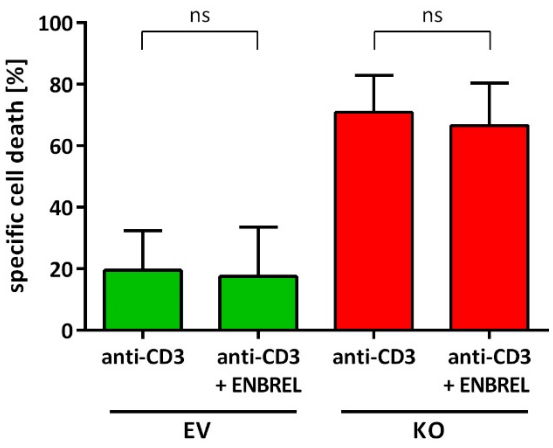

Supplementary Figure 3: Blocking TNFα does not influence AICD.
EV and TXNIP KO clones were treated with or without ENBREL and restimulated with anti-CD3 antibodies for 48 h to induce AICD. Cell death was assessed by flow cytometry using AnxV-FITC and 7AAD and calculated as "specific cell death" normalised to untreated cells. Bars represent "specific cell death" as a mean of the three EV and TXNIP KO clones of one experiment. Statistical significance was calculated using unpaired t-test (mean and SD, ns: $p > 0.05$).

Effect of TXNIP knockout on basal proliferation

TXNIP is involved in the regulation of cell proliferation. On the one hand, by controlling Trx activity, TXNIP affects functions of Trx which promote cell proliferation *e.g.* activation of transcription factors [40]. On the other hand, TXNIP itself inhibits cell division by influencing the activity of cyclins [230, 337]. Hence, we investigated whether TXNIP expression affects basal proliferation of Jurkat T cells. As illustrated in Supplementary Figure 4, EV and TXNIP KO clones exhibited comparable basal proliferation indicating that TXNIP has no impact on general proliferation of Jurkat T cells.

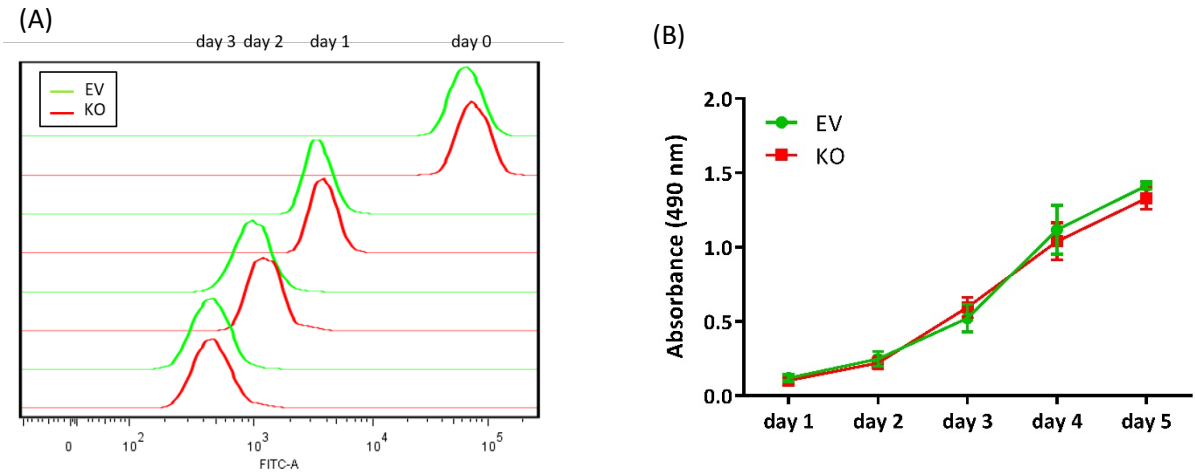

Supplementary Figure 4: Comparable basal proliferation in EV and TXNIP KO clones.
(A) EV and TXNIP KO clones were labelled with CFSE and cultured for up to 3 days. Proliferation was monitored by flow cytometry. The panel shows a representative analysis of two independent experiments. (B) EV and TXNIP KO clones were cultured for up to 5 days and every day, proliferation was measured using a colorimetric assay kit. The panel shows mean values and SD of three EV and TXNIP KO clones of one representative analysis of two independent experiments.

List of Figures